DISSERTATION / DOCTORAL THESIS

Titel der Dissertation /Title of the Doctoral Thesis

“Evaluation of bioavailability and influencing factors thereof in antineoplastic drugs: in silico predictions and in vivo analyses”

verfasst von / submitted by

Mag.pharm. Andrea Gruber

angestrebter akademischer Grad / in partial fulfilment of the requirements for the degree of

Doktorin der Naturwissenschaften (Dr.rer.nat.)

Wien, 2019 / Vienna, 2019<

Studienkennzahl lt. Studienblatt / degree programme code as it appears on the student record sheet:	A 796 610 449
Dissertationsgebiet lt. Studienblatt / field of study as it appears on the student record sheet:	Pharmazie
Betreut von / Supervisor:	ao. Univ.-Prof. Mag.pharm. Dr. Martin Czejka

Acknowledgements

I would like to express my sincere gratitude to my supervisor Univ.-Prof. Dr. Martin Czejka (Department of Clinical Pharmacy and Diagnostics, University of Vienna) who continuously supported me with his experience, scientific knowledge, encouragement and motivation. This thesis would not have been possible in this form without his help.

In addition, I would like to cordially thank Dr. Michael Lawless from Simulation Plus Inc. for his generous support with the software tools ADMET Predictor ™ and GastroPlus™ and Univ.-Prof. Dr. Christian Dittrich, head of the Applied Cancer Research - Institution for Translational Research, Vienna (ACR-ITR VIEnna) for the valuable cooperation regarding publications of the current thesis.

My sincere thanks also go to Dr. Marie Kitzmueller for the years of support, collaboration and friendship during our shared PhD-experience as well as my colleges at the Department of Clinical Pharmacy and Diagnostics, Dr. Nairi Kirchbaumer-Baroian, Dr. Azra Sahmanovic-Hrgovcic and Dr. Philipp Buchner for their motivation and companionship.

I also want to specifically thank my sister, who encouraged me to start my PhD in the first place, always lent me an ear in difficult situations, pep talked me whenever necessary and shared my joy after accomplishing my goals. Moreover, I am grateful for the support and encouragement of my parents, who are always there for me.

Lastly, I wish to thank my friends for listening, offering me advice, and supporting me throughout this entire period. Thank you for going through all the fun and stressful times with me as well as understanding and supporting my decisions to follow my way.

TABLE OF CONTENTS

1 Abstract

The present work examines various methods to assess the bioavailability of selected compounds as well as several influences thereof, before administration to a patient. It is important to consider the safety aspects of drugs, not only by assessing toxicities and monitoring plasma concentrations of drugs in pharmacokinetic (PK) studies, but also by illuminating the underlying mechanisms leading to adverse events or ineffective treatment. Additionally, it is crucial to understand the impact of molecular properties on the PK performance of a compound and connect those properties with a susceptibility to certain co-variate influences. This strategy will not replace in vivo studies on animals and humans but has the potential to drastically reduce both and thus manage safety and efficacy trials with a much smaller budget. In this thesis, four chemotherapeutic agents, erlotinib, selumetinib, capecitabine and irinotecan, have been investigated regarding their bioavailability and influences thereof, based on their molecular properties, in a physiologically based pharmacokinetic (PBPK) model and animal model. Erlotinib is an orally administered tyrosine kinase inhibitor (TKI) with physicochemical properties of a weak base and therefore exhibits pH-sensitive absorption characteristics. The concomitant administration of erlotinib with acid-reducing agents resulted in drug concentrations below the activity threshold in patients and thus an ineffective chemotherapeutic treatment. It was demonstrated in the PBPK model that the underlying mechanism responsible for this drug-drug interaction (DDI) was the reduced solubility of the compound in a higher pH-range of the stomach, induced by the acid reducing agents, which decreased the dissolution and solubility of erlotinib and thus led to considerably reduced plasma concentrations in patients. Additionally, erlotinib plasma concentrations exhibited a generally high inter-patient variability in the analyzed PK profiles. The PBPK model showed that physiological differences such as variations in the plasma protein binding rate as well as differences in the hepatic clearance considerably affected the bioavailability of the drug. Those variations can result from co-medication, different stages of the respective disease and the overall performance, including organ dysfunctions. Selumetinib, another orally administered TKI with similar physicochemical characteristics as erlotinib, but lower aqueous solubility, was administered to patients in formulations containing excipients to enhance the absorption and thus the bioavailability of the drug. The PK profile of selumetinib consequently changed when administered with excipients, and the

bioavailability enhancing mechanisms were demonstrated in a PBPK model. Additionally, physiological differences affected the plasma concentrations of selumetinib, resulting in high inter-patient variability, similar to erlotinib. The PBPK model however displayed no significant impact of acid reducing agents on the plasma concentrations of selumetinib, due to the formulation, which provided a stable solubility over the physiological pH-range. Overall, the PBPK model demonstrated its usefulness in formulation development by increasing the understanding of the compound's properties and their impact on the bioavailability. Capecitabine has been designed as triple prodrug and is transformed to the active moiety 5-fluorouracil (5FU) in liver and tumor tissue, which allows the drug to reach its target more specifically. This strategy also helped to decrease haematotoxicity, which was observed in 5FU-based treatment, due to the higher concentration of the chemotherapeutic agent in tumor tissue and less in the systemic circulation. The PBPK model of capecitabine therefore included its metabolites as well as the enzymatic cascade leading to 5FU. Influences on the metabolic steps and their effect on the 5FU concentration in various compartments were demonstrated, which can derive from physiological or genetic differences, as well as DDIs. The model can thus also serve as basis for further investigations of the clinical relevance of connected genetic polymorphisms. Irinotecan, another established chemotherapeutic drug, was also designed as prodrug, with the active compound being SN-38. It is usually administered as intravenous infusion, however to reduce its systemic effects, it can also be applied as hepatic arterial infusion. The administration of irinotecan was further investigated as hepatic arterial infusion in combination with two different embolization particles in an animal model for the indication of colorectal liver metastases. This specific administration method was used to increase the local concentration of irinotecan in the tumor tissue and thus further increase the cytotoxic effect in the liver metastases and additionally embolize small blood vessels in the tumor tissue to reduce the tumor growth by lowering the blood supply. Plasma, tumor and liver samples were then analyzed to detect the impact of different administration methods and embolization particles on the antitumoral effect.

Altogether, the thesis encourages the combination of various PK tools to effectively increase the safety and efficacy of chemotherapeutic treatment for patients.

2 Zusammenfassung

Die vorliegende Arbeit untersucht verschiedene Methoden zur Bestimmung der Bioverfügbarkeit und darauf Einfluss nehmende Faktoren, anhand ausgewählter chemotherapeutischer Arzneistoffe. Eine sichere Arzneimittel-Anwendung sollte nicht nur durch eine Überwachung von Plasmakonzentrationen oder Evaluierung von Toxizitäten in pharmakokinetischen (PK) Studien gewährleistet werden, sondern auch durch Aufklärung der zugrunde liegenden Mechanismen, die zu unerwünschten Nebenwirkungen oder unwirksamen Behandlungen führen. Darüber hinaus ist es wichtig, den Einfluss molekularer Eigenschaften auf die PK Parameter einer Substanz zu verstehen und diese mit einer Anfälligkeit für bestimmte Co-Faktoren zu verknüpfen. Dieser Ansatz wird Studien an Tieren und Menschen bezüglich Sicherheit und Wirksamkeit nicht ersetzen, kann diese jedoch deutlich reduzieren und somit die Ausgaben in der Arzneimittelentwicklung senken. In dieser Arbeit wurden vier Chemotherapeutika, Erlotinib, Selumetinib, Capecitabin und Irinotecan, hinsichtlich ihrer Bioverfügbarkeit und ihrer molekularen Eigenschaften untersucht und darauf Einfluss nehmende Faktoren in einem physiologisch-basierten pharmakokinetischen (PBPK) Modell und einem Tiermodell dargestellt.

Erlotinib ist ein oral verabreichter Tyrosinkinase-Inhibitor (TKI) mit den physikochemischen Eigenschaften einer schwachen Base und zeigt daher pH-abhängige Absorptionseigenschaften. Die gleichzeitige Anwendung von Erlotinib mit säurereduzierenden Arzneistoffen führte bei Patienten zu Plasmakonzentrationen unterhalb der Aktivitätsschwelle und somit zu einer unwirksamen chemotherapeutischen Behandlung. Im PBPK-Modell wurde gezeigt, dass der Grund für diese Arzneimittelwechselwirkung in der verringerten Löslichkeit von Erlotinib im höheren pH-Bereich liegt, der durch die säurereduzierenden Arzneistoffe im Magen verursacht wurde. Dieser Prozess verringerte sowohl die Lösung als auch die Löslichkeit von Erlotinib und führte somit zu deutlich reduzierten Plasmakonzentrationen bei Patienten. Darüber hinaus haben Erlotinib-Plasmakonzentrationen eine generell hohe Variabilität in den analysierten PK-Profilen der Patienten gezeigt. Das PBPK-Modell veranschaulichte, dass physiologische Unterschiede z.B. in der Plasmaprotein-Bindungsrate oder in der Leber-Clearance, die Bioverfügbarkeit des Arzneimittels erheblich beeinflussen können. Diese Schwankungen können durch eine gleichzeitig verabreichte Co-Medikation, einem

unterschiedlichen Stadium der Erkrankung oder durch mögliche Organschwächen in Patienten entstehen.

Selumetinib, ein weiterer oral verabreichter TKI mit ähnlichen physikochemischen Eigenschaften, aber einer geringeren Wasserlöslichkeit als Erlotinib, wurde Patienten in Formulierungen mit Resorptions-verstärkenden Hilfsstoffen verabreicht, um die Bioverfügbarkeit des Arzneistoffs zu verbessern. Das PK-Profil von Selumetinib änderte sich folglich durch die Verabreichung mit den Hilfsstoffen. Die Mechanismen, die zur Verbesserung der Bioverfügbarkeit führten, konnten in einem PBPK-Modell analysiert werden. Zusätzlich haben jedoch, ähnlich wie bei Erlotinib, physiologische Unterschiede die Plasmakonzentrationen von Selumetinib beeinflusst, was zu einer hohen Variabilität in den PK-Profilen von Patienten führte. Das PBPK-Modell zeigte jedoch anders als bei Erlotinib, keinen signifikanten Einfluss von säurereduzierenden Arzneistoffen auf die Plasmakonzentration von Selumetinib, da durch die Formulierung die Löslichkeit von Selumetinib über den physiologischen pH-Bereich hinweg stabil gehalten wurde. Diese Anwendung verdeutlicht, dass PBPK-Modelle auch bei der Entwicklung von geeigneten Formulierungen eingesetzt werden können, indem sie die Eigenschaften des Arzneistoffs und deren Einfluss auf die Bioverfügbarkeit veranschaulichen.

Capecitabin ist ein Prodrug und wird durch dreifachen Metabolismus in Leber- und Tumorgewebe zur aktiven Substanz 5-Fluorouracil (5FU) umgewandelt. Durch die spezifische Aktivierung von Capecitabin zu 5FU im Tumor kommt es zu einer höheren Konzentration des Arzneistoffs im Tumorgewebe und daher zu geringeren Konzentrationen in der systemischen Zirkulation. Diese Strategie wurde unter anderem entwickelt um die Hämatotoxizität der 5FU Therapie zu reduzieren, die durch die erhöhte systemische Verfügbarkeit zustande kommt. Das PBPK Modell von Capecitabin umfasst zusätzlich alle Metaboliten bis hin zu 5FU und die dazugehörigen enzymatischen Metabolisierungsschritte. Im Modell konnten Einflüsse auf die Metabolisierung und ihre Auswirkung auf die 5FU-Konzentration in verschiedenen Kompartimenten gezeigt werden, die sich aus physiologischen oder genetischen Unterschieden sowie DDIs ergeben können. Das Modell kann somit auch als Grundlage für weitere Untersuchungen zur Prüfung der klinischen Relevanz genetischer Polymorphismen dienen.

Irinotecan, ein weiterer etablierter chemotherapeutischer Arzneistoff, wurde ebenfalls als Prodrug entwickelt, und wird im Körper zum aktiven Wirkstoff SN-38 metabolisiert. Irinotecan wird in der Regel als intravenöse Infusion verabreicht, kann jedoch in der Indikation kolorektaler Lebermetastasen zur Verringerung seiner systemischen Wirkungen auch als hepato-arterielle Infusion appliziert werden. Die hepato-arterielle Verabreichung von Irinotecan wurde in einem Tiermodell zusätzlich in Kombination mit zwei verschiedenen Embolisations-Partikeln untersucht. Diese spezifische Verabreichungsmethode wurde verwendet, um die lokale Konzentration von Irinotecan im Tumorgewebe zu erhöhen und dadurch die zytotoxische Wirkung in den Lebermetastasen weiter zu steigern. Außerdem wurden durch die mitverabreichten Partikeln kleine Blutgefäße im Tumor embolisiert, um so das Tumorwachstum zusätzlich durch eine verringerte Blutversorgung zu hemmen. Anschließend wurden Plasma-, Tumor- und Leberproben analysiert, um den Einfluss der verschiedenen Verabreichungsmethoden und Embolisations-Partikeln auf die Tumor-reduzierende Wirkung zu untersuchen.

Zusammenfassend soll die aktuelle Arbeit einen Einblick in die Vielzahl von PK Untersuchungsmethoden geben und den Einsatz von Kombinationen verschiedener Methoden in der Arzneimittelentwicklung und klinischen Routine anregen um letztlich die Sicherheit und Wirksamkeit einer chemotherapeutischen Behandlung für Patienten zu erhöhen.

3 Introduction

3.1 Pharmacokinetics and bioavailability

Pharmacokinetics (PK) describes the time dependent course of a drug and its metabolites in different compartments in a physiological system (1). The steps a drug undertakes on its way through the body can be summarized as absorption, distribution, metabolism and excretion (ADME) processes (2). The sum of these steps determines the bioavailability of the compound, defined by the US Food and Drug Administration (FDA) as the “rate and extent to which the active ingredient or active moiety is absorbed from a drug product and becomes available at the site of action” (3). The PK profile, including the bioavailability of a drug is dependent upon the physicochemical properties of a compound, as well as the formulation, application method and site of the drug and the physiology of the target population (4-8). For a better understanding of the PK pathways of the drug and hence to predict its in vivo performance, molecular properties and ADME parameters can be measured by in vitro and in vivo methods or calculated by in silico tools to approximate its fate. Understanding the PK pathways is essential to anticipate problems in the clinical use, such as low bioavailability at the target site. The obtained insights can be used in drug development to assist in optimization of either the molecule, the formulation or the administration route. Drug metabolism and pharmacokinetics (DMPK) has emerged as scientific discipline to understand and illustrate the fate of the drug in physiological environment to ensure the availability of the drug at the target site for an efficiently executed pharmacological action and reduced incidence of adverse events (9). The field has been greatly expanded from in vitro and in vivo animal studies to in silico methods more recently, which allows the process to be more time- and cost-effective. It has improved success rates of drug discovery and development over the last 15-20 years and thus plays an important role in drug development for drug safety and efficacy (9-11).

3.1.1 PK drug profiling

Drug profiles are usually measured in plasma, even though the central compartment is mostly not the target site. The measured bioavailability thus only indirectly indicates the efficacy of the treatment but allows a standardized characterization of the drug in the intended dosage and route of administration (12). Important PK parameters include

the area under the curve (AUC_{0-t}), describing the disposition of the drug, the peak concentration (C_{max}) and the time to peak concentration (T_{max}) as well as the clearance rate (Cl), volume of distribution (Vd) and the elimination half-life ($t½_{el}$). Most analytical methods have been developed for plasma samples, however the analysis of additional samples from e.g. blood, serum, tissue, biopsy, saliva, urine or feces can be necessary to accurately predict the distribution in the body (13). The PK profile can also be obtained by in silico predictions with suited software tools using information of the molecular properties of the drug and the physiology of the target population. These physiologically-based pharmacokinetic (PBPK) models are based upon mathematical calculations following the ADME steps (14-17). Most predictions refer to standard conditions, which often differ from the clinical situation observed in patients. It is therefore important to consider possible changes in parameters and their effect on the drug disposition and bioavailability. Changes in physiological parameters can have a considerable influence on the drug profile and may result in concentrations outside the therapeutic window, defined as the concentration range, where a drug has a therapeutic, but not toxic effect in a patient (18). Hence, exceeding this range can cause ineffective treatment or a higher incidence of adverse events. Reasons for variability in the plasma concentration and therefore bioavailability can derive from parameters in all ADME steps.

3.1.2 Variabilities

Drug concentrations in patients are pursued to occur as steadily as possible, because a high variability in the PK profile of a drug can cause unpredictable effects during the treatment of patients (19-21). However, drug administrations other than continuous infusion imply a natural fluctuation of drug concentration in the PK profile. It is therefore essential to adapt the dosing schedules to the PK profile of a drug to maintain optimal steady state levels. For drugs with a high risk of variability, due to interferences in the treatment, therapeutic drug monitoring (TDM) has been established to monitor drug levels in patients to ensure a safe and efficient treatment (22-23). However, the link between observed variabilities and PK interactions can often only been drawn retrospectively by statistical analysis of the PK data. Additionally, it is difficult to include TDM in a regular clinical routine or outpatient regimens, which gave rise to PBPK modeling, aiming to detect and understand the co-variate influences and their clinical

relevance in the physiology of the target population before administration to the patient (24-30). A transparent PK pathway and prediction of the clinical relevance of co-variate influences, such as drug-drug-interactions (DDIs) or physiological changes, can thus decidedly reduce inter-and intra-patient variabilities. PBPK models can also predict the drug levels in additional compartments, e.g. target organs or tissues linked to adverse events, which are often difficult to analyze in vivo (31-32).

3.1.3 Bioavailability assessment - in vitro/in silico/in vivo methods

There are several methods available to predict and approximate the PK profile in patients, which support the decision for advancing, holding or terminating a drug candidate during drug development. DMPK has not only advanced the understanding of target physiologies and research tools but has demonstrated that the selection of an appropriate model, including a specific strategy and correct data interpretation, is critical for the success of the process (9). In vitro methods as well as animal models have been favored for decades in drug discovery and development, whereas often quantity dominated over quality regarding the extractable information. Nonetheless, automated high-throughput screening (HTS) methods can be of great use to effectively assess PK parameters on a large set of compounds in early stages of drug development (2). In the prediction of physicochemical properties of compounds, in silico methods have in many cases superseded in vitro screenings, for a quick determination of the drug-likeness of a compound. In the field of ADME parameters, still many in vitro tools and animal models are used to describe the PK profiles of new drug candidates and especially toxicology and risk assessment still strongly rely on animal models, even though a slow tendency to replace, refine and reduce the use of these models can be observed (3Rs) (33-35). In addition, the development of in silico tools for the prediction of ADME parameters has advanced and decidedly benefits from the extensive curation of in vitro data, which can be used to improve the predictive strength of in silico models. However, even though in silico and in vitro models rapidly develop to facilitate the drug development process, some investigations still require in vivo studies. The following sections describe several methods to determine in vivo bioavailability in a target population and examine their potential to increase safety and efficacy of treatments.

3.2 Key parameters in bioavailability predictions

3.2.1 Molecular properties

The physicochemical properties of a compound determine and correlate with many ADME and PK parameters and are thus an important first step of characterizing a possible drug candidate in early drug development (36-37). Some general standards have been established to guide development decisions. Lipinski et al predicted an increased risk of lower permeability, absorption and consequently bioavailability if the compound fulfills certain criteria. These outlines are summarized as the rule of five (RO5) and limit the lipophilicity, measured as logP (<5), the molecular weight (<500 Da) and the number of hydrogen bond donors (<5, expressed as the sum of all OH's and NH's) and acceptors (<10, expressed as the sum of all O's and N's) of a compound for drug-likeness (38-40). It can be further extended by the Veber rule, limiting the number of rotatable bonds (<10), the polar surface area (<140 A) and the total number of hydrogen bonds (<12) (41).

Measurements of the physicochemical properties of most compound libraries showed an increased tendency for compounds with at least one of those criteria, indicating that the chemical space in which the potential drug candidates occur is likely differing from the compound libraries used in drug development, often resulting in low bioavailability compounds (38). The lipophilicity of a compound is usually measured as octanol/water coefficient, which describes the distribution of the compound in the water (hydrophilic) or octanol (lipophilic) phase of a mixture. There is a positive correlation between lipophilicity and permeability, therefore the lipophilicity can be used as first estimation of the passive permeability through the intestinal membrane (2,42-45). The logP value is pH sensitive and it is therefore important to measure the logP at the appropriate pH (7.4 for the blood and 6.8 for the intestine). The consideration of molecular weight (MW) is important for the absorption, because the process can be hindered when the molecules are too big for permeating passively through the membrane (46). The passage is then dependent upon active transport, which generally comes with a lower bioavailability and higher variability. To cross membranes, the hydrogen bonds to water molecules must be stripped off and a high number of hydrogen bond donors and acceptors in the molecular structure makes the process energetically more expensive and therefore unlikely (47). The number of hydrogen bond donors and acceptors can be calculated as the sum of oxygen and nitrogen atoms or from the calculation of the

polar surface area. It is also dependent upon the ionization of a compound, and therefore by its pKa values, which should be measured in an adequate pH range. The ionization constant displays the strength of acidity or basicity of a compound and therefore also determines the ionization at a given pH in an aqueous solution. This is important, because non-ionized compounds are more likely to permeate passively through the membrane (48). For a better estimation of the ability to permeate the intestinal membrane, the pH-dependent logD could therefore be used instead of logP, which has been demonstrated by Kokate et al 2008 (49). The polar surface area is the sum of surfaces of polar atoms such as oxygen and nitrogen including attached hydrogens in a compound. It has also shown to correlate well with the permeability of membranes (50). It can be calculated by generating a 3D geometry to determine the surface. In drug development, it is now however usually calculated by software tools (51-52).

Many different software tools focus on the prediction of physicochemical characteristics to replace HTS methods by either substructure-based or property-based calculations (53-62). Calculations based on fragments or on single-atom levels divide the molecular structure into substructures and then summarize the known contributions of individual fragments under application of correction factors to the requested parameter. The prediction results have shown to improve when the contributions of atoms, structural fragments and intramolecular interactions were combined in the calculations. Property-based methods employ descriptors of the entire molecule and calculate the prediction based on parameters derived from empirical methods, or by using 3D structure- or topological descriptors (60). In the field of property-based methods, models based on artificial neural network ensembles (ANNE) showed the best results for the prediction of the physiochemical parameters pKa and logP (59).

However, in all cases of in silico predictions of physicochemical or PK properties, the curation of reliable data is crucial in the model building process as well as the establishment of a clear endpoint with little variability (59). It is also highly beneficial to use training sets with compounds that cover a large chemical space for a broad application of the model.

3.2.2 ADME parameters

Predictions of ADME parameters are still mostly based on in vitro and in vivo methods (63-64). In silico methods have nevertheless been developed to predict ADME parameters, even though it is more difficult to establish these models, due to the often more unstable endpoints and in general less data than for molecular properties, which can be relevant for the establishment of these models, since they rely on both, quantity and quality of data (65-67). Tools such as the ADMET Predictor™ (Simulations Plus, CA), which operates with ANNE based models, are able to deliver predictions of relevant ADME parameters based on the molecular properties of a compound (68). These include predictions of solubility and permeability for an estimation of the absorption properties of a compound, plasma protein binding and distribution in to red blood cells for an assessment of the distribution, or sites of metabolism, V_{max} and Km values as well as intrinsic clearance, calculated for the main drug metabolizing cytochrome P (CYP) 450 enzymes (69-70). However, even though these predictions can give a first impression of the PK performance of the compound, it is recommended to compare the obtained data with in vitro data to check if the evaluated compounds are within the limits of the chemical space the model was trained and tested with. Users must also be aware that the predictions are approximations, based on in vitro data of similar compounds, which can underly variations and errors just as any in vitro experiment. Additionally, all ADME parameters produce a static image of the molecule instead of picturing the dynamic equilibrium in physiological environment. Therefore, in vivo studies are still the gold standard in evaluating the PK profile of a new drug candidate. However, also PBPK models can depict the dynamic situation of drugs in physiological environment, thus greatly enriching and facilitating the entire process of candidate selection for further development (30,71-76). PBPK models combine information of the molecular characteristics and PK properties of a drug with a selected physiology, therefore relying on the correct input data of the molecular and PK properties of the analysed compounds. It is crucial for the model development process to understand the methods and conditions under which the data was obtained from in vitro experiments to correctly apply the information to the model. Thus, also small differences, such as different measurement methods or even temperature can influence the outcome of the experiment and consequently the prediction. The model hence underlies several basic variabilities, which must be minimized by following the recommended modelling guidelines including important validation steps in the model

building process to improve the accuracy and the predictive power of these models and thus increase the reliability to enable a more frequent use in drug development (14-16).

Absorption

In pharmacokinetics the term absorption process mainly focusses on the intestinal absorption because most drugs are designed for oral administration. The intestinal absorption requires two main steps, the solubility of the compound, including the dissolution from the dosage form and the permeability across the gut wall (77-78). These two parameters have been combined in the Biopharmaceutics Classification System (BCS) to map compounds, based on their properties, for a quick evaluation of their absorption characteristics. Drugs are divided into four classes, I - high solubility, high permeability; II – low solubility, high permeability; III – high solubility, low permeability and IV – low solubility and low permeability compounds (79-84). The BCS was originally intended as guidance for generic drug biowaivers, but advanced in recent years to a valuable scientific framework in early drug development to estimate the absorption characteristics of a drug (74,85-88). It can also reveal possible absorption difficulties leading to low bioavailability, which are often associated with certain BCS classes.

Solubility and permeability can be predicted from the molecular structure of a drug candidate (89-95). Additionally, the absorption process can be simulated in a PBPK model (96-97). In vitro absorption related experiments must be conducted in the intended dose strength and formulation, because solubility and permeability are also dependent upon formulation. The solubility of a compound should be tested in the highest dose strength or highest single dose administered in 250 ml aqueous media and a pH range of 1 – 6.8, at 37 ± 1 °C to cover the relevant physiological range in the intestine. A drug considered highly soluble, must be soluble in 250 ml aqueous media, across the measured pH range in the highest intended dose strength (98). The 250 ml refer to common study protocols of administration of a drug to a fasting person with an 8-ounce glass of water. Solubility measurements should include the testing of a compound's solubility in intestinal fluid media, which can differ to the aqueous media by composition. Especially the fed state media contains a high number of bile salts, which can increase the solubility of poorly water-soluble compounds (99-103). Bile salts can stabilize highly lipophilic molecules and thus prevent nucleation and

precipitation at the absorption site, which would inhibit the absorption of the compound. The dissolution of the drug from the formulation is a prerequisite for absorption and another part of the solubility measurements. In vitro dissolution testing is not only imperative for regulatory purposes, it is also a valuable tool in formulation development, in quality control and for monitoring the manufacturing process (104-106). The dissolution is guided by many factors, including the dosage form, particle size, dose strength or the dissolution media. There are standard methods for solid dosage forms, with the United States Pharmacopeia (USP) apparatus USP 1 (basket method) and USP 2 (paddle method), stirring rates, defined medium and temperature, however deviation from those standard methods is accepted if properly justified (107-108). The testing must be robust and reproducible as well as economical and simple and must fit dosage form characteristics and the intended route of administration. The extraction of the compound of the solid-state matrix into solution is then expressed as percent released over time in a dissolution plot. High solubility drugs are expected to release 80% of the drug in a time course of 30 minutes (98). The dissolution test can also be used for the comparison of dosage forms and potencies or measuring the effect of excipients or surfactants as well as particle size on the formulation (2).

The second step of the absorption process is the transport of the drug from the gastrointestinal lumen into the systemic circulation, hence the permeation through the intestinal membrane. There are several possibilities to cross the intestinal membrane, depending on the properties of the drug. The transcellular route through the enterocytes can be passed actively or passively, whereas the paracellular pathway occurs passively by bypassing the enterocytes at tight junctions, adherens junctions or desmosomes (109-110). The paracellular route allows the diffusion of ions and molecules with a low MW aside the enterocytes. Paracellular permeability can be increased in certain pathological conditions, resulting in unspecific crossing of the epithelial layer for molecules with higher MW. The more frequent route for oral drugs however is the transcellular pathway. The type of passage depends on the molecular properties, mainly on the lipophilicity/hydrophilicity of a compound, as well as the ionization state at a pH of approximately 6.8 and the molecular weight. Due to the architecture of the membrane, moderately lipophilic compounds can readily permeate passively, resulting in adequate permeation and steady absorption (111-112). Highly lipophilic compounds however often show a greater variability in their absorption rate, which could be due to a deficient solubility at the absorption site (113-115). Hydrophilic

compounds and compounds with a higher MW are generally dependent upon active transport through the membrane. These mechanisms require influx transporters, such as the organic anion transporting polypeptides (OATP). There are however also efflux transporters present in the enterocytes, such as breast cancer resistance protein (BCRP), P-glycoprotein (P-GP) and ATP binding cassette (ABC) transporters, resulting in varying or poor absorption rates for these compounds (116-122). There are many ways to measure the permeability, however the chosen method should reflect the transport mechanisms involved. The BCS permeability classification is indirectly based on the extent of absorption of a compound and can thus be determined through in vivo or in vitro studies. In vivo studies include mass balance studies with unlabelled stable isotopes or radiolabelled drug substance or from bioavailability calculations, using intravenous administration as reference. In vitro methods involve permeation studies on cultured epithelial cells or human or animal tissue, as well as in situ perfusion of human or animal tissue. In vitro methods are considered appropriate for drugs using passive transport and many of those methods have been thoroughly validated in many studies. The most common cultured cell assays include CaCo-2 cells (human epithelial colon adenocarcinoma cell lines), which express several transporters, including dipeptide carriers and P-GP for an estimation of active transport involvement in the absorption process, as well as Madin-Darby canine kidney (MDCK) cells or 2/4/A1 cell lines, able to depict the paracellular transport (123-130). Isolated sections of human or animal tissue can also be used for the measurement of intestinal permeability, mounted in a chamber as barrier between two compartments. In situ perfusion involves either an isolated segment or the whole small intestinal tract, remaining in situ while being perfused, and the measurement of the disappearance of the drug from the solution (2,131-132). A drug is considered highly permeable if the absolute bioavailability is > 85 % or if > 85 % of the drug is recovered unchanged or as parent and metabolites in urine (98). In general, in vivo studies are more common, however they fail to illustrate the underlying absorption mechanisms, therefore often a combination of methods is recommended. Excipients, as well as surfactants and stabilizing agents in the formulation can influence the absorption rate, however they mostly influence solubility and stability at the absorption site instead of the permeation itself (5,133-137).

Distribution

Once the compound is absorbed and reaches the systemic circulation, it is distributed into different compartments of the body, which enables the compound to reach its pharmacological target. The unbound fraction of the drug is available for pharmacological action, whereas the remaining drug is bound to intrinsic structures, such as plasma proteins, erythrocytes or tissue (12,138-143). If the drug is bound, it can neither perform any therapeutic action, nor can it be metabolized or eliminated. The extent of distribution and binding can be described by the PK parameter volume of distribution (Vd), which is defined as the theoretical volume of body fluid that holds the total amount of an administered drug at the same concentration as observed in the blood plasma (144). It is thus a proportionality factor that relates the amount of drug in the body to the concentration of drug measured in a biological fluid. Drugs with a high Vd are therefore highly distributed into tissue or bound to plasma proteins or erythrocytes and very little is present and circulating in plasma. Low Vd drugs on the other hand are present in plasma almost fully unbound and thus require little more theoretical volume than the body plasma volume. Measuring the concentration of a drug in plasma can visualize the availability of the drug in the systemic circulation, however it cannot depict the drug concentration at the target site. Depending on the target organ or target site, the analysis of biopsy or fluid samples can be necessary for a full monitoring of the distribution kinetics of the substance. This is however rarely possible, therefore the bioavailability of the drug at the target site is usually estimated with distribution coefficients for each organ or tissue, based on the physicochemical properties of the compound and physiological parameters of the target population (145-149). Apart from the distribution into tissues, the binding of drugs to plasma proteins and red blood cells can be essential for the kinetics and availability and thus the pharmacological action of the drug. This is mainly relevant for lipophilic drugs, since they occur to a higher extent bound to plasma proteins for transport through the central compartment. For highly bound drugs, the free and therefore active fraction is small, hence changes in protein binding can then result in a distinct variability in drug disposition if e.g. another highly bound drug is administered concomitantly, and both drugs compete for the binding site of plasma proteins (150-151). Furthermore, organ dysfunctions can cause alterations in plasma protein levels, resulting in varying bioavailability of highly protein bound drugs (152-154). As a result, the unbound concentration can suddenly increase significantly, which can be clinically relevant if the

increased concentrations exceed the range of the therapeutic window and thus lead to a higher rate of adverse events or toxicities. The plasma proteins mostly involved in drug binding are alpha-acidic glycoprotein (AGP) and human serum albumin (HSA) (155). There are two main methods to assess the plasma protein biding rate of a drug, ultrafiltration and equilibrium dialysis, and additionally the TRANSIL® method has evolved more recently. Ultrafiltration is performed by filtering plasma, in which the drug is dissolved, through a membrane with hydrostatic pressure. The membrane cannot be passed by larger molecules, such as proteins as well as drugs bound to these proteins. It is therefore possible to separate the free drug fraction of the drug for analysis. However, often leakages and adsorption of the drug to the device were observed to interfere with the analysis, leading to imprecise outcomes (156). Equilibrium dialysis works through the diffusion of drug dissolved in plasma across a semipermeable membrane into isotonic protein-free buffer. Only the free fraction of the drug can permeate and after reaching equilibrium, the concentration in the buffer can be measured. Difficulties in this method arose by adsorption of the drug to the device, as well as from volume shift, because buffer can also permeate through the membrane and dilute the plasma-drug-solution (157). The TRANSIL® method is based on the distribution of the drug between plasma water, plasma proteins and a solid-supported lipid membrane representing erythrocytes and showed an overall lower susceptibility to interferences than the ultrafiltration and equilibrium dialysis. The method can also be used for membrane affinity studies, regarding the intestinal membrane or the blood/brain barrier (159-160). The extent of binding to erythrocytes and partitioning into the red blood cells (RBCs) can be measured in vitro, by adding drug to an RBC suspension. After reaching an equilibrium, the concentration of drug can be measured in plasma water and erythrocytes (161). It can also be assessed ex vivo, by drawing blood samples after drug administration and separating the RBCs from plasma by centrifuge before analyzing the samples. Many drugs exhibit a fast partitioning, therefore in vitro method can be applied in most cases, also it is much easier and cheaper. Ex vivo can be more specific concerning the equilibrium time, however the drug can simultaneously distribute into tissue, especially when the partitioning step is generally slow, and thus again result in inaccuracy. An exact measurement of partitioning into and onto RBC is important for drugs with a high binding rate, which is often elevated in lipophilic drugs or drugs which are easily partitioning into RBCs, such as compounds with low molecular weight (<150kDa) (2,161).

Metabolism

Metabolism describes the biotransformation of a drug towards a more hydrophilic compound for an easier and quicker excretion by the organism. It is thus closely related to the elimination phase of the ADME process (162). Metabolic reactions mainly take place in the liver and to a minor extent in the intestine, lung and plasma, and can be divided into two phases. Phase I reactions can result in three possible outcomes; the drug becomes inactive trough metabolism, both the parent drug and the metabolite are pharmacologically active, or the inactive parent drug is a prodrug and can be transformed into the active metabolite (163-164). The reactions include dealkylation, oxidation, aliphatic and aromatic hydroxylation and deamination (165). In phase II metabolism ionizable groups are attached to the molecule to transform them into compounds soluble enough to be excreted in urine or bile. These phase II metabolites are unlikely to be pharmacologically active. However, they can be retransformed into active components through intestinal enzymes and reabsorbed through the gut wall, in an enterohepatic circle (166). This reuptake can be described as phase III metabolism. Most phase I enzymes are part of the CYP450 family, acting as monooxygenases, dioxygenases and hydrolases (167). CYP enzymes can be divided in numerous subfamilies, responsible for the metabolism of xenobiotics and endobiotics and their activity can be crucial for the bioavailability of a drug. It is hence necessary to know the phase I metabolism pathways and the enzymatic activity of the metabolizing enzymes to properly predict the fate of a drug in the body. For drugs exhibiting a high first pass effect, this mechanism can be bypassed by e.g. administering a prodrug as inactive precursor, which is then transformed to the active metabolite by enzymatic conversion or by co-administering an enzyme inhibitor to ensure a stable concentration of the active moiety in the systemic circulation. The rate and extent of metabolic conversion as well as its saturation can be described by the Michaelis Menten constant (Km) and the velocity of the reaction (V_{max}). The metabolic conversion can decisively influence the overall bioavailability and variations in enzyme expression levels or metabolic activity can have a considerable impact on the safety and efficacy of a treatment (170). The insights into the metabolic pathway as well as the extent of the enzymatic reaction or any interferences therewith are important for a further combination of the drug in clinical use. Many DDIs are based on metabolic inhibition or induction, therefore new drug candidates are now regularly checked for such interactions, if their metabolic pathway includes the common enzymatic reactions.

Phase II enzymes catalyze glucuronidation, sulfation, methylation, acetylation, glutathione and amino acid conjugation (171). Phase II enzymes are mostly transferases, with the most common UDP-glucuronosyltransferases (UGTs) and sulfotransferases (SULTs) as well as N-acetyltransferases (NATs), glutathione-S-transferases (GSTs) and several methyl-transferases (COMT, TPMT). The abundance of phase I and II enzymes changes with age, gender, diseases or genetics and as such underlies variations (172). Therefore, the determination of metabolic pathways should always consider the circumstances and conditions of the target population for an adequately accurate bioavailability prediction of the drugs. There are various methods to illustrate the metabolic pathways of a drug, based on in vitro or in silico methods to create a metabolic profile of the drug (173-175). Since most enzymes involved in drug metabolism occur in the liver, there are various essays based on homogenized liver and liver fractions, e.g. liver S9-, cytosolic, or microsomal fraction, as well as liver slices or isolated perfused liver (2). However, also cell based and hepatocyte cultures, as well as microsomes containing recombinant human enzymes play a big role in metabolism assays. The closest system to in vivo experiments is the isolated perfused liver, because it can show phase I and II metabolism (176). It can be used as open or closed system and various parameters can be adapted to display in vivo situations. Hepatocytes are relatively easy to handle and control and well-accepted for predictions of the metabolic stability and the metabolic profile and are also able to depict drug-drug interactions based on the metabolic activity of a drug (177). Liver homogenates, such as microsomal, cytosolic or S9 fractions contain several phase I and II enzymes and usually require additional co-factors, such as NADPH. The enzyme content of the assays must be defined to adequately calculate the metabolic activity. The in vitro metabolic profile of a drug further helps to choose an appropriate preclinical safety species, able to demonstrate the fate of the drug closest to a human in vivo system. Various species show a different distribution of enzymes and therefore drug metabolism, hence a species with similar distribution is required for an appropriate metabolic profile (178).

Elimination

After the drug has been metabolized and transformed to a more hydrophilic compound, it can be excreted through urine or bile, unless it is reabsorbed in enterohepatic

circulation. Parameters influencing the elimination phase are mostly based on the physiology of the target organism, such as renal or hepatic clearance rates. The renal function can be approximated by the creatinine clearance, however, for a specific drug clearance, it is necessary to analyze the excreted drug fraction in urine or feces from a human model (179). Variations, such as renal or hepatic impairment, as well as dialysis can strongly influence the bioavailability of a drug. If the excretion of a drug is hindered, it can accumulate in the body and consequently exceed the concentrations of the therapeutic window resulting in toxicities. Depending on the impaired organ, the state of impairment and the route of elimination for a drug, precautions such as dose reductions or a change in the therapeutic regimen must be considered (23,180-182). This is especially necessary for drugs with a narrow therapeutic window, where a close monitoring of plasma concentrations as well as the renal and hepatic function is recommended. Dialysis can affect plasma concentrations of a drug, due to the clearing effect, where fractions of the drug can be filtered from the blood and thus result in a reduced availability in plasma (183). This is however in most cases manageable by adapting the administered dose and timing according to the dialysis schedule. The drug might also bind to the dialysis equipment and therefore result in reduced plasma concentrations, which can however be easily predicted if relevant in in vitro experiments. PK studies focusing on the effect of renal/hepatic impairment on the plasma concentrations and bioavailability are usually conducted in vivo. However, also PBPK modeling can illustrate the effects of hepatic or renal impairment by implementing physiological changes accompanying these conditions, such as reduced excretion or modified plasma protein binding rates, in the model (184).

3.3 Influencing factors on bioavailability

Influences on the bioavailability of a drug can be population- or drug-based. Alterations based on the population can derive from physiological differences or medical conditions of patients and drug-based changes can originate from DDIs of concomitantly applied co-medication or from the formulation or administration method and -site (22,182,185-187). Those changes are responsible for inter- and intra-patient variabilities in the observed plasma concentrations, which can be clinically relevant. Physiological differences can be based on e.g. age, body weight, gender or race (152,188-190). Age and body weight can alter the distribution of the drug, by

differences in cardiac output and therefore distribution in the systemic circulation or partitioning of lipophilic drugs into adipose tissue (191). Gender differences can change distribution kinetics, with different plasma protein binding rates in men and women or differences of distribution into red blood cells, due to a natural diversity between women's and men's hematocrit. Furthermore, enzyme expression levels and activities can vary due to gender, resulting in alterations in drug metabolism. The overall health status of a patient can also change the bioavailability, if the renal or hepatic function is impaired (182,192-193). Polymorphisms of enzymes, transporters or other intrinsic structures can also affect the bioavailability and the extent of alteration determines if the change has a physiological or pathological effect on the patient. If the polymorphism affects a drug eliminating enzyme it is highly likely to have grave effects on the drug disposition, resulting in accumulation or non-effective treatment (194). Of the drug-based influences, co-medication is mainly responsible for bioavailability alterations throughout all ADME stages, but also formulation and administration can strongly impact the bioavailability of a drug. Influences in absorption can derive from complexation, physiochemical interactions or inhibition of drug transporting enzymes (170,195). Complexation mostly results in insufficient absorption, alike physicochemical interactions, derived from e.g. acid reducing agents, which increase the stomach pH and therefore result in reduced solubility for drugs with a pH sensitive dissolution and disintegration. Some drugs are also known to inhibit important drug transporters and thus the absorption of other drugs, or contrarily, helping a drug to be absorbed by inhibiting relevant efflux transporters in the intestine (116-117). This mechanism can be used in formulation development, especially for BCS class IV drugs, which are often susceptible to drug efflux and show an overall difficulty in absorption process, due to their low solubility and permeability (5). These drugs can either be changed and optimized to obtain molecular properties better fit to the requirements of the administration, or their formulation can correct their disabilities. Specific formulation development is thus mostly required for BCS class II and IV drugs, with low solubility, which can be enhanced by excipients (196-197). An increase in permeability is often more difficult to accomplish without optimizing the molecule, but also BCS class IV drugs have shown to improve their bioavailability through an improved formulation. Class IV drugs often exhibit a high molecular weight or high lipophilicity, which makes them susceptible to efflux transporters. One strategy to enhance the permeability is therefore to inhibit these efflux transporters for an

increased absorption of the compound. It is often also necessary to add surfactants and stabilizing agents to the formulation to prevent the drug from precipitation in the intestine (133-137). Naturally, the body uses bile salts to enable absorption for lipophilic compounds from food (26,198). This effect can be used for the absorption of drugs. Some drugs are therefore recommended to be administered with or after food, thus enhancing their chances for absorption from the intestine. Co-medication can also alter the protein binding of drugs, which can affect highly protein bound drugs with a small free fraction of the drug available for pharmacological action (150-151). For drugs with a narrow therapeutic window, concentrations can then result outside their therapeutic index and cause a higher rate of treatment emergent adverse events (TEAE). Another influence on the drug disposition is the administration. Even though most drugs are designed for oral use, there are many possible administration routes and it is usually necessary to define those in advance, because certain routes require specific properties and contrarily, certain properties limit the variety of administration routes (187). Different routes or methods can however also arise for already approved drugs. Especially in oncology, where the cytotoxic effects of the drugs should be limited to the cancerous cells and tissues to minimally affect healthy tissues, the administration with additives has been successfully implemented in therapy (199). Increased drug concentrations in specific cancer tissues or metastases can increase the pharmacological effect of the drug and reduce the systemic exposure and therefore also adverse events and toxicities. The specific administration can be e.g. investigated in animal models. Many DDIs also derive from interactions in metabolism, based on inhibition or induction of certain metabolic pathways or genetic variations thereof (170,194,200). If a degradation of a drug is thus limited it can easily result in accumulation and therefore cause severe toxicities and adverse events. On the contrary, an induced metabolism can reduce the effective drug concentration in the systemic circulation to a level where the treatment is ineffective. Both scenarios are highly undesirable, therefore a transparent analysis of the metabolic pathways has proved to be highly beneficial for the clinical safety. If a drug is highly and rapidly metabolized, which strongly limits its pharmacological action, it can be designed as prodrug, which is ideally transformed into the active compound at the target site and thus perform its pharmacological action more precisely and efficiently (201-202).

3.4 Outlook

The central role of PK studies is to gain understanding of underlying processes occurring after drug administration and to optimize drug candidates by balancing the physicochemical and ADME properties with the efficacy of the drug (2). This process requires a comprehensive assessment of the overall compound quality, which not only focusses on the potency against the target, but also on the ADME parameters (203). A shift from PK studies only serving regulatory affairs to integrating PK into drug development to guide decisions for further development and increase the understanding of the compounds properties is highly beneficial. Additionally, combining PK with pharmacodynamic (PD) in PK/PD models can facilitate the bridging from preclinical to clinical stages of drug development (204). Transforming PD aims into measurable endpoints also helps to define therapy success and leads towards a more individualized therapy (205-206). It can furthermore increase the transparency of therapeutic regimen and guide treatment decisions. A measurable PD endpoint for every drug and disease would increase the application of PK/PD models instead of relying on semi empirical measurements for characterizing the safety and efficacy of a drug. In silico models have been the most cost-effective tool developed in drug development lately and regulatory offices take notice of its possibilities. Hence, the focus of future PK studies should include dynamic modeling by using the combination of in vitro in silico and in vivo methods to achieve relevant approximations of drug disposition at the target site and link them to therapeutic effects (14,207-208). However, it will be necessary to enhance the trust in the predictive power of in silico models through an increase of the understanding for the relative risk of extrapolations and the correct use of obtained data. Conclusively, this approach represents a more resource-orientated process to maximize the information obtained from animal or human studies and thus increase safety and efficacy of patient treatment in an evidence-based way.

4 References

1. Meibohm B, Derendorf H. Basic concepts of pharmacokinetic/pharmacodynamic (PK/PD) modelling. Int J Clin Pharmacol Ther. 1997;35:401-413.

2. Ruiz-Garcia A, Bermejo M, Moss A, et al. Pharmacokinetics in drug discovery. J Pharm Sci. 2008;97:654-690.

3. U.S. Department of Health and Human Services Food and Drug Administration Center for Drug Evaluation and Research (CDER). Bioavailability Studies Submitted in NDAs or INDs — General Considerations, Guidance for Industry. https://www.fda.gov/media/121311/download. Accessed 08.05.2019.

4. Lin L, Wong H. Predicting Oral Drug Absorption: Mini Review on Physiologically-Based Pharmacokinetic Models. Pharmaceutics. 2017;9:41.

5. Ghadi R, Dand N. BCS class IV drugs: Highly notorious candidates for formulation development. J Control Release. 2017;248:71-95. doi: 10.1016/j.jconrel.2017.01.014.

6. Yu LX, Lipka E, Crison JR, Amidon GL. Transport approaches to the biopharmaceutical design of oral drug delivery systems: prediction of intestinal absorption. Adv Drug Deliv Rev. 1996;19:359-376.

7. Sun D, Yu LX, Hussain MA, et al. In vitro testing of drug absorption for drug 'developability' assessment: forming an interface between in vitro preclinical data and clinical outcome. Curr Opin Drug Discov Devel. 2004;7:75-85.

8. Dahan A, Beig A, Lindley D, et al. The solubility-permeability interplay and oral drug formulation design: Two heads are better than one. Adv Drug Deliv Rev. 2016;101:99-107. doi: 10.1016/j.addr.2016.04.018.

9. Zhang D, Gang L, Xinxin D, et al. Preclinical experimental models of drug metabolism and disposition in drug discovery and development. Acta Pharm Sin B. 2012;2:549-561 https://doi.org/10.1016/j.apsb.2012.10.004.

10. Roberts SA. Drug metabolism and pharmacokinetics in drug discovery. Curr Opin Drug Discov Devel. 2003;6:66-80.

11. Webborn PJ. The role of pharmacokinetic studies in drug discovery: where are we now, how did we get here and where are we going? Future Med Chem. 2014;6:1233-1235. doi: 10.4155/fmc.14.76.

12. Poulin P. A paradigm shift in pharmacokinetic-pharmacodynamic (PKPD) modeling: rule of thumb for estimating free drug level in tissue compared with plasma to guide drug design. J Pharm Sci. 2015;104:2359-2368. doi: 10.1002/jps.24468.

13. Langer O, Müller M. Methods to assess tissue-specific distribution and metabolism of drugs. Curr Drug Metab. 2004;5:463-481.

14. Kuepfer L, Niederalt C, Wendl T, et al. Applied Concepts in PBPK Modeling: How to Build a PBPK/PD Model. CPT Pharmacometrics Syst Pharmacol. 2016;5:516-531. doi: 10.1002/psp4.12134.

15. Thelen K, Coboeken K, Willmann S, et al. Evolution of a detailed physiological model to simulate the gastrointestinal transit and absorption process in humans, part 1: oral solutions. J Pharm Sci. 2011;100:5324-45. doi: 10.1002/jps.22726.

16. Thelen K, Coboeken K, Willmann S, et al. Evolution of a detailed physiological model to simulate the gastrointestinal transit and absorption process in humans, part II: extension to describe performance of solid dosage forms. J Pharm Sci. 2012;101:1267-1280. doi: 10.1002/jps.22825.

17. Pang KS, Durk MR. Physiologically-based pharmacokinetic modeling for absorption, transport, metabolism and excretion. J Pharmacokinet Pharmacodyn. 2010;37:591-615. doi: 10.1007/s10928-010-9185-x.

18. Tamargo J, Le Heuzey JY, Mabo P. Narrow therapeutic index drugs: a clinical pharmacological consideration to flecainide. Eur J Clin Pharmacol. 2015;71: 549–567. doi: 10.1007/s00228-015-1832-0.

19. Gross AS. Best practice in therapeutic drug monitoring. Br J Clin Pharmacol. 1998;46:95–99. doi: 10.1046/j.1365-2125.1998.00770.x.

20. Undevia SD, Gomez-Abuin G, Ratain MJ. Pharmacokinetic variability of anticancer agents. Nat Rev Cancer. 2005;5:447-458.

21. Thanki K, Gangwal RP, Sangamwar AT, et al. Oral delivery of anticancer drugs: challenges and opportunities. J Control Release. 2013;170:15-40. doi: 10.1016/j.jconrel.2013.04.020.

22. Gao B, Yeap S, Clements A, et al. Evidence for therapeutic drug monitoring of targeted anticancer therapies. J Clin Oncol. 2012;30:4017-4025. doi: 10.1200/JCO.2012.43.5362.

23. Kang JS, Lee MH. Overview of Therapeutic Drug Monitoring Korean J Intern Med. 2009;24:1–10. doi: 10.3904/kjim.2009.24.1.1

24. Kostewicz ES, Aarons L, Bergstrand M, et al. PBPK models for the prediction of in vivo performance of oral dosage forms. Eur J Pharm Sci. 2014;57:300-321. doi: 10.1016/j.ejps.2013.09.008.

25. Paixão P, Gouveia LF, Morais JA. Prediction of the human oral bioavailability by using in vitro and in silico drug related parameters in a physiologically based absorption model. Int J Pharm. 2012;429:84-98. doi: 10.1016/j.ijpharm.2012.03.019.

26. Parrott N, Lukacova V, Fraczkiewicz G, et al. Predicting pharmacokinetics of drugs using physiologically based modeling--application to food effects. AAPS J. 2009;11:45-53. doi: 10.1208/s12248-008-9079-7.

27. Cheeti S, Budha NR, Rajan S, et al. A physiologically based pharmacokinetic (PBPK) approach to evaluate pharmacokinetics in patients with cancer. Biopharm Drug Dispos. 2013;34:141-154. doi: 10.1002/bdd.1830.

28. Sjögren E, Westergren J, Grant I, et al. In silico predictions of gastrointestinal drug absorption in pharmaceutical product development: application of the mechanistic absorption model GI-Sim. Eur J Pharm Sci. 2013;49:679-698. doi: 10.1016/j.ejps.2013.05.019.

29. Jones HM, Parrott N, Jorga K, et al. A novel strategy for physiologically based predictions of human pharmacokinetics. Clin Pharmacokinet. 2006;45:511-542.

30. Parrott N, Lave T. Applications of physiologically based absorption models in drug discovery and development. Mol Pharm. 2008;5:760-775. doi: 10.1021/mp8000155.

31. Jones HM, Chen Y, Gibson C, et al. Physiologically based pharmacokinetic modeling in drug discovery and development: a pharmaceutical industry perspective. Clin Pharmacol Ther. 2015;97:247-262. doi: 10.1002/cpt.37.

32. Thompson MD, Beard DA. Physiologically-based pharmacokinetic tissue compartment model selection in drug development and risk assessment. J Pharm Sci. 2012;101:424–435. doi: 10.1002/jps.22768

33. Chapman KL, Holzgrefe H, Black LE et al. Pharmaceutical toxicology: designing studies to reduce animal use, while maximizing human translation. Regul Toxicol Pharmacol. 2013;66:88-103. doi: 10.1016/j.yrtph.2013.03.001.

34. Doke SK, Dhawale SC. Alternatives to animal testing: A review. Saudi Pharm J. 2015;23:223-229. doi: 10.1016/j.jsps.2013.11.002.

35. Denayer T, Stöhr T, Roy MV. Animal models in translational medicine: Validation and prediction. New Horiz Transl Med. 2014;2:5–11. doi: https://doi.org/10.1016/j.nhtm.2014.08.001.

36. Segall MD. Multi-parameter optimization: identifying high quality compounds with a balance of properties. Curr Pharm Des. 2012;18:1292-1310.

37. Meanwell NA. Improving drug candidates by design: a focus on physicochemical properties as a means of improving compound disposition and safety. Chem Res Toxicol. 2011;24:1420-1456. doi: 10.1021/tx200211v.

38. Lipinski CA. Drug-like properties and the causes of poor solubility and poor permeability. J Pharmacol Toxicol Methods. 2000;44:235-249.

39. Benet LZ, Hosey CM, Ursu O, et al. BDDCS, the Rule of 5 and drugability. Adv Drug Deliv Rev. 2016;101:89-98. doi: 10.1016/j.addr.2016.05.007.

40. Bergström CAS, Porter CJH. Understanding the Challenge of Beyond-Rule-of-5 Compounds. Adv Drug Deliv Rev. 2016;101:1-5. doi: 10.1016/j.addr.2016.05.016.

41. Veber DF, Johnson SR, Cheng HY, et al. Molecular properties that influence the oral bioavailability of drug candidates. J Med Chem. 2002;45:2615-2623.

42. Klopman G, Zhu H. Recent methodologies for the estimation of n-octanol/water partition coefficients and their use in the prediction of membrane transport properties of drugs. Mini Rev Med Chem. 2005;5:127-133.

43. Kubinyi H. Lipophilicity and drug activity. Prog Drug Res. 1979;23:97-198.

44. Testa, B., Crivori, P., Reist, M. et al. The influence of lipophilicity on the pharmacokinetic behavior of drugs: Concepts and examples. Perspectives in Drug Discovery and Design. 2000;19:179–211. https://doi.org/10.1023/A:1008741731244.

45. Hill AP, Young RJ. Getting physical in drug discovery: a contemporary perspective on solubility and hydrophobicity. Drug Discov Today. 2010;15:648-655. doi: 10.1016/j.drudis.2010.05.016.

46. Yang NJ, Hinner MJ. Getting Across the Cell Membrane: An Overview for Small Molecules, Peptides, and Proteins. Methods Mol Biol. 2015;1266:29–53. doi: 10.1007/978-1-4939-2272-7_3.

47. Goodwin JT, Conradi RA, Ho NFH, et al. Physicochemical Determinants of Passive Membrane Permeability: Role of Solute Hydrogen-Bonding Potential and Volume. J. Med. Chem. 2001;44:3721–3729. doi: 10.1021/jm010253i.

48. Wan H, Ulander J. High-throughput pKa screening and prediction amenable for ADME profiling. Expert Opin Drug Metab Toxicol. 2006;2:139-155.

49. Kokate A, Li X, Singh P, et al. Effect of thermodynamic activities of the unionized and ionized species on drug flux across buccal mucosa. J Pharm Sci. 2008;97:4294-4306. doi: 10.1002/jps.21301.

50. Hou TJ, Zhang W, Xia K, et al. ADME evaluation in drug discovery. 5. Correlation of Caco-2 permeation with simple molecular properties. J Chem Inf Comput Sci. 2004;44:1585-1600.

51. Ertl P, Rohde B, Selzer P. Fast Calculation of Molecular Polar Surface Area as a Sum of Fragment-Based Contributions and Its Application to the Prediction of Drug Transport Properties J. Med. Chem. 2000;43:3714–3717. doi: 10.1021/jm000942e.

52. Yang Y, Engkvist O, Llinàs A, et al. Beyond size, ionization state, and lipophilicity: influence of molecular topology on absorption, distribution, metabolism, excretion, and toxicity for druglike compounds. J Med Chem. 2012;55:3667-3677. doi: 10.1021/jm201548z.

53. Liao C, Nicklaus MC. Comparison of nine programs predicting pK(a) values of pharmaceutical substances. J Chem Inf Model. 2009;49:2801-2812. doi: 10.1021/ci900289x.

54. Fraczkiewicz R. (2013) In Silico Prediction of Ionization. In: Reedijk, J. (Ed.) Elsevier Reference Module in Chemistry, Molecular Sciences and Chemical Engineering. Waltham, MA: Elsevier. 11-Sep-13 doi: 10.1016/B978-0-12-409547-2.02610-X.

55. Milletti F, Storchi L, Goracci L, et al. Extending pKa prediction accuracy: high-throughput pKa measurements to understand pKa modulation of new chemical series. Eur J Med Chem. 2010;45:4270-4279. doi: 10.1016/j.ejmech.2010.06.026.

56. Lee AC, Crippen GM. Predicting pKa. J Chem Inf Model. 2009;49:2013-2033. doi: 10.1021/ci900209w.

57. Milletti F, Storchi L, Sforna G, et al. New and original pKa prediction method using grid molecular interaction fields. J Chem Inf Model. 2007;47:2172-2181.

58. Cruciani G, Milletti F, Storchi L, et al. In silico pKa prediction and ADME profiling. Chem Biodivers. 2009;6:1812-1821. doi: 10.1002/cbdv.200900153.

59. Fraczkiewicz R, Lobell M, Göller AH, et al. Best of both worlds: combining pharma data and state of the art modeling technology to improve in Silico pKa prediction. J Chem Inf Model. 2015;55:389-397. doi: 10.1021/ci500585w.

60. Mannhold R, Poda GI, Ostermann C, et al. Calculation of molecular lipophilicity: State-of-the-art and comparison of log P methods on more than 96,000 compounds. J Pharm Sci. 2009;98:861-893. doi: 10.1002/jps.21494.

61. Wenlock MC, Barton P. In silico physicochemical parameter predictions. Mol Pharm. 2013;10:1224-1235. doi: 10.1021/mp300537k.

62. Tetko IV, Poda GI, Ostermann C, et al. Large-scale evaluation of log P predictors: local corrections may compensate insufficient accuracy and need of experimentally testing every other compound. Chem Biodivers. 2009;6:1837-1844. doi: 10.1002/cbdv.200900075.

63. Li AP. Screening for human ADME/Tox drug properties in drug discovery. Drug Discov Today. 2001;6:357-366.

64. Yu H, Adedoyin A. ADME-Tox in drug discovery: integration of experimental and computational technologies. Drug Discov Today. 2003;8:852-861.

65. Waldman M, Fraczkiewicz R, Clark RD. Tales from the war on error: the art and science of curating QSAR data. J Comput Aided Mol Des. 2015;29:897-910. doi: 10.1007/s10822-015-9865-0.

66. Boobis A, Gundert-Remy U, Kremers P, et al. In silico prediction of ADME and pharmacokinetics. Report of an expert meeting organised by COST B15. Eur J Pharm Sci. 2002;17:183-193.

67. van de Waterbeemd H, Gifford E. ADMET in silico modelling: towards prediction paradise? Nat Rev Drug Discov. 2003;2:192-204.

68. Simulations Plus Inc (2019) ADMETPredictor™ user manual.

69. Hosea NA, Jones HM. Predicting pharmacokinetic profiles using in silico derived parameters. Mol Pharm. 2013;10:1207-1215. doi: 10.1021/mp300482w.

70. Grime KH, Barton P, McGinnity DF. Application of in silico, in vitro and preclinical pharmacokinetic data for the effective and efficient prediction of human pharmacokinetics. Mol Pharm. 2013;10:1191-206. doi: 10.1021/mp300476z.

70. Kesisoglou F, Chung J, van Asperen J et al. Physiologically Based Absorption Modeling to Impact Biopharmaceutics and Formulation Strategies in Drug Development-Industry Case Studies. J Pharm Sci. 2016;105:2723-2734. doi: 10.1016/j.xphs.2015.11.034.

72. Sager JE, Yu J, Ragueneau-Majlessi I, et al. Physiologically Based Pharmacokinetic (PBPK) Modeling and Simulation Approaches: A Systematic Review of Published Models, Applications, and Model Verification. Drug Metab Dispos. 2015;43:1823-1837. doi: 10.1124/dmd.115.065920.

73. Willmann S, Edginton AN, Kleine-Besten M, et al. Whole-body physiologically based pharmacokinetic population modelling of oral drug administration: inter-individual variability of cimetidine absorption. J Pharm Pharmacol. 2009;61:891-899. doi: 10.1211/jpp/61.07.0008.

74. Hansmann S, Darwich A, Margolskee A, et al. Forecasting oral absorption across biopharmaceutics classification system classes with physiologically based

pharmacokinetic models. J Pharm Pharmacol. 2016;68:1501-1515. doi: 10.1111/jphp.12618.

75. Kersting G, Willmann S, Würthwein G, et al. Physiologically based pharmacokinetic modelling of high- and low-dose etoposide: from adults to children. Cancer Chemother Pharmacol. 2012;69:397-405. doi: 10.1007/s00280-011-1706-9.

76. Eissing T, Kuepfer L, Becker C, et al. A computational systems biology software platform for multiscale modeling and simulation: integrating whole-body physiology, disease biology, and molecular reaction networks. Front Physiol. 2011;2:1-10. doi: 10.3389/fphys.2011.00004.

77. Avdeef A. Physicochemical profiling (solubility, permeability and charge state). Curr Top Med Chem. 2001;1:277-351.

78. Mudie DM, Amidon GL, Amidon GE. Physiological parameters for oral delivery and in vitro testing. Mol Pharm. 2010;7:1388-1405. doi: 10.1021/mp100149j.

79. Amidon GL, Lennernäs H, Shah VP, et al. A theoretical basis for a biopharmaceutic drug classification: the correlation of in vitro drug product dissolution and in vivo bioavailability. Pharm Res. 1995;12:413-420.

80. Dahan A, Miller JM, Amidon GL. Prediction of solubility and permeability class membership: provisional BCS classification of the world's top oral drugs. AAPS J. 2009;11:740-746. doi: 10.1208/s12248-009-9144-x.

81. Shah VP, Amidon GL. G.L. Amidon, H. Lennernas, V.P. Shah, and J.R. Crison. A theoretical basis for a biopharmaceutic drug classification: the correlation of in vitro drug product dissolution and in vivo bioavailability, Pharm Res 12, 413-420, 1995--backstory of BCS. AAPS J. 2014;16:894-898. doi: 10.1208/s12248-014-9620-9.

82. Lennernäs H. Regional intestinal drug permeation: biopharmaceutics and drug development. Eur J Pharm Sci. 2014;57:333-341. doi: 10.1016/j.ejps.2013.08.025.

83. Lindenberg M, Kopp S, Dressman JB. Classification of orally administered drugs on the World Health Organization Model list of Essential Medicines according to the biopharmaceutics classification system. Eur J Pharm Biopharm. 2004;58:265-278.

84. Takagi T, Ramachandran C, Bermejo M, et al. A provisional biopharmaceutical classification of the top 200 oral drug products in the United States, Great Britain, Spain, and Japan. Mol Pharm. 2006;3:631-643.

85. Benet LZ. The role of BCS (biopharmaceutics classification system) and BDDCS (biopharmaceutics drug disposition classification system) in drug development. J Pharm Sci. 2013;102:34-42. doi: 10.1002/jps.23359.

86. Davit BM, Kanfer I, Tsang YC, et al. BCS Biowaivers: Similarities and Differences Among EMA, FDA, and WHO Requirements. AAPS J. 2016;18:612-618. doi: 10.1208/s12248-016-9877-2.

87. Larregieu CA1, Benet LZ. Distinguishing between the permeability relationships with absorption and metabolism to improve BCS and BDDCS predictions in early drug discovery. Mol Pharm. 2014;11:1335-1344. doi: 10.1021/mp4007858.

88. Parr A, Hidalgo IJ, Bode C, et al. The Effect of Excipients on the Permeability of BCS Class III Compounds and Implications for Biowaivers. Pharm Res. 2016;33:167-176. doi: 10.1007/s11095-015-1773-4.

89. Hewitt M, Cronin MT, Enoch SJ, et al. In silico prediction of aqueous solubility: the solubility challenge. J Chem Inf Model. 2009;49:2572-2587. doi: 10.1021/ci900286s.

90. Cappelli CI, Manganelli S, Lombardo A, et al. Validation of quantitative structure-activity relationship models to predict water-solubility of organic compounds. Sci Total Environ. 2013;463-464:781-789. doi: 10.1016/j.scitotenv.2013.06.081.

91. Bergström CA, Luthman K, Artursson P. Accuracy of calculated pH-dependent aqueous drug solubility. Eur J Pharm Sci. 2004;22:387-398.

92. Hansen NT, Kouskoumvekaki I, Jørgensen FS, et al. Prediction of pH-dependent aqueous solubility of druglike molecules. J Chem Inf Model. 2006;46:2601-2609.

93. Jorgensen WL, Duffy EM. Prediction of drug solubility from structure. Adv Drug Deliv Rev. 2002;54:355-366.

94. Faller B, Ertl P. Computational approaches to determine drug solubility. Adv Drug Deliv Rev. 2007;59:533-545.

95. Delaney JS. Predicting aqueous solubility from structure. Drug Discov Today. 2005;10:289-295.

96. Chow EC, Talattof A, Tsakalozou E, et al. Using Physiologically Based Pharmacokinetic (PBPK) Modeling to Evaluate the Impact of Pharmaceutical Excipients on Oral Drug Absorption: Sensitivity Analyses. AAPS J. 2016;18:1500-1511.

97. Willmann S, Schmitt W, Keldenich J, et al. A physiological model for the estimation of the fraction dose absorbed in humans. J Med Chem. 2004;47:4022-4031.

98. U.S. Department of Health and Human Services Food and Drug Administration Center for Drug Evaluation and Research (CDER). Waiver of In Vivo Bioavailability and Bioequivalence Studies for Immediate-Release Solid Oral Dosage Forms Based on a Biopharmaceutics Classification System, Guidance for Industry. https://www.fda.gov/media/70963/download. Accessed 08.05.2019.

99. Augustijns P, Wuyts B, Hens B, et al. A review of drug solubility in human intestinal fluids: implications for the prediction of oral absorption. Eur J Pharm Sci. 2014;57:322-332. doi: 10.1016/j.ejps.2013.08.027.

100. Bergström CA, Holm R, Jørgensen SA, et al. Early pharmaceutical profiling to predict oral drug absorption: current status and unmet needs. Eur J Pharm Sci. 2014;57:173-199. doi: 10.1016/j.ejps.2013.10.015.

101. Kou D, Dwaraknath S, Fischer Y, et al. Biorelevant Dissolution Models for a Weak Base To Facilitate Formulation Development and Overcome Reduced Bioavailability Caused by Hypochlordyria or Achlorhydria. Mol Pharm. 2017;14:3577-3587. doi: 10.1021/acs.molpharmaceut.7b00593.

102. Mercuri A, Wu S, Stranzinger S, et al. In vitro and in silico characterisation of Tacrolimus released under biorelevant conditions. Int J Pharm. 2016;515:271-280. doi: 10.1016/j.ijpharm.2016.10.020.

103. Ottaviani G, Wendelspiess S, Alvarez-Sánchez R. Importance of critical micellar concentration for the prediction of solubility enhancement in biorelevant media. Mol Pharm. 2015;12:1171-1179. doi: 10.1021/mp5006992.

104. Anand O, Yu LX, Conner DP, et al. Dissolution testing for generic drugs: an FDA perspective. AAPS J. 2011;13:328-335. doi: 10.1208/s12248-011-9272-y.

105. Jakubiak P, Wagner B, Grimm HP, et al. Development of a Unified Dissolution and Precipitation Model and Its Use for the Prediction of Oral Drug Absorption. Mol Pharm. 2016;13:586-598. doi: 10.1021/acs.molpharmaceut.5b00808.

106. Costa P, Sousa Lobo JM. Modeling and comparison of dissolution profiles. Eur J Pharm Sci. 2001;13:123-133.

107. Particle Sciences- Drug development services. In Vitro Dissolution Testing for solid oral dosage forms. Technical Brief. 2010:5.

108. Duque MD, Issa MG, Silva DA, et al. Intrinsic dissolution simulation of highly and poorly soluble drugs for BCS solubility classification. Dissolut. Technol. 2017;6-11. dx.doi.org/10.14227/DT240417P6.

109. Laksitorini M, Prasasty VD, Kiptoo PK, et al. Pathways and Progress in Improving Drug Delivery through the Intestinal Mucosa and Blood-Brain Barriers. Ther Deliv. 2014;5:1143–1163. doi: 10.4155/tde.14.67.

110. Deli MA. Potential use of tight junction modulators to reversibly open membranous barriers and improve drug delivery. Biochim Biophys Acta. 2009;1788:892-910. doi: 10.1016/j.bbamem.2008.09.016.

111. Lee Y, Choi SQ. Quantitative analysis for lipophilic drug transport through a model lipid membrane with membrane retention. Eur J Pharm Sci. 2019;134:176-184. doi: 10.1016/j.ejps.2019.04.020.

112. Zhu C, Jiang L, Chen TM, et al. A comparative study of artificial membrane permeability assay for high throughput profiling of drug absorption potential. Eur J Med Chem. 2002;37:399-407.

113. Pang KS. Modeling of intestinal drug absorption: roles of transporters and metabolic enzymes (for the Gillette Review Series). Drug Metab Dispos. 2003;31:1507-1519.

114. Bennion BJ, Be NA, McNerney MW, et al. Predicting a Drug's Membrane Permeability: A Computational Model Validated With in Vitro Permeability Assay Data. J Phys Chem B. 2017;121:5228-5237. doi: 10.1021/acs.jpcb.7b02914.

115. Bergström CAS, Charman WN, Porter CJH, et al. Computational prediction of formulation strategies for beyond-rule-of-5 compounds. Adv Drug Deliv Rev. 2016;101:6-21. doi: 10.1016/j.addr.2016.02.005.

116. Hetal PT, Jagruti LD. Influence of excipients on drug absorption via modulation of intestinal transporters activity. Asian J Pharmaceutics. 2015;9:69-82. doi: 10.4103/0973-8398.154688.

117. de Gooijer MC, Zhang P, Weijer R, Buil LCM, Beijnen JH, van Tellingen O. The impact of P-glycoprotein and breast cancer resistance protein on the brain pharmacokinetics and pharmacodynamics of a panel of MEK inhibitors. Int J Cancer. 2018;142:381-391. doi: 10.1002/ijc.31052.

118. Porat D, Dahan A. Active intestinal drug absorption and the solubility-permeability interplay. Int J Pharm. 2018;537:84-93. doi: 10.1016/j.ijpharm.2017.10.058.

119. Robinson AN, Tebase BG, Francone SC, et al. Co-expression of ABCB1 and ABCG2 in a Cell Line Model Reveals Both Independent and Additive Transporter Function. Drug Metab Dispos. 2019. pii: dmd.118.086181. doi: 10.1124/dmd.118.086181.

120. Safar Z, Kis E, Erdo F, et al. ABCG2/BCRP: variants, transporter interaction profile of substrates and inhibitors. Expert Opin Drug Metab Toxicol. 2019;15:313-328. doi: 10.1080/17425255.2019.1591373.

121. Harwood M, Zhang M, Pathak S, et al. The regional-specific relative and absolute expression of gut transporters in adult Caucasians: A meta-analysis. Drug Metab Dispos. 2019. pii: dmd.119.086959. doi: 10.1124/dmd.119.086959.

122. Marchitti SA, Mazur CS, Dillingham CM, et al. Inhibition of the Human ABC Efflux Transporters P-gp and BCRP by the BDE-47 Hydroxylated Metabolite 6-OH-BDE-47: Considerations for Human Exposure. Toxicol Sci. 2017;155:270-282. doi: 10.1093/toxsci/kfw209.

123. Antoine D, Pellequer Y, Tempesta C, et al. Biorelevant media resistant co-culture model mimicking permeability of human intestine. Int J Pharm. 2015;481:27-36. doi: 10.1016/j.ijpharm.2015.01.028.

124. Kataoka M, Tsuneishi S, Maeda Y, et al. A new in vitro system for evaluation of passive intestinal drug absorption: establishment of a double artificial membrane

permeation assay. Eur J Pharm Biopharm. 2014;88:840-846. doi: 10.1016/j.ejpb.2014.09.009.

125. van Breemen RB, Li Y. Caco-2 cell permeability assays to measure drug absorption. Expert Opin Drug Metab Toxicol. 2005;1:175-185.

126. Press B, Di Grandi D. Permeability for intestinal absorption: Caco-2 assay and related issues. Curr Drug Metab. 2008;9:893-900.

127. Reis JM, Sinkó B, Serra CH. Parallel artificial membrane permeability assay (PAMPA) - Is it better than Caco-2 for human passive permeability prediction? Mini Rev Med Chem. 2010;10:1071-1076.

128. Jin X, Luong TL, Reese N, et al. Comparison of MDCK-MDR1 and Caco-2 cell based permeability assays for anti-malarial drug screening and drug investigations. J Pharmacol Toxicol Methods. 2014;70:188-194. doi: 10.1016/j.vascn.2014.08.002.

129. Volpe DA. Drug-permeability and transporter assays in Caco-2 and MDCK cell lines. Future Med Chem. 2011;3:2063-2077. doi: 10.4155/fmc.11.149.

130. Tavelin S, Taipalensuu J, Hallböök F, et al. An improved cell culture model based on 2/4/A1 cell monolayers for studies of intestinal drug transport: characterization of transport routes. Pharm Res. 2003;20:373-381.

131. Doluisio JT, Billups NF, Dittert LW, et al. Drug absorption. I. An in situ rat gut technique yielding realistic absorption rates. J Pharm Sci. 1969;58:1196-1200.

132. Patel N, Forbes B, Eskola S, et al. Use of simulated intestinal fluids with Caco-2 cells and rat ileum. Drug Dev Ind Pharm. 2006;32:151-161.

133. Zheng W, Jain A, Papoutsakis D, et al. Selection of oral bioavailability enhancing formulations during drug discovery. Drug Dev Ind Pharm. 2012;38:235-247. doi: 10.3109/03639045.2011.602406.

134. Gupta S, Kesarla R, Omri A. Formulation strategies to improve the bioavailability of poorly absorbed drugs with special emphasis on self-emulsifying systems. ISRN Pharm. 2013;2013:848043. doi: 10.1155/2013/848043.

135. Savjani KT1, Gajjar AK, Savjani JK. Drug solubility: importance and enhancement techniques. ISRN Pharm. 2012;2012:195727. doi: 10.5402/2012/195727.

136. Shekhawat P, Pokharkar V. Understanding peroral absorption: regulatory aspects and contemporary approaches to tackling solubility and permeability hurdles. Acta Pharm Sin B. 2017;7:260-280. doi: 10.1016/j.apsb.2016.09.005.

137. Kollipara S, Gandhi RK. Pharmacokinetic aspects and in vitro-in vivo correlation potential for lipid-based formulations. Acta Pharm Sin B. 2014;4:333-349. doi: 10.1016/j.apsb.2014.09.001.

138. Stepensky D. Use of unbound volumes of drug distribution in pharmacokinetic calculations. Eur J Pharm Sci. 2011;42:91-98. doi: 10.1016/j.ejps.2010.10.011.

139. Ruark CD, Hack CE, Robinson PJ, et al. Predicting passive and active tissue:plasma partition coefficients: interindividual and interspecies variability. J Pharm Sci. 2014;103:2189-2198. doi: 10.1002/jps.24011.

140. Mariappan TT, Mandlekar S, Marathe P. Insight into tissue unbound concentration: utility in drug discovery and development. Curr Drug Metab. 2013;14:324-340.

141. Smith DA, Di L, Kerns EH. The effect of plasma protein binding on in vivo efficacy: misconceptions in drug discovery. Nat Rev Drug Discov. 2010;9:929-939. doi: 10.1038/nrd3287.

142. Mueller M, de la Peña A, Derendorf H. Issues in pharmacokinetics and pharmacodynamics of anti-infective agents: kill curves versus MIC. Antimicrob Agents Chemother. 2004;48:369-377.

143. Mouton JW, Theuretzbacher U, Craig WA, et al. Tissue concentrations: do we ever learn? J Antimicrob Chemother. 2008;61:235-237.

144. Yates JW, Arundel PA. On the volume of distribution at steady state and its relationship with two-compartmental models. J Pharm Sci. 2008;97:111-122.

145. De Buck SS, Sinha VK, Fenu LA, et al. The prediction of drug metabolism, tissue distribution, and bioavailability of 50 structurally diverse compounds in rat using mechanism-based absorption, distribution, and metabolism prediction tools. Drug Metab Dispos. 2007;35:649-659.

146. Lombardo F, Berellini G, Obach RS. Trend Analysis of a Database of Intravenous Pharmacokinetic Parameters in Humans for 1352 Drug Compounds. Drug Metab Dispos. 2018;46:1466-1477. doi: 10.1124/dmd.118.082966.

147. Berellini G, Springer C, Waters NJ, et al. In silico prediction of volume of distribution in human using linear and nonlinear models on a 669 compound data set. J Med Chem. 2009;52:4488-4495. doi: 10.1021/jm9004658.

148. Keldenich J. Prediction of human clearance (CL) and volume of distribution (VD). Drug Discov Today Technol. 2004;1:389-395. doi: 10.1016/j.ddtec.2004.10.007.

149. Sui X, Sun J, Li H, et al. Prediction of volume of distribution values in human using immobilized artificial membrane partitioning coefficients, the fraction of compound ionized and plasma protein binding data. Eur J Med Chem. 2009;44:4455-4460. doi: 10.1016/j.ejmech.2009.06.004.

150. Palleria C, Di Paolo A, Giofrè C, et al. Pharmacokinetic drug-drug interaction and their implication in clinical management. J Res Med Sci. 2013;18:601-610.

151. Yang F, Zhang Y, Liang H. Interactive association of drugs binding to human serum albumin. Int J Mol Sci. 2014;15:3580-3595. doi: 10.3390/ijms15033580.

152. Ignjatovic V, Lai C, Summerhayes R, et al. Age-related differences in plasma proteins: how plasma proteins change from neonates to adults. PLoS One. 2011;6:e17213. doi: 10.1371/journal.pone.0017213.

153. Grainger-Rousseau TJ, McElnay JC, Collier PS. The influence of disease on plasma protein binding of drugs. Int J Pharm. 1989;54:1-13.

154. Keller F, Maiga M, Neumayer HH, et al. Pharmacokinetic effects of altered plasma protein binding of drugs in renal disease. Eur J Drug Metab Pharmacokinet. 1984;9:275-282.

155. McNamara PJ, Meiman D. Predicting Drug Binding to Human Serum Albumin and Alpha One Acid Glycoprotein in Diseased and Age Patient Populations. J Pharm Sci. 2019. pii: S0022-3549(19)30167-4. doi: 10.1016/j.xphs.2019.03.018.

156. Barrail A, Le Tiec C, Paci-Bonaventure S, et al. Determination of amprenavir total and unbound concentrations in plasma by high-performance liquid chromatography and ultrafiltration. Ther Drug Monit. 2006;28:89-94.

157. Shippenberg TS, Thompson AC. Overview of microdialysis. Curr Protoc Neurosci. 2001;7:7.1. doi: 10.1002/0471142301.ns0701s00.

158. Hammarlund-Udenaes M. Microdialysis as an Important Technique in Systems Pharmacology-a Historical and Methodological Review. AAPS J. 2017;19:1294-1303. doi: 10.1208/s12248-017-0108-2.

159. Schuhmacher J, Kohlsdorfer C, Bühner K, et al. High-throughput determination of the free fraction of drugs strongly bound to plasma proteins. J Pharm Sci. 2004;93:816-830.

160. Longhi R, Corbioli S, Fontana S, et al. Brain tissue binding of drugs: evaluation and validation of solid supported porcine brain membrane vesicles (TRANSIL) as a novel high-throughput method. Drug Metab Dispos. 2011;39:312-321. doi: 10.1124/dmd.110.036095.

161. Hinderling PH. Red blood cells: a neglected compartment in pharmacokinetics and pharmacodynamics. Pharmacol Rev. 1997;49:279-295.

162. Smith DA, Beaumont K, Maurer TS, et al. Clearance in Drug Design. J Med Chem. 2019;62:2245-2255. doi: 10.1021/acs.jmedchem.8b01263.

163. Iyanagi T. Molecular mechanism of phase I and phase II drug-metabolizing enzymes: implications for detoxification. Int Rev Cytol. 2007;260:35-112.

164. Dhaneshwar S, Jain A, Tewari K. Design and applications of bioprecursors: a retrometabolic approach. Curr Drug Metab. 2014;15:291-325.

165. Zeng M, Yang L, He D, et al. Metabolic pathways and pharmacokinetics of natural medicines with low permeability. Drug Metab Rev. 2017;49:464-476. doi: 10.1080/03602532.2017.1377222.

166. Roberts MS, Magnusson BM, Burczynski FJ, et al. Enterohepatic circulation: physiological, pharmacokinetic and clinical implications. Clin Pharmacokinet. 2002;41:751-790.

167. Anzenbacher P, Anzenbacherová E. Cytochromes P450 and metabolism of xenobiotics. Cell Mol Life Sci. 2001;58:737-747.

168. Walther R, Rautio J, Zelikin AN. Prodrugs in medicinal chemistry and enzyme prodrug therapies. Adv Drug Deliv Rev. 2017;118:65-77. doi: 10.1016/j.addr.2017.06.013.

169. Abet V, Filace 1, Recio J ,et al. Prodrug approach: An overview of recent cases. Eur J Med Chem. 2017;127:810-827. doi: 10.1016/j.ejmech.2016.10.061.

170. van Leeuwen RW, van Gelder T, Mathijssen RH, et al. Drug-drug interactions with tyrosine-kinase inhibitors: a clinical perspective. Lancet Oncol. 2014;15:e315-26. doi: 10.1016/S1470-2045(13)70579-5.

171. Jancova P, Anzenbacher P, Anzenbacherova E. Phase II drug metabolizing enzymes. Biomed Pap Med Fac Univ Palacky Olomouc Czech Repub. 2010;154:103-116.

172. Perucca E. Age-related changes in pharmacokinetics: predictability and assessment methods. Int Rev Neurobiol. 2007;81:183-199.

173. Weiss M1. Analysis of metabolite formation pharmacokinetics after intravenous and oral administration of the parent drug using inverse Laplace transformation. Drug Metab Dispos. 1998;26:562-565.

174. Grime KH, Bird J, Ferguson D, et al. Mechanism-based inhibition of cytochrome P450 enzymes: an evaluation of early decision making in vitro approaches and drug-drug interaction prediction methods. Eur J Pharm Sci. 2009;36:175-191. doi: 10.1016/j.ejps.2008.10.002.

175. Heikkinen AT, Fowler S, Gray L, et al. In vitro to in vivo extrapolation and physiologically based modeling of cytochrome P450 mediated metabolism in beagle dog gut wall and liver. Mol Pharm. 2013;10:1388-1399. doi: 10.1021/mp300692k.

176. Bruinsma BG, Sridharan GV, Weeder PD, et al. Metabolic profiling during ex vivo machine perfusion of the human liver. Sci Rep. 2016;6:22415. doi: 10.1038/srep22415.

177. Gómez-Lechón MJ, Donato MT, Castell JV, et al. Human hepatocytes as a tool for studying toxicity and drug metabolism. Curr Drug Metab. 2003;4:292-312.

178. Martignoni M, Groothuis GM, de Kanter R. Species differences between mouse, rat, dog, monkey and human CYP-mediated drug metabolism, inhibition and induction. Expert Opin Drug Metab Toxicol. 2006;2:875-894.

179. Levy G. Pharmacokinetics in renal disease. Am J Med. 1977;62:461-465.

180. Jones GR. Estimating renal function for drug dosing decisions. Clin Biochem Rev. 2011;32:81-88.

181. Talal AH, Venuto CS, Younis I. Assessment of Hepatic Impairment and Implications for Pharmacokinetics of Substance Use Treatment. Clin Pharmacol Drug Dev. 2017;6:206-212. doi: 10.1002/cpdd.336.

182. Dymond AW, Martin P, So K, et al. Pharmacokinetics of a Single Oral Dose of the MEK1/2 Inhibitor Selumetinib in Subjects With End-Stage Renal Disease or Varying Degrees of Hepatic Impairment Compared With Healthy Subjects. J Clin Pharmacol. 2017;57:592-605. doi: 10.1002/jcph.848.

183. U.S. Department of Health and Human Services Food and Drug Administration Center for Drug Evaluation and Research (CDER). Pharmacokinetics in Patients with Impaired Renal Function — Study Design, Data Analysis, and Impact on Dosing and Labeling, Guidance for Industry. https://www.fda.gov/media/78573/download. Accessed 08.05.2019.

184. Varma MV, Pang KS, Isoherranen N, et al. Dealing with the complex drug-drug interactions: towards mechanistic models. Biopharm Drug Dispos. 2015;36:71-92. doi: 10.1002/bdd.1934.

185. Hussaarts KGAM, Veerman GDM, Jansman FGA, et al. Clinically relevant drug interactions with multikinase inhibitors: a review. Ther Adv Med Oncol. 2019;11:1758835918818347. doi: 10.1177/1758835918818347.

186. Banerji U, Camidge DR, Verheul HM, et al. The first-in-human study of the hydrogen sulfate (Hyd-sulfate) capsule of the MEK1/2 inhibitor AZD6244 (ARRY-142886): a phase I open-label multicenter trial in patients with advanced cancer. Clin Cancer Res. 2010;16:1613-1623. doi: 10.1158/1078-0432.CCR-09-2483.

187. Mocellin S, Pilati P, Lise M, et al. Meta-analysis of hepatic arterial infusion for unresectable liver metastases from colorectal cancer: the end of an era? J Clin Oncol. 2007;25:5649-5654.

188. Karlsson Lind L, von Euler M, Korkmaz S, et al. Sex differences in drugs: the development of a comprehensive knowledge base to improve gender awareness prescribing. Biol Sex Differ. 2017;8:32. doi: 10.1186/s13293-017-0155-5.

189. de Man FM, Veerman GDM, Oomen-de Hoop E, et al. Comparison of toxicity and effectiveness between fixed-dose and body surface area-based dose capecitabine. Ther Adv Med Oncol. 2019;11:1758835919838964. doi: 10.1177/1758835919838964.

190. Ilich AI, Danilak M, Kim CA, et al. Effects of gender on capecitabine toxicity in colorectal cancer. J Oncol Pharm Pract. 2016;22:454-460. doi: 10.1177/1078155215587345.

191. Reeve E, Wiese MD, Mangoni AA. Alterations in drug disposition in older adults. Expert Opin Drug Metab Toxicol. 2015;11:491-508. doi: 10.1517/17425255.2015.1004310.

192. Czejka M, Sahmanovic A, Buchner P, et al. Disposition of Erlotinib and Its Metabolite OSI420 in a Patient with High Bilirubin Levels. Case Rep Oncol. 2013;6:602-608. doi: 10.1159/000357211.

193. Twelves C, Glynne-Jones R, Cassidy J, et al. Effect of hepatic dysfunction due to liver metastases on the pharmacokinetics of capecitabine and its metabolites. Clin Cancer Res. 1999;5:1696-1702.

194. Lam SW, Guchelaar HJ, Boven E. The role of pharmacogenetics in capecitabine efficacy and toxicity. Cancer Treat Rev. 2016;50:9-22. doi: 10.1016/j.ctrv.2016.08.001.

195. Parrott NJ, Yu LJ, Takano R, et al. Physiologically Based Absorption Modeling to Explore the Impact of Food and Gastric pH Changes on the Pharmacokinetics of Alectinib. AAPS J. 2016;18:1464-1474.

196. Pouton CW. Formulation of poorly water-soluble drugs for oral administration: physicochemical and physiological issues and the lipid formulation classification system. Eur J Pharm Sci. 2006;29:278-287.

197. Stegemann S, Leveiller F, Franchi D, et al. When poor solubility becomes an issue: from early stage to proof of concept. Eur J Pharm Sci. 2007;31:249-261.

198. Porter CJ, Trevaskis NL, Charman WN. Lipids and lipid-based formulations: optimizing the oral delivery of lipophilic drugs. Nat Rev Drug Discov. 2007;6:231-248.

199. Gruber-Rouh T, Marko C, Thalhammer A, et al. Current strategies in interventional oncology of colorectal liver metastases. Br J Radiol. 2016;89:20151060. doi: 10.1259/bjr.20151060.

200. Bode C. The nasty surprise of a complex drug-drug interaction. Drug Discov Today. 2010;15:391-395. doi: 10.1016/j.drudis.2010.02.013.

201. Mathijssen RH, van Alphen RJ, Verweij J, et al. Clinical pharmacokinetics and metabolism of irinotecan (CPT-11). Clin Cancer Res. 2001;7:2182-2194.

202. Blesch KS, Gieschke R, Tsukamoto Y, et al. Clinical pharmacokinetic/pharmacodynamic and physiologically based pharmacokinetic modeling in new drug development: the capecitabine experience. Invest New Drugs. 2003;21:195-223.

203. Gallo JM. Pharmacokinetic/ pharmacodynamic-driven drug development. Mt Sinai J Med. 2010;77:381-388. doi: 10.1002/msj.20193.

204. Visser SAG, Bueters TJH. Assessment of translational risk in drug research: Role of biomarker classification and mechanism-based PKPD concepts. Eur J Pharm Sci. 2017;109:72-77. doi: 10.1016/j.ejps.2017.08.006.

205. Gerretsen P, Müller DJ, Tiwari A, et al. The intersection of pharmacology, imaging, and genetics in the development of personalized medicine. Dialogues Clin Neurosci. 2009;11:363-376.

206. Knibbe CA, Danhof M. Individualized dosing regimens in children based on population PKPD modelling: are we ready for it? Int J Pharm. 2011;415:9-14. doi: 10.1016/j.ijpharm.2011.02.056.

207. Zhang X, Lionberger RA, Davit BM, et al. Utility of physiologically based absorption modeling in implementing Quality by Design in drug development. AAPS J. 2011;13:59-71. doi: 10.1208/s12248-010-9250-9.

208. Chetty M, Rose RH, Abduljalil K, et al. Applications of linking PBPK and PD models to predict the impact of genotypic variability, formulation differences, differences in target binding capacity and target site drug concentrations on drug responses and variability. Front Pharmacol. 2014;5:258. doi: 10.3389/fphar.2014.00258.

5 Aim of the thesis

The in vivo bioavailability of a drug or drug candidate is based on the physicochemical properties of the compound as well as the drug formulation, application method and -site and the physiology of the target population. DMPK, which nowadays represents an integral part in drug development, provides a wide range of tools to investigate the PK characteristics and thus also the bioavailability of a compound. There are various in vitro, in silico or in vivo methods available to predict the in vivo PK profile of a drug, but the applied method should be selected carefully in consideration of the desired outcome. Several physicochemical properties of a compound can be related to parameters in the ADME process, which describe the PK profile of a drug. It has thus become possible to predict drug PK profiles by in silico methods, based on the molecular properties of a compound and a mathematical description of the ADME steps. These PBPK models have now advanced to predict drug profiles in various physiologies, including several application methods or formulations. The aim of this work was to evaluate the impact of influences derived from variations in physiology, formulation or administration site or -method on the bioavailability of selected drugs. The four investigated antineoplastic compounds, erlotinib, selumetinib, capecitabine and irinotecan, were selected as role models to demonstrate the impact of these influences on their bioavailability.

Erlotinib is an orally administered TKI and exhibits a high inter-patient variability in the PK profiles of patients. The compound is characterized by a pH-sensitive absorption, with low aqueous solubility in a higher pH range, hence the concomitant administration of acid reducing agents can alter the absorption and result in plasma concentrations below the therapeutic threshold. The interaction was detected by analysis of patient data but is however not solely responsible for the observed variability in plasma concentrations. We wanted to investigate if the observed DDI could be predicted more easily by a PBPK model, based on the physicochemical properties of erlotinib, before administration to a patient and if the model can elucidate the main mechanisms responsible for the inter-patient variability.

Selumetinib, another orally administered TKI, which is currently in phase III investigations, exhibits similar molecular properties as erlotinib but has a low aqueous solubility over the whole physiological pH-range, which limits the absorption and

consequently the bioavailability of the drug. It has thus been administered to patients in formulations containing excipients to enhance its absorption. We wanted to illustrate the impact of the deployed excipients on the PK profile of the compound and highlight the application of in silico tools in formulation development.

Capecitabine was designed as triple prodrug of the chemotherapeutic drug 5-fluorouracil and as such exhibits an extensive metabolic cascade. TEAEs of capecitabine have been observed to increase when combined with other cytotoxic agents. Insights were therefore required concerning underlying mechanisms leading to the high number of TEAEs and the observed variability in plasma concentrations of patients, to detect if these events were based on a DDI or an accumulation of side effects. Additionally, several genetic polymorphisms have been identified in capecitabine metabolizing enzymes, however their exact influence on the safety and efficacy of capecitabine treatment has not yet been reported. We therefore wanted to elucidate the impact of physiological differences and influences in the metabolic cascade on the PK profile of capecitabine and its metabolites in plasma, liver and tumor tissue.

Irinotecan, a prodrug of the active moiety SN-38 is a well-established chemotherapeutic agent and is used in treatments for various solid cancers but causes numerous toxicities of which many can be related to the SN-38 presence in the systemic circulation. A new application method was therefore proposed for the treatment of colorectal liver metastases, which includes hepatic arterial infusion instead of systemic infusion as well as the use of embolization particles to increase SN-38 concentrations in tumor tissue and simultaneously decrease its systemic exposure. The purpose of the investigation was to analyze irinotecan and SN-38 concentrations in liver, tumor and plasma samples in an animal model to illustrate the differences that result from the varying application methods and routes, including the use of two different embolization particles. Additionally, we wanted to evaluate the individual antitumoral effect of each application method and their applicability in clinical routine.

6 Results

6.1 Original articles and manuscripts

Gruber A, Czejka M, Buchner P, Kitzmueller M, Kirchbaumer Baroian N, Dittrich C, Sahmanovic Hrgovcic A. Monitoring of erlotinib in pancreatic cancer patients during long-time administration and comparison to a physiologically based pharmacokinetic model. Cancer Chemother Pharmacol. 2018;81:763-771. doi: 10.1007/s00280-018-3545-4.

Kauffels A, Kitzmüller M, Gruber A, Nowack H, Bohnenberger H, Spitzner M, Kuthning A, Sprenger T, Czejka M, Ghadimi M, Sperling J. Hepatic arterial infusion of irinotecan and EmboCept® S results in high tumor concentration of SN-38 in a rat model of colorectal liver metastases. Clin Exp Metastasis. 2019;36:57-66. doi: 10.1007/s10585-019-09954-5.

I performed HPLC analyses of plasma and tissue samples for irinotecan and SN-38 quantification.

Gruber A, Czejka M. Physiologically based pharmacokinetic modeling of the MEK 1/2 inhibitor selumetinib: impact of pharmaceutical formulation and co-variates on the plasma disposition. AAPS PharmSciTech. (Impact factor 2.666).

Submitted: May 2019.

Gruber A, Czejka M, Dittrich C. Pharmacokinetic modeling of the sequential metabolism of capecitabine to 5-fluorouracil (5FU) for evaluation of influencing factors on 5FU disposition in plasma, liver and tumor tissue and assessment of related toxicities. Cancer Chemother Pharmacol. (Impact factor 2.808).

Submitted: May 2019.

6.1.1 Erlotinib

Monitoring of erlotinib in pancreatic cancer patients during long-time administration and comparison to a physiologically based pharmacokinetic model.

Gruber A, Czejka M, Buchner P, Kitzmueller M, Kirchbaumer Baroian N, Dittrich C, Sahmanovic Hrgovcic A.

Cancer Chemother Pharmacol. 2018

Cancer Chemotherapy and Pharmacology (2018) 81:763–771
https://doi.org/10.1007/s00280-018-3545-4

ORIGINAL ARTICLE

Monitoring of erlotinib in pancreatic cancer patients during long-time administration and comparison to a physiologically based pharmacokinetic model

Andrea Gruber[1] · Martin Czejka[1,3] · Philipp Buchner[1,3] · Marie Kitzmueller[1] · Nairi Kirchbaumer Baroian[1] · Christian Dittrich[2] · Azra Sahmanovic Hrgovcic[1]

Received: 25 January 2018 / Accepted: 12 February 2018 / Published online: 16 February 2018

Abstract

Purpose In this study, a therapeutic drug monitoring (TDM) of erlotinib in pancreatic cancer patients was performed over 50 weeks to reveal possible alterations in erlotinib plasma concentrations. Additionally, a physiologically based pharmacokinetic (PBPK) model was created to assess such variations in silico.

Methods Patients with advanced pancreatic cancer received a chemotherapeutic combination of 100 mg erlotinib q.d., 500–900 mg capecitabine b.d. and 5 mg/kg bevacizumab q.2wks. Samples were analyzed by HPLC and the results were compared to a PBPK model, built with the software GastroPlus™ and based on calculated and literature data.

Results The erlotinib plasma concentrations did not show any accumulation, but displayed a high inter-patient variability over the whole investigated period. Trough plasma concentrations ranged from 0.04 to 1.22 µg/ml after day 1 and from 0.01 to 2.4 µg/ml in the long-term assessment. 7% of the patients showed concentrations below the necessary activity threshold of 0.5 µg/ml during the first week. The impact of some co-variates on the pharmacokinetic parameters C_{max} and $AUC_{0–24}$ were shown in a PBPK model, including food effects, changes in body weight, protein binding or liver function and the concomitant intake of gastric acid reducing agents (ARAs).

Conclusion This study presents the approach of combining TDM and PBPK modeling for erlotinib, a drug with a high interaction potential. TDM is an important method to monitor drugs with increased inter-patient variability, additionally, the PBPK model contributed valuable insights to the interaction mechanisms involved, resulting in an effective combination from a PK perspective to ensure a safe treatment.

Keywords Erlotinib · Long-time administration · Therapeutic drug monitoring · Interaction assessment · PBPK model

Introduction

Erlotinib (Tarceva®, OSI Pharmaceuticals, Melville, NY, USA; Roche, Basel, Switzerland; Genetech, South San Francisco, USA) is a potent and reversible inhibitor of the epidermal growth factor receptor (EGFR) tyrosine kinase and has been approved for the treatment of patients with metastatic non-small cell lung cancer and the treatment of patients with locally advanced, unresectable or metastatic pancreatic cancer, in combination with gemcitabine [1, 2]. It is available as a 25, 100 or 150 mg tablet and is given once daily at a fixed dose. The combination of erlotinib with capecitabine, bevacicumab or oxaliplatinum has been under investigation in the treatment of advanced pancreatic cancer [3, 4].

As a weak base, erlotinib quickly dissolves in the gastric acid of the stomach, but shows limited solubility at a

✉ Andrea Gruber
andrea.gruber@univie.ac.at

1 Division of Clinical Pharmacy and Diagnostics, Faculty of Life Sciences, University of Vienna, Althanstrasse 14, 1090 Vienna, Austria

2 Applied Cancer Research - Institution for Translational Research Vienna (ACR-ITR VIEnna) and Ludwig Boltzmann Institute for Applied Cancer Research (LBI-ACR VIEnna), Centre for Oncology and Hematology, Kaiser Franz Josef-Spital, Bernardgasse 24/2, 1070 Vienna, Austria

3 Austrian Society of Applied Pharmacokinetics, Krottenbachstrasse 184, 1190 Vienna, Austria

pH above its pKa value of 5.4. Therefore, a physicochemical interaction with co-administered acid reducing agents (ARAs), increasing the gastric pH, is very likely to occur and has been reported before [5–7]. However, as a recent study showed, the negative influence of ARAs on erlotinib absorption can be diminished by drinking acidic beverages [8]. Erlotinib is well absorbed with mean peak plasma levels of 2–4 h after oral ingestion, resulting in an estimated bioavailability of 60% [1, 9]. Since the absorption of erlotinib can be influenced by food, its bioavailability is considered unpredictable after absorption to a fed state and can vary from 60 to 100% [1]. Hence, the intake of erlotinib is recommended to a minimum of 2 h after and 1 h before a meal. Due to its high lipophilicity, erlotinib is highly bound to plasma proteins at approximately 95%, mainly to albumin and α-1 acid glycoprotein [10], therefore the concomitant administration of drugs with high plasma protein binding can lead to altered unbound erlotinib plasma concentrations [11]. Erlotinib is primarily metabolized by CYP3A4 and to a minor extent by CYP1A2 and CYP1A1. A pre- or co-treatment with CYP3A4 inducers or inhibitors can alter the bioavailability of erlotinib and should thus be avoided during the treatment with erlotinib [12, 13]. Smokers should be advised to stop smoking during erlotinib therapy, due to a CYP induction and hence reduced plasma concentrations in comparison to non-smokers [14]. Gender aspects have been investigated, but resulted in a non-significant difference [15].

Due to the various possible pharmacokinetic interactions, plasma concentrations of erlotinib have been reported to show a high inter-patient variability [16]. In this study, the primary endpoint was to conduct a TDM of erlotinib over a long-time period to evaluate possible undesired changes in plasma concentrations. TDM is an effective tool in routine cancer care to reveal therapeutic interferences and to ensure that plasma concentrations of a drug are above the necessary threshold [17–19]. However, TDM is expensive and in case the influential co-variates on the plasma disposition are known, it would be easier and more economical to predict the concentration profile in a defined patient by a suitable software. In silico methods have shown to be of assistance in the drug development process since many years, but their support in later stages has been promoted only more recently [20–22]. Hence, the secondary objective of this study was to create a physiologically based pharmacokinetic (PBPK) model to predict a concentration–time curve with the software GastroPlus™ and use it to identify characteristics that may lead to altered erlotinib plasma concentrations, such as variations in body weight, liver function, certain co-medication or drug administration to a fasted or fed state.

Methods

Erlotinib study

Study population

Patients eligible for this phase 1b study suffered from histologically or cytologically documented adenocarcinoma of the pancreas with locally advanced not radically resectable or metastatic disease. Inclusion criteria for this study were ECOG performance status 0–2, age ≥ 18 years, life expectancy of ≥ 12 weeks, adequate bone marrow function (absolute neutrophil count (ANC) ≥ 1.5×10^9/l, platelet count ≥ 100×10^9/l, hemoglobin (Hb) ≥ 9 g/dl) adequate liver function (serum (total) bilirubin ≤ 3 × upper limit of normal (ULN), aspartate aminotransferase (AST), alanine aminotransferase (ALT) ≤ 2.5/5 × ULN (patients without/with liver metastases), albumin ≥ 25 g/l) and adequate renal function (serum creatinine ≤ 2 × ULN or creatinine clearance ≥ 50 ml/min). Patients must not have been treated for metastatic or locally advanced diseases, but were allowed prior adjuvant radiotherapy and previous adjuvant chemotherapy, excluding the three therapeutic agents used in this trial, capecitabine, erlotinib and bevacizumab. Amongst several further exclusion criteria, the most important were history or evidence of not controlled brain metastases or seizures, major surgical procedure planned within 28 days prior to study treatment, pregnant or lactating females or evidence of any disease or metabolic dysfunction that contradicts the use of the investigational drugs or puts the patient at high risk from treatment complications. All concomitant medication was reported and the intake of drugs inhibiting or inducing CYP3A4 was prohibited during the study, along with medication specifically contraindicated to one of the three study drugs [1, 23, 24]. All patients were asked to keep a diary during their treatment, containing co-medication and health status to retrace possible interactions and treatment failures.

Study design

The study was originally designed to evaluate the PK performance of erlotinib in the combination therapy of erlotinib, capecitabine and bevacizumab over a week, before the amendment for an evaluation of erlotinib plasma concentration over a longer period was approved by the Ethical Committee of the City of Vienna (vote EK 08-159-0908, EudraCT number 2008-004444-36) as a separate amendment to the clinical study protocol. Patients had been informed about the aim of this investigation and had given their written consent. The patients were divided into

4 dose levels, with constant erlotinib (100 mg, p.o., q.d.) and bevacizumab doses (5 mg/kg, i.v., q2wks), but different capecitabine doses (500, 650, 800, 900 mg, p.o., b.d.). Serial blood samples were obtained on day 1 pre-dose, 1, 2, 3, 4, 5, 6, 8 and 24 h after erlotinib ingestion. Blood samples on days 2–8 were drawn pre-dose and 4 h after administration of erlotinib. Further blood samples were obtained in the long-term evaluation once a week before erlotinib ingestion, hence 24 h after the last erlotinib dose. The C_{trough} value was selected as sampling time for the pharmacokinetic monitoring of erlotinib as recommended in literature [19].

Sample preparation, analysis and PK calculations

After removing the blood cells from the samples by centrifugation (10 min for 4000 rpm), erlotinib was separated from the plasma by solid phase extraction using Oasis® HLB C18 cartridges. Erlotinib was quantified by a sensitive and selective, validated, reversed phase HPLC assay as described in the literature [25].

For the pharmacokinetic analysis of plasma concentration data on day 1, Phoenix WinNonlin version 6.2.1 software (Pharsight Corporation, a Certara™ company) was used to calculate the PK parameters C_{peak}, C_{trough}, T_{max}, $AUC_{0–24}$ as well as the volume of distribution (V_d), total body clearance (Cl_{tot}) and terminal half-life ($T_{1/2el}$). For this purpose, the noncompartmental model 303 of the WinNonlin library was chosen. From day 2 until day 8, the trough and peak concentrations were analyzed, but only the trough concentrations were evaluated until the end of the study. The parameters were calculated as arithmetic mean ± SD and the range (min–max) was calculated for comparison to the simulation output.

The statistical evaluation of the plasma data was performed using the scientific software GraphPad Prism version 6.00 for Windows (GraphPad Software, La Jolla California USA).

PBPK modeling

The erlotinib plasma concentration–time profile was created in a PBPK model using the GastroPlus™ software version 9.5. (Simulations Plus Inc., Lancaster, California, USA). A general description of the software is available in the user manual [26]. PBPK simulations differ from compartmental PK simulations in the calculation of diffusion coefficients for all compartments, for a more precise distribution of the compound into different tissues over time [27]. The physicochemical and absorption–distribution–metabolism–elimination (ADME) properties used in this model were calculated by the ADMET Predictor™ module of the software and are summarized in Table 1. Some parameters were optimized, using parameter sensitivity analysis (PSA) to obtain a good fit for the model.

Table 1 Input parameters for the erlotinib PBPK model in GastroPlus™

Parameter	Predicted value	Optimized value
Molecular weight (g/mol)	393.45	393.45
LogP (neutral)	3.13	2.7
Basic pKa	4.46	5.4
Intrinsic solubility (mg/ml)	0.078	0.0089
Solubility at pH = 2 (mg/ml)	22.44	0.40
Solubility factor	334.44	50.0
Permeability (cm/s × 10^{-4})	2.7	2.7
Fraction unbound in plasma (%)	4.57	4.57
Blood plasma ratio	0.71	0.71
Liver clearance (l/h)	40.0	4.0
FaSSIF (mg/ml)	0.003	0.003
FeSSIF (mg/ml)	0.117	0.7
Solubilization ratio	1.03E+04	8.01E+04
Particle radius/diameter (µm)	25/50	15/30
Mean precipitation time (s)	900	100

Solubility factor: ratio of the solubility of ionized to unionized drug; FaSSIF: compound solubility in intestinal fluid in fasted state; FeSSIF: compound solubility in intestinal fluid in fed state; solubilization ratio: effect of bile salt concentration in FaSSIF and FeSSIF media on solubility of the compound

Input data for the model

Tarceva® 100 mg tablets contain 109.3 mg erlotinib hydrochloride, which is equal to 100 mg erlotinib free base [1]. The properties of the erlotinib base were used as input parameters for the PBPK model. Erlotinib is a weak base and a lipophilic compound, with a good intestinal permeability. The free base is only very slightly soluble in water, but the solubility of the hydrochloride salt is higher at a lower pH, indicating that the drug will easily dissolve in the acidic environment of the stomach. With the overall low solubility and a high permeability, the drug is considered a Biopharmaceutics Classification System (BCS) class II compound [28].

Modeling strategy

The general workflow of PBPK modeling has been described in many publications and tutorials [29–31]. The preliminary model in this case was based solely on the physicochemical data from the ADMET Predictor™ module of GastroPlus™, using a human PBPK model of a standard 30-year old, healthy man, which was subsequently changed to a man of 60 years and 60 kg, corresponding to the study population. The physicochemical parameters logP,

pKa and intrinsic solubility were updated based on literature data [1, 32]. The best suited distribution model was the Lukacova model, which was chosen according to the properties of the compound for the perfusion-limited tissue distribution coefficients of erlotinib [26]. The liver clearance, calculated by ADMET Predictor™ was implemented and adjusted to match the observed Cl_{tot} in the population. Since the majority of erlotinib is metabolized in the liver, the gut metabolism was excluded in this model. Concerning the oral absorption modeling, the dissolution was best described by the Johnson model and the particle size was adapted to depict the quick dissolution of erlotinib in the acidic environment of the stomach. The selected gut physiology calculation method was the human-physiological-fasted model with the Opt logD Model SA/V 6.1 for the calculation of the absorption scale factors. Ultimately, the solubilization ratio (SR) and the mean precipitation time were optimized by PSA to fit the oral absorption. The SR is calculated by GastroPlus™ according to the solubility of the compound in simulated intestinal fluids in fasted (FaSSIF) and fed state (FeSSIF) and gives an idea on how much additional solubility can be gained through the increased intestinal bile salt concentration in a fed state [26].

The PBPK model was calculated as a single and a population simulation, whereas the population simulation was set up with 25 American patients of 50–70 years and was used as comparison to the erlotinib plasma concentrations of the population studied. The simulation output was formulated as arithmetic mean with a 90% confidence interval (CI) and the corresponding range (min–max). The single simulation of a standard patient of 60 years and 60 kg, receiving erlotinib at a fasted state was used to evaluate the impact of possible co-variates on the plasma concentration of erlotinib. The selected co-variates include ingestion of erlotinib at a fasted or fed state, changes in body weight, protein binding and liver function and the influence of a concomitant use of ARAs during the erlotinib therapy. For the fed state, the absorption model human-physiological-fed was chosen and the liver blood flow was adapted [26]. Differences in body weight, liver clearance and protein binding were considered by modifying the according parameters. The concomitant intake of ARAs was modeled by changing the stomach pH from 1.3 to 5.0 and increasing the transit time from 0.25 to 0.5 h [33].

Results

Patients characteristics

26 Patients with advanced, metastatic pancreatic cancer were selected to participate in the first week of the study. A subsequent set of 10 out of the 26 patients was chosen according to the selection criteria specified in the Methods section, to participate in the amendment of the study for a longer period. The demographics of the patients are listed in Table 2. Since there was no sign of interference from the different capecitabine doses on erlotinib plasma concentrations, the four dose levels with varying capecitabine doses, but constant bevacizumab and erlotinib doses, were pooled for the pharmacokinetic calculations. All 26 patients completed the first week of the study, but only 2 out of 10 patients completed the therapy up to 50 weeks; 8 patients were discontinued due to progression of the disease. The patients were checked upon every week concerning their performance status and 3 patients were therefore temporarily discontinued during the 50 weeks, because of toxicity and side effects.

Long time performance

The analyses of the plasma samples on day 1 showed a mean erlotinib peak concentration of 0.84 µg/ml at 2 h after administration, but revealed a high variability of $C_{peak,}$ from 0.21 to 1.82 µg/ml. The mean trough concentration at 24 h after ingestion was 0.33 µg/ml in a range of 0.04–1.22 µg/ml. The $AUC_{0–24}$ ranged from 1.23 to 36.37 µg h/ml with a mean value of 12.47 µg h/ml. With a bioavailability of 60% [1, 11], the calculated V_d is 97.86 l, the Cl_{tot} is 5.51 l/h and the mean $T_{1/2el}$ is 18.72 h. The key PK parameters are summarized in Table 3.

Based on the analyses of the first day, the parameters C_{peak} and C_{trough} were expected to illustrate a continuously high variation in the first week. The steady state was reached 6 days after the first administration with a mean C_{peak} of 1.38 µg/ml in a range of 0.11–3.24 µg/ml. The mean C_{trough} value after 6 days was 0.72 µg/ml and varied from 0.05 to 2.27 µg/ml. Although the mean C_{peak} and C_{trough} values were above the activity threshold of 0.5 µg/ml, 10 of the

Table 2 Patient demographics

Characteristics	Week 1 ($n=26$)	Week 2–50 ($n=10$)
Gender *n* (%)		
Female	14 (53.8%)	6 (60%)
Male	12 (46.2%)	4 (40%)
Age (years)		
Median (min–max)	65.5 (47–80)	65.5 (55–74)
Body weight (kg)		
Median (min–max)	68.5 (44–97)	63.0 (44–84)
Body height (cm)		
Median (min–max)	170.0 (156.0–186.0)	170.0 (156.0–186.0)
Body surface (m^2)		
Median (min–max)	1.79 (1.36–2.22)	1.69 (1.36–2.06)

Table 3 Observed and simulated PK parameters of erlotinib for day 1, 3 and 6

Time	Parameters	Dimension	Observed			Simulated		
			Mean[a]±SD	Min–max	*N*	Mean[a]	Min–max	*N*
Day 1	C_{peak}	µg/ml	0.84 ± 0.54	0.21–1.82	26	0.78	0.60–0.99	25
	C_{last}	µg/ml	0.33 ± 0.29	0.04–1.22	26	0.30	0.29–0.31	25
	T_{max}	h	2.00	1.00–8.00	26	1.89	1.20–2.90	25
	$AUC_{0–24}$	µg-h/ml	12.47 ± 9.38	1.23–36.37	26	11.47	9.57–14.07	25
	$T_{1/2el}$	h	18.72 ± 13.10	4.10–59.00	26	10.90	nc	25
	V_d	l	97.86 ± 61.72	18.00–268.09	26	67.80	nc	25
	Cl_{tot}	l/h	5.51 ± 5.73	0.47–30.09	26	4.30	nc	25
Day 3	C_{trough}	µg/ml	0.45 ± 0.37	0.003–1.51	26	0.44	0.40–0.48	25
	C_{peak}	µg/ml	1.04 ± 0.62	0.19–2.99	26	1.04	0.98–1.10	25
Day 6	C_{trough}	µg/ml	0.72 ± 0.53	0.05–2.20	26	0.51	0.46–0.56	25
	C_{peak}	µg/ml	1.38 ± 0.66	0.11–3.24	26	1.09	1.02–1.15	25

C_{peak} peak plasma concentration, C_{last} plasma concentration of the last analyzed sample, T_{max} time of peak plasma concentration, $AUC_{0–24}$ area under the curve for the time 0–24 h, $T_{1/2el}$ terminal elimination half-life, V_d volume of distribution, Cl_{tot} total body clearance, C_{trough} plasma concentration before subsequent drug ingestion, *nc* not calculable

[a]T_{max} data are expressed as median, all other PK parameters are calculated as arithmetic mean

Table 4 Mean trough concentrations ± SD (µg/ml) during long time administration of 100 mg erlotinib q.d.

Patients	Weeks	*N*	C_{trough}[a]	Min–max
Pat.1	1–15	10	1.67 ± 0.44	0.77–2.20
Pat.2[b]	1–9	9	0.16 ± 0.04	0.12–0.23
Pat.3	1–50	50	0.89 ± 0.68	0.09–2.68
Pat.4	1–8	7	0.66 ± 0.27	0.14–1.06
Pat.5[b]	1–4	4	0.37 ± 0.09	0.25–0.46
Pat.6	1–8	8	1.78 ± 0.74	0.73–3.06
Pat.7	1–9	9	1.20 ± 0.51	0.31–1.80
Pat.8[b]	1–16	16	0.27 ± 0.38	0.02–1.31
Pat.9[b]	1–50	47	0.06 ± 0.04	0.01–0.16
Pat.10[b]	1–11	11	0.16 ± 0.06	0.07–0.31

[a]All mean C_{trough} values are calculated as arithmetic mean

[b]Patients with co-medication of acid reducing agents

26 patients did not reach the threshold within 24 h after the first administration and 2 of the 26 patients never reached the threshold in the first week of erlotinib therapy. The administration of capecitabine and bevacizumab was continued for treatment purpose.

In the long-term monitoring, the erlotinib plasma concentrations did not show any significant accumulation in the blood over the whole investigated period. However, the high variability persisted throughout the rest of the study (Table 4). Mean erlotinib trough concentrations in the long-term study were calculated for each patient and ranged from 0.06 to 1.78 µg/ml. The long-term analysis showed C_{trough} values below the activity threshold for 5 of the 10 patients, who all received ARAs concomitantly. An unpaired *t* test demonstrated a statistically significant difference ($P < 0.002$) between the ARA and non-ARA group in the calculated trough concentrations.

PBPK basic model

The workflow for building, optimizing and verifying the erlotinib model is described in the "Methods" section. The preliminary model resulted in an underprediction of C_{max} and $AUC_{0–24}$ by 37 and 90%, respectively, corresponding to the observed values; hence a further optimization was necessary. Therefore, the physicochemical parameters logP, pKa, intrinsic solubility and the maximum solubility of the hydrochloride salt as well as the physiology settings and the liver clearance were adjusted. The optimized model was evaluated with in vivo data of an i.v. application of 100 mg erlotinib and resulted in an underprediction of 20% in $AUC_{0–24}$ and an overprediction of 12% for the C_{peak}, compared to the mean parameter values of the study [34]. For the modeling of the oral absorption, the dissolution and absorption models were implemented and the particle size, SR and the mean precipitation time were modified. The population simulation resulted in a slight underprediction of $AUC_{0–24}$ by 9% and C_{max} was underpredicted by 13% in comparison to the mean plasma concentration of the erlotinib study, but both values were still well within the observed concentration range as can be examined in Fig. 1.

Co-variates

Figure 2 illustrates the effect of possible co-variates on erlotinib plasma concentration. Insert a displays the comparison

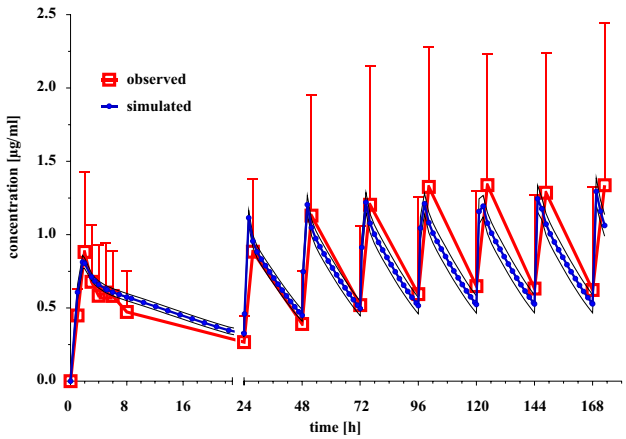

Fig. 1 Comparison of the observed mean erlotinib plasma concentration (±SD) for the days 1–8, to the simulated mean erlotinib plasma concentration (±90% CI), calculated by the population simulation model of GastroPlus™

of the mean observed concentration in patients, who received erlotinib to a fasted state, without any relevant co-medication to the predicted GastroPlus™ single simulation, matching the settings of the standard patient of the study. C_{peak} differed by 8.5% but $AUC_{0–24}$ achieved a 100% fit to the observed values, concluding that the prediction can be used for further modifications. The administration of erlotinib at a fed state, resulted in an increased bioavailability and AUC [1], as could be shown in insert b for the $AUC_{0–24}$, which increased by 12% from 14.1 to 15.8 µg h/ml. Body weight has no impact on the total body clearance of the drug [35], but has a potential effect on the C_{max} and the V_d, as shown in insert c. A reduced body weight resulted in a 16% higher C_{max} and a 25% lower V_d and the increased body weight caused a decrease in C_{max} by 20% and higher distribution into the tissue by 42%. Insert d depicts the difference in C_{max} and $AUC_{0–24}$, due to co-administered ARAs, which reduced the $AUC_{0–24}$ by 39% and C_{max} by 49% in the simulation, compared to a reduction by 52 and 56% respectively, in the study population. The physicochemical drug–drug interaction has been reported [7–9] and the PBPK model, as well as the analyses of the plasma samples of patients who received ARA co-medication in this study, support these findings. Changes in the hepatic clearance are displayed in insert e, from an elevated hepatic clearance of 10 l/h to a reduced liver clearance of 2 l/h. This range was obtained from the PK analyses of the plasma concentrations of the study. In the simulated high hepatic clearance patient, C_{max} decreased by 26% and $AUC_{0–24}$ by 55%, and in the low hepatic clearance patient C_{max} increased by 12% and $AUC_{0–24}$ by 41% in comparison to the values of the average patient. The fraction unbound of erlotinib in plasma was estimated to be 4.6%, but when changed to 10%, due to a possible pharmacokinetic interaction with a strongly protein-bound co-medication, and therefore a higher fraction unbound of erlotinib, as shown in insert f, the plasma concentration did not result as expected in a higher C_{max} and $AUC_{0–24}$, but was distributed to a higher extent into adipose and liver tissue, and resulted in a higher Cl_{tot} of 7.66 l/h and lower C_{max} and $AUC_{0–24}$ by 33 and 49%, respectively.

Discussion

TDM has shown to be beneficial in oncological patients to ensure a safe and effective treatment, especially when drugs with high inter-patient variabilities are used. To date, TDM of erlotinib has been reported up to a maximum of 30 days [4, 36]. In this study, it is the first time that erlotinib levels have been monitored closely for 1 week and further once a week for up to 50 weeks. The daily administration of erlotinib over a long-time period did not lead to drug accumulation in the central compartment. Steady state was reached within 6 days after the first erlotinib ingestion, but the variability in plasma concentrations remained high throughout the study. However, based solely on the limited knowledge about the study population, the co-variates, influencing the plasma concentrations, were difficult to deduce.

PBPK models have gained more importance with the increased progress of their features and are useful in many stages of drug development. In this case, the PBPK model was built to demonstrate the influence of co-variates on the erlotinib plasma concentration. The administration of TKIs to a fed state has often been discussed to increase the AUC and bioavailability [12], which was shown accordingly in the model. The influence of body weight on the distribution of a lipophilic compound such as erlotinib was also shown and matched our expectations, as did the differences in hepatic clearance. When a higher or lower liver clearance rate was implemented, the elimination changed accordingly. However, the simulation of an increased unbound fraction of erlotinib did not result in the expected elevated plasma concentration, but in a higher distribution into adipose and liver tissue and therefore an increased elimination and lower plasma concentration. The biggest influence though seemed to come from the concomitant intake of ARAs, which has been reported before in patients [7, 8] and healthy subjects [9]. The decreased $AUC_{0–24}$ and C_{peak} levels often result in an ineffective treatment below the activity threshold. Patients receiving both, erlotinib and ARA were advised to terminate the use of ARAs, but due to gastrointestinal side effects, some patients continued a combined intake.

In conclusion, a PBPK model can demonstrate effects of co-variates that are known in advance. However, although assumptions about possible interactions can be drawn from other drugs of the same class of compounds, the list might not be complete and some influences might still be

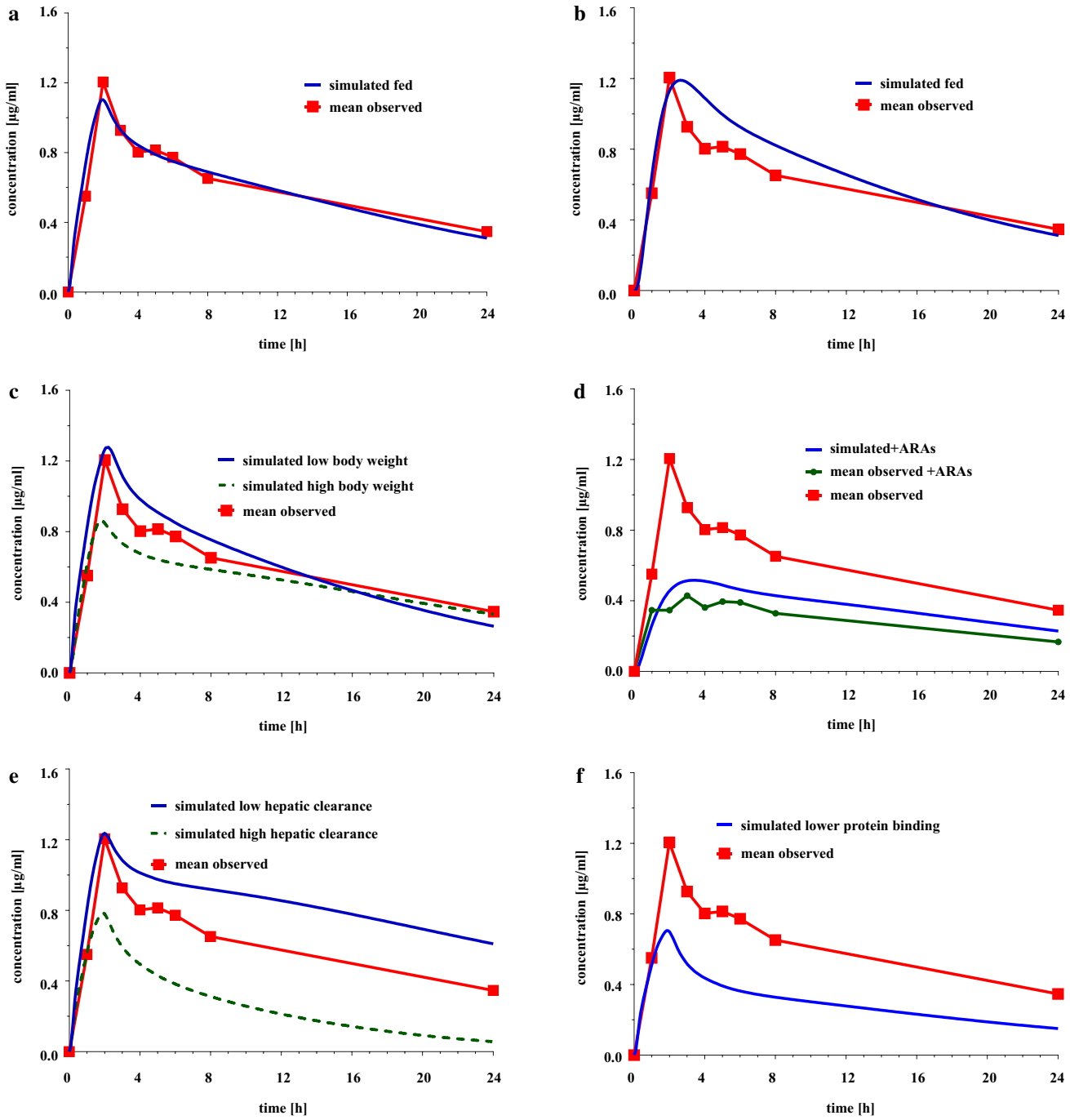

Fig. 2 Simulated impact of co-variates on erlotinib plasma concentration vs observed mean concentration. **a** Standard patient without co-variates, **b** ingestion of erlotinib at a fed state, **c** patients with elevated (85 kg) and reduced (45 kg) body weight, **d** concentrations with co-medication of acid reducing agents (ARAs) vs observed concentration without ARAs, **e** patients with elevated (10 l/h) and reduced (2 l/h) hepatic clearance, **f** patients with decreased protein binding (10% fraction unbound)

unrevealed. Therefore, a TDM is nonetheless recommended for drugs with a high interaction profile and a narrow therapeutic window and cannot be replaced entirely by in silico predictions. From a PK point of view, PBPK modeling combined with TDM represents a new strategy to evaluate the therapy of drugs with high inter-patient variability.

Acknowledgements Open access funding provided by University of Vienna.

Funding This project was funded by Hoffmann La Roche Austria (Grant number: FA555004 of the University of Vienna).

Compliance with ethical standards

Conflict of interest CD has reported honoraria or consultation fees from Roche Austria and (un)restricted grants donated to a research institute directed by him. The other authors declare that they have no conflict of interest.

Ethical approval All procedures performed in studies involving human participants were in accordance with the ethical standards of the institutional and/or national research committee and with the 1964 Helsinki declaration and its later amendments or comparable ethical standards.

Informed consent Informed consent was obtained from all individual participants included in the study.

References

1. US Food and Drug Administration-Center for Drug Evaluation and Research (2004) Erlotinib hydrochloride (Tarceva®) NDA 021743 Clinical pharmacology and biopharmaceutics review. https://www.accessdata.fda.gov/drugsatfda_docs/nda/2004/21-743_Tarceva_biopharmr.PDF. Accessed 12 Dec 2017
2. Shepherd FA, Rodrigues Pereira J, Ciuleanu T et al (2005) Erlotinib in previously treated non-small-cell lung cancer. N Engl J Med 353:123–132
3. Sahmanovic A, Buchner P, Lichtneckert M et al (2013) P-0042 pharmacokinetics of erlotinib and its main metabolite OSI420 in advanced pancreatic cancer patients when combined with escalating doses of capecitabine. Ann Oncol 24:iv48-iv48
4. Van Cutsem E, Verslype C, Beale P et al (2008) A phase Ib dose-escalation study of erlotinib, capecitabine and oxaliplatin in metastatic colorectal cancer patients. Ann Oncol 19:332–339
5. Ter Heine R, Fanggiday JC, Lankheet NAG et al (2010) Erlotinib and pantoprazole: a relevant interaction or not? Br J Clin Pharmacol 70:908–911
6. Chu MP, Ghosh S, Chambers CR et al (2015) Gastric acid suppression is associated with decreased erlotinib efficacy in non-small-cell lung cancer. Clin Lung Cancer 16:33–39
7. Kletzl H, Giraudon M, Abt M et al (2015) Effect of gastric pH on erlotinib pharmacokinetics in healthy individuals: omeprazole and ranitidine. Anticancer Drugs 26:565–572
8. Planchard D, Roussy G (2016) Can an acidic beverage reduce interactions between proton pump inhibitors and erlotinib? J Clin Oncol 34:1292–1294
9. Frohna P, Lu J, Eppler S et al (2006) Evaluation of the absolute oral bioavailability and bioequivalence of erlotinib, an inhibitor of the epidermal growth factor receptor tyrosine kinase, in a randomized, crossover study in healthy subjects. J Clin Pharmacol 46:282–290
10. O'Bryant CL, Haluska P, Rosen L et al (2011) An open-label study to describe pharmacokinetic parameters of erlotinib in patients with advanced solid tumors with adequate and moderately impaired hepatic function. Cancer Chemother Pharmacol 69:605–612
11. Scripture CD, Figg WD (2006) Drug interactions in cancer therapy. Nat Rev Cancer 6:546–558
12. Van Leeuwen RWF, Van Gelder T, Mathijssen RHJ, Jansman FGA (2014) Drug–drug interactions with tyrosine-kinase inhibitors: a clinical perspective. Lancet Oncol 15:e315–e326
13. Peereboom DM, Ahluwalia MS, Ye X et al (2013) NABTT 0502: a phase II and pharmacokinetic study of erlotinib and sorafenib for patients with progressive or recurrent glioblastoma multiforme. Neuro-Oncol 15:490–496
14. Hamilton L, Wolf JL, Rusk J et al (2006) Effects of smoking on the pharmacokinetics of erlotinib. Clin Cancer Res 12:2166–2171
15. Kraut EH, Rhoades C, Zhang Y et al (2011) Phase I and pharmacokinetic study of erlotinib (OSI-774) in combination with docetaxel in squamous cell carcinoma of the head and neck (SSCHN). Cancer Chemother Pharmacol. https://doi.org/10.1007/s00280-010-1332-y
16. Herviou P, Thivat E, Richard D et al (2016) Therapeutic drug monitoring and tyrosine kinase inhibitors. Oncol Lett 12:1223–1232
17. Josephs DH, Fisher DS, Spicer J et al (2013) Clinical pharmacokinetics of tyrosine kinase inhibitors: implications for therapeutic drug monitoring. Ther Drug Monit 35:562–587
18. Lankheet NAG, Knapen LM, Schellens JHM et al (2014) Plasma concentrations of tyrosine kinase inhibitors imatinib, erlotinib, and sunitinib in routine clinical outpatient cancer care. Ther Drug Monit 36:326–334
19. Gao B, Yeap S, Clements A et al (2012) Evidence for therapeutic drug monitoring of targeted anticancer therapies. J Clin Oncol 30:4017–4025
20. Jones MH, Gardner IB, Watson KJ (2009) Modelling and PBPK simulation in drug discovery. AAPS J 1:155–166
21. Parrott N, Lukacova V, Fraczkiewicz G et al (2009) Predicting Pharmacokinetics of drugs using physiologically based modeling—application to food effects. AAPS J 11:45–53
22. Kostewicz ES, Aarons L, Bergstrand M et al (2014) PBPK models for the prediction of in vivo performance of oral dosage forms. Eur J Pharm Sci 57:300–321
23. US Food and Drug Administration - Center for Drug Evaluation and Research (2005) Capecitabine (Xeloda®) NDA 020896 Clinical pharmacology and biopharmaceutics review https://www.accessdata.fda.gov/drugsatfda_docs/nda/98/20896-chem-pharm.pdf. Accessed 12 Dec 2017
24. US Food and Drug Administration - Center for Drug Evaluation and Research (2004) Bevacizumab (Avastin®) BLA 125085 Clinical pharmacology and biopharmaceutics review. https://www.accessdata.fda.gov/drugsatfda_docs/nda/2004/STN-125085_Avastin_BioPharmr.pdf. Accessed 12 Dec 2017
25. Lepper ER, Swain SM, Tan AR et al (2003) Liquid-chromatographic determination of erlotinib (OSI-774), an epidermal growth factor receptor tyrosine kinase inhibitor. J Chromatogr B Analyt Technol Biomed Life Sci 796:181–188
26. Simulations Plus Inc (2015) Gastro Plus user manual
27. Pang KS, Durk MR (2010) Physiologically-based pharmacokinetic modeling for absorption, transport, metabolism and excretion. J Pharmacokinet Pharmacodyn 37:591–615
28. Amidon GL, Lennernäs H, Shah VP et al (1995) A theoretical basis for a biopharmaceutic drug classification: the correlation of in vitro drug product dissolution and in vivo bioavailability. Pharm Res 12:413–420
29. Thelen K, Coboeken K, Willmann S et al (2011) Evolution of a detailed physiological model to simulate the gastrointestinal transit and absorption process in humans, part 1: oral solutions. J Pharm Sci 100:5324–5345
30. Thelen K, Coboeken K, Willmann S et al (2012) Evolution of a detailed physiological model to simulate the gastrointestinal

transit and absorption process in humans, part II: extension to describe performance of solid dosage forms. J Pharm Sci 101:1267–1280
31. Parrott NJ, Yu LJ, Takano R et al (2016) Physiologically based absorption modeling to explore the impact of food and gastric pH changes on the pharmacokinetics of alectinib. AAPS J 18:1464–1474
32. Wishart DS, Jewison T, Guo AC et al (2013) HMDB 3.0-The Human Metabolome Database in 2013. Nucleic Acids Res 41:D801–D807
33. Rasmussen L, Oster-Jørgensen E, Qvist N et al (1999) The effects of omeprazole on intragastric pH, intestinal motility, and gastric emptying rate. Scand J Gastroenterol 34:671–675
34. Ranson M, Shaw H, Wolf J et al (2010) A phase I dose-escalation and bioavailability study of oral and intravenous formulations of erlotinib (Tarceva, OSI-774) in patients with advanced solid tumors of epithelial origin. Cancer Chemother Pharmacol 66:53–58
35. Lu J-F, Eppler SM, Wolf J et al (2006) Clinical pharmacokinetics of erlotinib in patients with solid tumors and exposure-safety relationship in patients with non-small cell lung cancer. Clin Pharmacol Ther 80:136–145
36. Yamamoto N, Horiike A, Fujisaka Y et al (2008) Phase I dose-finding and pharmacokinetic study of the oral epidermal growth factor receptor tyrosine kinase inhibitor Ro50-8231 (erlotinib) in Japanese patients with solid tumors. Cancer Chemother Pharmacol 61:489–496

6.1.2 Irinotecan

Hepatic arterial infusion of irinotecan and EmboCept® S results in high tumor concentration of SN-38 in a rat model of colorectal liver metastases.

Kauffels A, Kitzmüller M, Gruber A, Nowack H, Bohnenberger H, Spitzner M, Kuthning A, Sprenger T, Czejka M, Ghadimi M, Sperling J.

Clin Exp Metastasis. 2019

Clinical & Experimental Metastasis
https://doi.org/10.1007/s10585-019-09954-5

RESEARCH PAPER

Hepatic arterial infusion of irinotecan and EmboCept® S results in high tumor concentration of SN-38 in a rat model of colorectal liver metastases

Anne Kauffels[1] · Marie Kitzmüller[2] · Andrea Gruber[2] · Hannah Nowack[1] · Hanibal Bohnenberger[3] · Melanie Spitzner[1] · Anja Kuthning[4] · Thilo Sprenger[1] · Martin Czejka[2,5] · Michael Ghadimi[1] · Jens Sperling[1]

Received: 17 August 2018 / Accepted: 8 January 2019

Abstract

Intraarterial chemotherapy for colorectal liver metastases (CRLM) can be applied alone or together with embolization particles. It remains unclear whether different types of embolization particles lead to higher intratumoral drug concentration. Herein, we quantified the concentrations of CPT-11 and its active metabolite SN-38 in plasma, liver and tumor tissue after hepatic arterial infusion (HAI) of irinotecan, with or without further application of embolization particles, in a rat model of CRLM. Animals underwent either systemic application of irinotecan, or HAI with or without the embolization particles Embocept® S and Tandem™. Four hours after treatment concentrations of CPT-11 and SN-38 were analyzed in plasma, tumor and liver samples by high-performance liquid chromatography. Additionally, DNA-damage and apoptosis were analyzed immunohistochemically. Tumor tissue concentrations of SN-38 were significantly increased after HAI with irinotecan and EmboCept® S compared to the other groups. The number of apoptotic cells was significantly higher after both HAI with irinotecan and EmboCept® S or Tandem™ loaded with irinotecan compared to the control group. HAI with irinotecan and EmboCept® S resulted in an increased SN-38 tumor concentration. Both HAI with irinotecan and EmboCept® S or Tandem™ loaded with irinotecan were highly effective with regard to apoptosis.

Keywords Hepatic arterial infusion · Irinotecan · SN38

Background

Intraarterial chemotherapy for patients with colorectal liver metastases (CRLM) has been performed for decades, but is recently of increased interest [1]. Although intraarterial regimens alone failed to show any benefit compared to systemic application in first-line approaches [2], modern multimodal treatment strategies combining systemic and intraarterial application of chemotherapy show promising results [3, 4]. Even after resistance to first- or second-line systemic chemotherapy, patients with CRLM profited from intraarterial chemotherapy [5]. Moreover, intraarterial chemotherapy in unresectable CRLM resulted in high rates of conversion to resectability associated with prolonged overall survival [6, 7]. Even in primarily resectable CRLM perioperative intraarterial chemotherapy led to a significant longer survival [8].

Most commonly intraarterial chemotherapy is administered as hepatic arterial infusion (HAI) or transarterial chemoembolization (TACE). These forms of locoregional

Electronic supplementary material The online version of this article (https://doi.org/10.1007/s10585-019-09954-5) contains supplementary material, which is available to authorized users.

✉ Anne Kauffels
anne.kauffels@med.uni-goettingen.de

1 Department of General, Visceral and Pediatric Surgery, University Medical Center Goettingen, Robert-Koch Str. 40, 37099 Göttingen, Germany

2 Division of Clinical Pharmacy and Diagnostics, University of Vienna, Vienna, Austria

3 Institute of Pathology, University Medical Center Goettingen, Göttingen, Germany

4 PharmaCept GmbH, Berlin, Germany

5 Austrian Society of Applied Pharmacokinetics, Vienna, Austria

Published online: 24 January 2019

application are thought to increase the concentration of the chemotherapeutic drug within the tumor tissue. The chemotherapeutic drugs can be combined with embolic agents such as lipiodol or embolization particles. The use of embolic agents should lead to an even greater increase of the drug concentration compared to the application of the drug alone. There are two types of embolization particles: Non-degradable hydrogel drug eluting beads (DEB) and degradable starch microspheres (DSM). Whereas DEB are loadable with irinotecan or doxorubicin before administration and persist within the tissue leading to vascular occlusion, DSM cannot be loaded and are completely degraded by serum α-amylases [9].

Irinotecan plays a key role as chemotherapeutic drug both for systemic and locoregional treatment of metastatic colorectal cancer [10]. It is administered as a prodrug (CPT-11) which requires metabolic conversion into its active metabolite SN-38 by carboxylesterases [11]. However, although SN-38 provides the anti-tumor effect of irinotecan, it is also responsible for adverse side effects associated with irinotecan therapy such as diarrhoea or hematotoxicity [12, 13]. Thus, it is of great interest to use an application form of irinotecan that provides a high concentration of SN-38 inside the tumor tissue. Moreover, the intraarterial application is theoretically capable to attenuate adverse side effects by lowering the systemic exposure to the chemotherapeutic drug. Therefore, a locoregional application form like HAI seems to be ideal to achieve these goals.

The present study was conducted to quantify the concentration of CPT-11 and SN-38 in plasma, liver and tumor tissue after HAI with irinotecan alone or in combination with one of two different type of embolization particles, EmboCept® S (DSM) or Tandem™ 40 µm (DEB), in a rat model of CRLM. The concentrations after systemic application were quantified for comparison. Additionally, immunohistochemical analyses were performed to detect apoptotic cell death and DNA-damage in tumor tissue.

Materials and methods

Drugs/embolization particles

Irinotecan was purchased as a liquid concentrate from Actavis (Puren Pharma GmbH&Co. KG, Munich, Germany) at a concentration of 20 mg/mL and was given in a dose of 90 mg/m^2. The body surface area was calculated according to "Meeh's formula": $A = KxW^{2/3}$, where A stands for body surface area; K is an animal specific constant (in the present study 9.1); and W stands for the body weight [14].

EmboCept® S (amilomer, degradable starch microspheres 35/50 µm) was obtained from PharmaCept GmbH (Berlin, Germany) at a concentration of 450 mg/7.5 mL. Tandem™ 40 µm drug eluting beads were purchased from CeloNova® BioSciences Germany GmbH (Ulm, Germany).

According to the user's guidelines EmboCept® S (DSM) and irinotecan were mixed shortly before administration; Tandem™ 40 µm beads (DEB) were loaded for at least 30 min with irinotecan before administration.

Cell culture

The syngeneic rat colon adenocarcinoma cell line CC531 was purchased from CLS Cell Lines Service GmbH (Eppelheim, Germany). Cells were expanded and stored in frozen aliquots (− 150 °C). After thawing the cells were cultured in RPMI-1640 (Roswell Park Memorial Institute) medium supplemented with 10% FCS (fetal calf serum) and 1% glutamine on 75 cm^2 culture flasks and kept at 37 °C and 5% CO_2 in a humidified incubator. After the third passage cells were counted and resuspended in PBS (phosphate buffered saline) at a concentration of 5×10^5 cells/100 µL for tumor cell implantation.

Animals

In total 37 male WAG/Rij rats (Charles River laboratories, Sulzfeld, Germany) aged 10–13 weeks with a mean body weight of 225 ± 6.88 g (mean ± SEM) were included in the experiment. The animals were kept in a temperature- and humidity-controlled 12 h day/night cycle enviroment with free access to water and standard laboratory chow (ssniff-Spezialdiäten GmbH, Soest, Germany). All experiments were approved by the regional legislation on animal protection (No. 14/1610). Experiments were performed in accordance to the Guidelines for the Welfare of Animals in Experimental Neoplasia of the United Kingdom Coordinating Committee on Cancer Research [15] and the Guide for Care and Use of Laboratory Animals [16].

Colorectal liver metastases model

Animals were anaesthetized by sevoflurane inhalation and underwent a median laparotomy of about 1.5 cm. To perform tumor cell implantation 5×10^5 CC531 cells were administered subcapsularly into the left and median liver lobe each using a 27 G needle (Sterican, B. Braun, Melsungen, Germany). Laparotomy was closed with a PDS 4-0 continuous suture (Ethicon/Johnson&Johnson Medical GmbH, Norderstedt, Germany).

Hepatic arterial infusion

On day 10 after tumor cell implantation animals received intraperitoneal injection of Ketamin/Cepetor® for anaesthesia and underwent relaparotomy. According to previously

described experiments, for HAI the gastroduodenal artery was canulated using a catheter (ID 0.28 mm, Smiths Medical International Ltd., Hythe, UK) [17]. The tip of the catheter was placed at the common hepatic artery without occluding the artery and allowing orthograde bloodflow. After HAI the catheter was removed and the gastroduodenal artery was ligated. For systemic treatment the subhepatic vena cava was punctured with a 27 G needle (Sterican, Braun, Melsungen, Germany) [18, 19]. Laparotomy was again closed with a PDS 4-0 continuous suture (Ethicon/Johnson&Johnson Medical GmbH, Norderstedt, Germany).

In a preliminary experiment one animal was sacrificed 4 h and one 24 h after systemic treatment to evaluate the ideal time point for analysis of plasma and tissue concentrations of CPT-11 and SN-38. As CPT-11 and SN-38 concentrations of both plasma and tissue were decisively lower or even not measurable after 24 h we continued the study with sacrificing the animals 4 h after drug administration (Supplementary Figs. 1 and 2).

Accordingly, 35 animals were randomly assigned to five study groups (n = 7 each). The animals underwent either HAI with NaCl 0.9% (Sham), irinotecan (HAI iri), irinotecan and EmboCept® S (HAI iri + Embo) or Tandem™ 40 µm loaded with irinotecan (HAI iri + Tandem). Moreover, one group received systemic application of irinotecan alone (sys iri). Body weight was measured at the time points of tumor implantation and treatment.

Tissue and blood samples

Four hours after treatment animals underwent relaparotomy under sevoflurane anaethesia. Blood was obtained by cardiac puncture and subsequently centrifuged with 8000 rpm for 5 min (Eppendorf AG, Hamburg, Germany). Plasma was stored at − 80 °C before high performance liquid chromatography (HPLC) analyses. The complete liver was removed and washed in PBS at 4 °C. Tissue samples of healthy liver and both tumors were collected and snap frozen in liquid nitrogen or fixed in 4% phosphate-buffered formalin and subsequently embedded in paraffin. Frozen samples were kept at − 80 °C before HPLC analyses.

Analytical assay for CPT-11 and SN-38

Total amounts of CPT-11 and SN-38 were quantified in plasma and tissue samples by an isocratic reversed-phase HPLC method, using fluorimetric detection as described previously [20, 21]. Shortly, the analytical procedure was as follows:

Blood samples: The thawed blood samples were mixed with ice-cold acetonitril (ACN) acidified with 8.5% H_3PO_4 and vortexed for 15 s (VELP® Scientifica Vortex Mixer, Velp Scientifica Srl, Usmate Velate MB, Italy). After protein precipitation had been completed, samples were centrifuged (VWR® Galaxy 16 DH, VWR International GmbH, Vienna, Austria) at 13 000 rpm for 5 min to obtain a clear supernatant.

Tissue samples: Thawed tissue samples (liver or tumor, about 50–100 mg) were weighed into tissue homogenizing tubes CK14 (Peqlab Biotechnologie GmbH, Erlangen, Germany), mixed with the 10 fold volume (mg/µL) of ice-cold ACN acidified with 8.5% H_3PO_4 and homogenized on a Minilys® (Bertin Technologies, Montigny le Bretonneux, France) at 8 000 rpm for 15 s (three cycles per sample). The resulting homogenate was centrifuged at 13 000 rpm for 5 min to obtain the clear supernatant for analysis.

Chromatography

Analysis was performed by use of a VWR-Hitachi Chromaster System (VWR International GmbH, Vienna, Austria) as described in the literature [22]. CPT-11 and metabolites were detected at an excitation wavelength of 360 nm and emission wavelength of 500 nm.

Histology and immunohistochemical analysis

Formalin fixed and paraffin embedded (FFPE) tissue of both tumor and liver was cut in 2 µm sections. Slices were stained with hematoxylin-eosin (HE) for exact localization of tumor site. For immunohistochemical analysis the sections from FFPE liver and tumor tissues were mounted on microscope slides (Starfrost, Light Laboratories, Dallas, Texas, USA). Epitope retrieval was performed with CC1 cell conditioner (60 min at 100 °C, Ventana Medical Systems, Tucson, Arizona, USA) and followed by primary antibody incubation (24 min at 37 °C) using the benchmark XT stainer (Ventana Medical Systems, Tucson, Arizona, USA). For visualization of the epitope-antibody complex and color development the ultraview universal DAB detection kit (Ventana Medical Systems, Tucson, Arizona, USA) was used. Counterstaining was performed with hematoxylin. Quantitative analyses were performed in a blinded fashion.

Caspase-3 as a marker for apoptotic cell death was detected using a rabbit monoclonal anti-cleaved caspase-3 antibody (1:1000; Cell Signaling Technology, Danvers, USA). Ten high-power-fields (HPF) were analyzed per specimen and positively stained tumor cells were counted and given as absolute number per HPF.

γH2AX as a marker for early DNA-damage was detected using a rabbit polyclonal anti-γH2AX antibody (1:100; abcam plc, Cambridge, UK). Ten HPF were analyzed per specimen and positively stained tumor cells were counted and given as absolute number per HPF.

PCNA as proliferation marker was detected using a mouse monoclonal anti-PCNA antibody (1:1500; invitrogen GmbH,

Carlsbad, USA). PCNA-positive tumor cells were estimated in percentage per HPF and analyzed using a score ranging from 0 to 4 ($0 \leq 1\%$, 1 = 1–10%, 2 = 10–30%, 3 = 30–50%, $4 \geq 50\%$ of PCNA-positive cells).

Statistical analysis

Statistical analysis was performed with the use of the software package STATISTICA (Systat Software, Germany). After analysis of normal distribution (quantile–quantile plot), pairwise comparison between each treatment group and Sham, each HAI group and sys iri, and HAI iri and both HAI iri + Embo and HAI iri + Tandem was performed by Student's t test (normal distribution) or Mann–Whitney u-test (non-normal distribution). Statistatical comparison of HAI iri + Embo and HAI iri + Tandem was not performed. Statistical significance was set at $p < 0.05$. All values are expressed as mean ± standard error of the mean (SEM).

Results

Health conditions and tumor establishment

All animals showed an appropriate increase in body weight from the day of tumor implantation (225 ± 6.88 g) until the day of treatment (240 ± 5.52 g). No animal showed any impairment due to tumor burden. Two animals developed disseminated tumors. These animals were excluded from further evaluation. All other animals developed single tumors of about 6 mm in diameter.

Chromatography

In plasma and tissue samples CPT-11 and SN-38 were quantified by a fluorimetric detection method. This procedure allows a selective and highly sensitive quantitation of the compounds. There were no peak interferences with matrix compounds or peaks resulting from drugs of premedication or sacrification procedure.

CPT-11 concentration

The measured CPT-11 concentrations are depicted in Fig. 1. Plasma concentrations of CPT-11 were in a similar range (1.0-2.5 µmol/L) after systemic application of irinotecan, HAI with irinotecan alone and HAI with irinotecan and EmboCept® S. However, HAI with Tandem™ 40 µm loaded with irinotecan led to low concentrations 4 h after treatment resulting in a significant difference compared to systemic application of irinotecan ($p = 0.019$) and HAI with irinotecan alone ($p < 0.0001$; Fig. 1A).

Mean liver tissue concentrations of CPT-11 after systemic application of irinotecan, HAI with irinotecan alone and HAI with irinotecan and EmboCept® S were about 10–20 fold higher compared to CPT-11 plasma concentrations. However, after HAI with Tandem™ 40 µm loaded with irinotecan only small amounts of CPT-11 were detectable and therefore resulted in a significant difference compared to systemic application of irinotecan ($p = 0.002$) and HAI with irinotecan alone ($p < 0.001$; Fig. 1b).

Mean CPT-11 concentrations in tumor tissue showed a larger interindividual variability and were about 50 to 150 fold higher in comparison to the plasma concentrations, with significantly higher concentrations after HAI with irinotecan alone and HAI with irinotecan and EmboCept® S compared to systemic application of irinotecan ($p < 0.001$ and $p = 0.003$, respectively). CPT-11 concentrations in tumor tissue after HAI with Tandem™ 40 µm loaded with irinotecan were significantly lower compared to the other application methods (Fig. 1c).

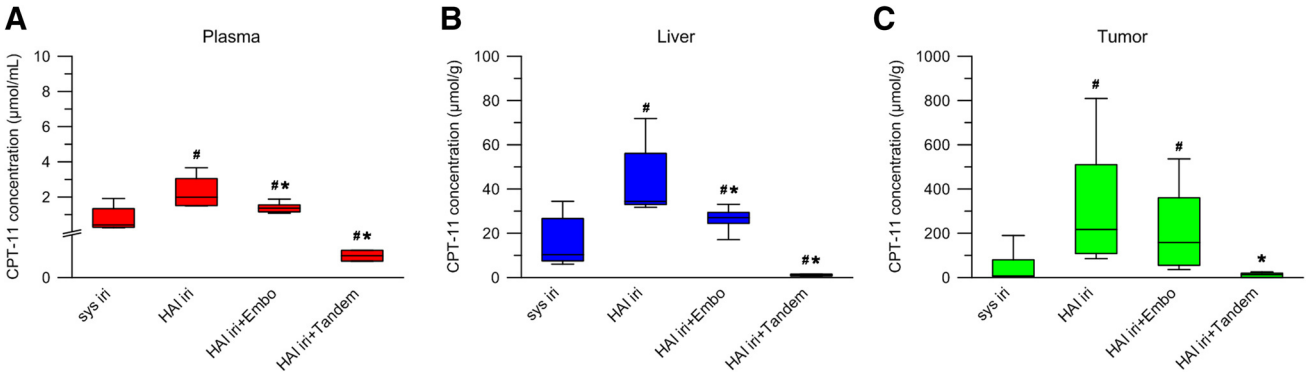

Fig. 1 CPT-11 concentrations of plasma (**a**), liver (**b**) and tumor tissue (**c**) of animals undergoing systemic administration of irinotecan (sys iri) or HAI with irinotecan alone (HAI iri), HAI with irinotecan + EmboCept® S (HAI iri + Embo), or HAI with irinotecan + Tandem™ 40 µM (HAI iri + Tandem). Mean ± SEM; #$p < 0.05$ versus sys iri, *$p < 0.05$ versus HAI iri

CPT-11 was not detectable in samples from Sham-treated animals.

SN-38 concentration

The measured SN-38 concentrations are displayed in Fig. 2. There was no difference in plasma concentrations between the systemic application of irinotecan, HAI with irinotecan alone and HAI with irinotecan and EmboCept® S at 4 h after administration. Of interest, after HAI with Tandem™ 40 µm loaded with irinotecan plasma concentrations of SN-38 were significantly lower compared to systemic application of irinotecan or HAI with irinotecan alone ($p < 0.001$, both; Fig. 2a).

SN-38 liver concentrations were about fivefold higher compared to plasma concentrations in all treatment groups with no significant difference between the groups with the exception of significantly lower concentrations after HAI with Tandem™ 40 µm loaded with irinotecan compared to systemic application of irinotecan or HAI with irinotecan alone ($p < 0.001$, both; Fig. 2b).

The SN-38 concentrations in the tumor tissue were similar after systemic application of irinotecan, HAI with irinotecan alone and HAI with Tandem™ 40 µm loaded with irinotecan. On the contrary, HAI with irinotecan and EmboCept® S resulted in significantly higher concentrations ($p = 0.032$ compared to systemic application of irinotecan and $p = 0.019$ compared to HAI with irinotecan alone) compared to the other groups. After HAI with Tandem™ 40 µm loaded with irinotecan SN-38 concentrations were increased compared to liver tissue concentrations (Fig. 2c).

SN-38 was not detectable in any sample from Sham-treated animals.

Immunohistochemical analysis

Immunohistochemical analysis of the protein expression of PCNA as a marker for cell proliferation showed comparable proliferation rates in the tumor tissue of all groups (Fig. 3a).

All treatment groups showed an increased phosphorylation of H2AX to γH2AX as a marker for DNA-damage compared to control animals (Sham), which was most pronounced after HAI with irinotecan and EmboCept® S, although without reaching statistical significance (Fig. 3b).

The expression of caspase-3 as a marker for apoptotic cell death was significantly higher after systemic application of irinotecan, HAI with irinotecan and EmboCept® S and HAI with Tandem™ 40 µm loaded with irinotecan ($p = 0.035$, $p = 0.003$ and $p = 0.009$, respectively) compared to control animals (Sham). Expression of caspase-3 after HAI with irinotecan alone compared to control animals was also increased, but failed to reach the level of statistical significance ($p = 0.0536$). Although the greatest level of expression of caspase-3 was detected after HAI with irinotecan and EmboCept® S and HAI with Tandem™ 40 µm loaded with irinotecan, there was no significant difference between the treatment groups (Fig. 3c).

Discussion

We herein describe for the first time the successful measurement of CPT-11 and SN-38 in a rat model of CRLM. Although quantitative analysis of CPT-11 and SN-38 has been performed successfully in plasma, urine, feces, liver and kidney of rats [23], the quantitative analysis of CPT-11 and SN-38 in preclinical cancer models has so far only been described in larger animals such as rabbits or pigs [24, 25]. In times of increased concern about animal welfare, small animal models are of great interest. In contrast to keeping

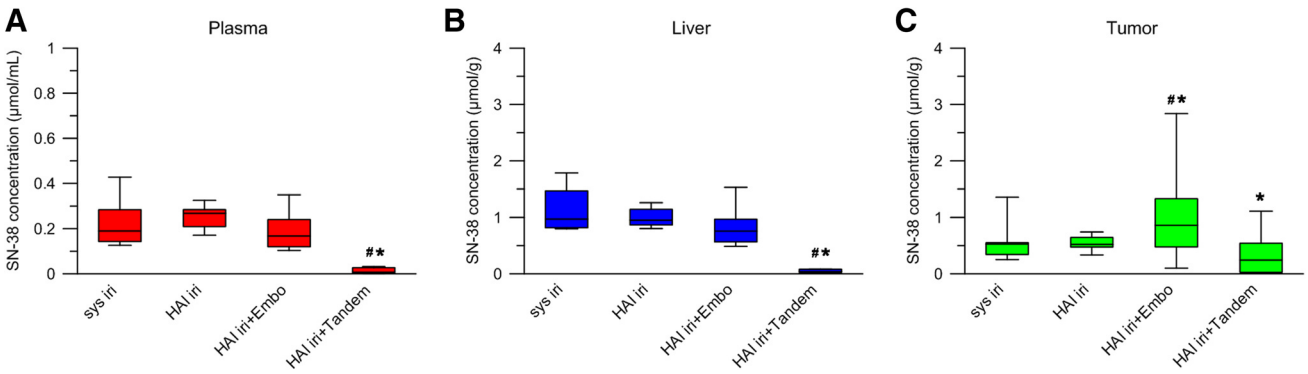

Fig. 2 SN-38 concentrations of plasma (**a**), liver (**b**) and tumor tissue (**c**) of animals undergoing systemic administration of irinotecan (sys iri) or HAI with irinotecan alone (HAI iri), HAI with irinotecan + EmboCept® S (HAI iri + Embo), or HAI with irinotecan + Tandem™ 40 µM (HAI iri + Tandem). Mean ± SEM; #$p < 0.05$ versus sys iri, *$p < 0.05$ versus HAI iri

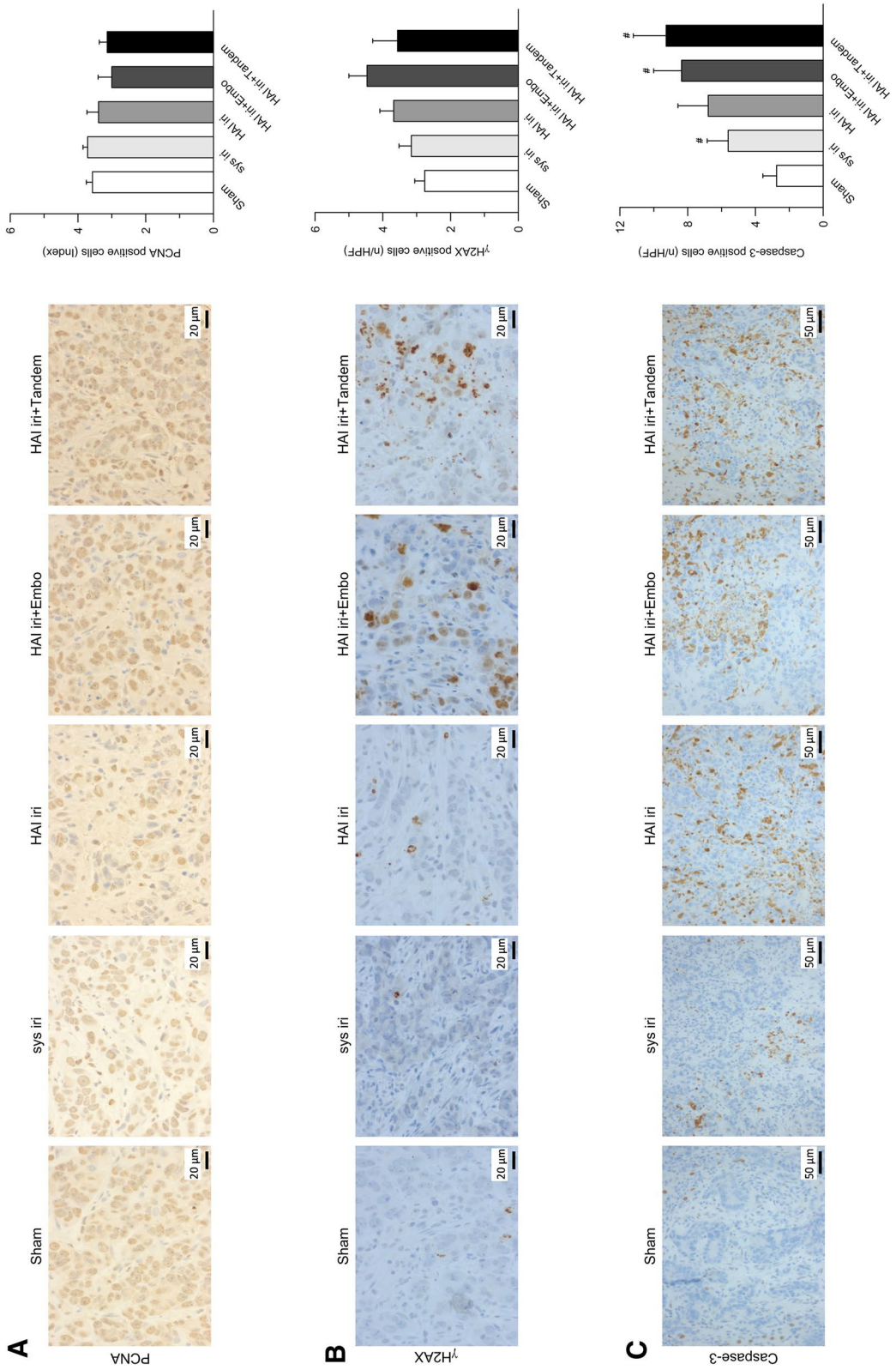

Fig. 3 Images and data of immunohistochemical analyses of tumor tissue of animals undergoing HAI with NaCl 0.9% (Sham), systemic administration of irinotecan (sys iri), HAI with irinotecan (HAI iri), HAI with irinotecan + EmboCept® S (HAI iri + Embo), or HAI with irinotecan + Tandem™ 40 µM (HAI iri + Tandem). **a** Images and data of immunohistochemical analysis of proliferating nuclear cell antibody (score $0 \leq 1\%$, $1 = 1–10\%$, $2 = 10–30\%$, $3 = 30–50\%$, $4 \geq 50\%$ of PCNA-positive cells). **b** Images and data analyses of γH2AX-positive cells (given as number per HPF). **c** Images and data analyses of caspase-3-positive cells (given as number per HPF). Mean ± SEM; $^{\S}p < 0.05$ versus Sham

large animals, housing small animals can be more species-appropriate due to the smaller body size and shorter life-span. Moreover, economic pressure does not allow every institution to perform experiments in large animal models [26].

The model of CC531 CRLM in WAGRij-rats [27, 28] is well established for the use of HAI [17–19, 29–31] and various other diagnostic tools or liver-directed therapies [32–34].

To date, it is not completely known to which degree the microvascular structure of the experimental CC531 CRLM is comparable to the microvascular structure in human CRLM. However, the anatomy of the human hepatic microvasculature has been analyzed in detail in various studies [35]. Thus, it is commonly understood that terminal hepatic arterioles and terminal portal venules, that supply the blood to the liver sinusoids, have a diameter of 15–35 µm [36]. Accordingly, the microvascular bed of the rat liver has also been well analyzed. Koo and colleagues investigated the diameter of the hepatic and portal venous system in rats in 1975 and described the diameter of these microvessels ranging from 45.6 ± 1.06 to 9.7 ± 0.18 µm on the portal venous side and from 42.0 ± 0.79 to 9.2 ± 0.26 µm on the hepatic side of the microvascular bed [37]. Thus, it can be stated, that the livers microvascular structure of rats and humans is at least comparable. In accordance with these findings we hypothesize that, although it consists of irregular tumor vessels, the microvasculature of CRLM in rats and humans is comparable. In this context Gonda et al. showed in a liver metastases model in Donryu rats, that the irregular tumor vessels measured from 12 to 105 µm in diameter and receive their main blood supply from the hepatic artery axis [38]. Thus, even though the authors used rat hepatoma cells to induce liver metastases, the tumor vessels match the diameter of the normal liver microvascular bed. Hence, we assume that the microvasculature associated with the CC531 experimental metastases resemble that seen in clinical colorectal metastases.

The CC531 model used in the present study proved to be feasible for quantative analyses of both the prodrug CPT-11 and its active metabolite SN-38 in plasma and tissue samples. A prior attempt of Buck et al. to evaluate SN-38 tumor tissue concentrations in a murine model of colorectal cancer failed, which the authors explained by the low conversion rate of CPT-11 to SN-38 and the even lower administration dose of irinotecan in mice [39]. It is also well known that CPT-11 has a very low affinity to the human carboxy esterase hCES2. Therefore only small amounts of SN-38 are generated in the human metabolism. Moreover, the concentration of SN-38 in plasma is not only dependent upon its formation by carboxy esterases, but also depends upon the redistribution from tissue into plasma. In humans conventional systemic administration of irinotecan at a dose of 180 mg/m^2 over 1 h led to CPT-11 peak concentrations measured in a range of 4000–6000 nmol/mL whereas SN-38 peak concentrations ranged from 40 to 100 nmol/mL, giving evidence for the very limited conversion rate [22].

However, the rat metabolism of CPT-11 differs at certain stages from the human metabolism. Rats do not express the cytochrome P450 enzyme 3A4, which is mostly responsible for conversion of CPT-11 into its inactive compounds aminopentanocamptothecin (APC) and norpentanocamptothecin (NPC) in humans [11]. It is therefore expected that rats are able to metabolize even more CPT-11 into its active metabolite SN-38 [40].

In the present study the plasma concentrations of CPT-11 were increased after HAI with irinotecan alone or HAI with irinotecan and EmboCept® S (DSM) compared to the systemic application. The low levels of plasma concentrations of CPT-11 after systemic application in humans can be explained by the high volume of distribution of irinotecan, which ranges at steady-state from 136 to 255 L/m^2 [41]. Distribution of CPT-11 into the liver tissue takes place rapidly and has shown to be completed within 1 h after the infusion in a study comparing plasma levels of CPT-11 and SN-38 in patients with CRLM [22]. Therefore, in these patients there was no significant difference in plasma concentrations of CPT-11 and SN-38 comparing application of irinotecan either by HAI or systemically 4 h after treatment. This was explained by the rapid distribution of CPT-11 from blood into tissue [22]. Interestingly, the authors found a higher metabolic conversion rate of CPT-11 into its active metabolite SN-38 after intraarterial application and concluded that this application form is beneficial from a pharmacokinetic point of view. This can be explained by the fact that liver tissue contains a high activity of human carboxy esterase hCES2 which is responsible for the formation of SN-38 [22]. This is in line with the findings of the present study, where HAI with irinotecan alone or in combination with EmboCept® S led to higher concentrations of the active metabolite SN-38 in liver and tumor tissue compared to the systemic application of irinotecan.

Only the concomitant application of irinotecan with EmboCept® S resulted in significantly higher tumor tissue concentrations of SN-38 compared to both systemic application of irinotecan and HAI of irinotecan alone. EmboCept® S as a DSM is degraded completely by serum α-amylases with a half-life of 35 min within the human metabolism [42], leading to an only temporary arterial occlusion. Accordingly, in the present study, a temporary arterial occlusion, provided by EmboCept® S led to a higher conversion of CPT-11 into SN-38 within the tumor tissue. The effect of the temporary arterial occlusion has also been described in a study with a pig model by Pieper et al. [43]. Thereby animals underwent HAI with EmboCept® S of a whole liver lobe. Subsequently, the arterial blood flow was not only completely

reconstituted, but there was also no sign of considerable liver damage [43]. These data support the potential use of EmboCept® S even in tumors which do not allow a highly selective vascular approach due to multiple tumor sites or vascular specificities.

In the present study the use of Tandem™ 40 µm (DEB) loaded with irinotecan did not lead to elevated tumor tissue concentrations neither of the prodrug CPT-11 nor its active metabolite SN-38. Moreover, it even led to significantly lower values compared to HAI with irinotecan alone. Quite the contrary, previous studies in preclinical models of rabbit and pig origin showed that the application of Tandem™ 40 µm loaded with irinotecan led to higher tissue concentrations of both CPT-11 and SN-38 compared to HAI with irinotecan alone. Additionally, after application of Tandem™ 40 µm loaded with irinotecan SN-38 was still detectable after 72 h, which was not the case after HAI of irinotecan alone [24, 25]. Accordingly, in a clinical study patients with unresectable CRLM showed a decrease in tumor size after intraarterial therapy with DEB loaded with irinotecan hinting to the effective anti-tumor qualities of the embolization agent in combination with the drug [44].

There are certainly limitations to our study with regard to the evaluation of Tandem™ 40 µm drug eluting beads. The loading with irinotecan was carried out following exactly the instructions from the users' guidelines, which should have ensured a correct loading process of the beads. We hypothesize that the low levels of CPT-11 and SN-38 concentrations are due to the slow release of irinotecan from the beads in vivo. This hypothesis is supported by the results from the previous studies mentioned above which showed the highest tissue concentration of SN-38 24 h after HAI with loaded beads and even measurable amounts of both CPT-11 and SN-38 after 72 h [24, 25]. Ideally, for the evaluation of Tandem™ 40 µm drug eluting beads repeated blood sampling and sacrification of animals at different time points after administration would have been necessary to create an area under the curve (AUC) and to enable exact evaluation of the drug release.

Finally, in the present study immunohistochemical analysis 4 h after treatment revealed that DNA-damage and apoptotic cell death was already detectable in the tumor tissue. Expression of caspase-3 as marker for apoptosis was even significantly higher in three of the treatment groups compared to Sham-treated animals. Although application of Tandem™ 40 µm loaded with irinotecan did not result in high tumor tissue concentrations of CPT-11 or SN-38, higher expression levels of caspase-3 were detectable. This finding supports the hypothesis that apoptosis is not only induced by irinotecan itself but might also be due to the permanent vascular occlusion caused by the DEB Tandem™ 40 µm.

The preclinical CC531/WAGRij model of CRLM is feasible for quantitative analysis of CPT-11 (prodrug) and SN-38 (active metabolite) after systemic application and HAI of irinotecan. The combined application of irinotecan and EmboCept® S via HAI led to significantly higher SN-38 tumor tissue concentrations compared to all other treatment groups. The time span of 4 h between administration of therapy and sacrification of the animals seemed too short to release CPT-11 quantitatively from the Tandem™ 40 µm drug eluting beads loaded with irinotecan. A longer time span would have been favorable for the detection of CPT-11 after Tandem™ 40 µm application. However, the study compared four different application methods (systemic application of irinotecan, HAI with irinotecan alone, HAI with irinotecan and EmboCept® S, HAI with irinotecan and Tandem™ 40 µm loaded with irinotecan) and therefore the sampling time of 4 h was chosen as a compromise to show the distribution of compounds in plasma and tissue after varying application ways. In addition to the pharmacological effects, immunohistochemical analyses with regard to apoptotic cell deaths and DNA-damage revealed a favorable effect when irinotecan was combined with embolization particles. Further studies are necessary to define the ideal type of embolization particle and to evaluate a potential benefit for the treatment of colorectal metastases.

Acknowledgements The authors thank Birgit Jünemann who helped to establish the immunohistochemistry staining.

Funding A Kauffels salary during the time of the study and part of the study itself has beend funded by the Else Kröner-Fresenius-Stiftung (EKFS), Bad Homburg v.d.H, Germany, due to a scholarship. The cost for HPLC-analyses in Vienna has been covered by PharmaCept GmbH, Berlin, Germany.

Compliance with Ethical Standards

Conflict of interest A Kuthning works for PharmaCept GmbH, Berlin. All other authors declare no potential conflict of interest.

Ethics approval All procedures performed in studies involving animals were in accordance with the ethical standards of the institution at which the studies were conducted (Niedersächsisches Landesamt für Verbraucherschutz und Lebensmittelsicherheit, ethics approval number 14/1610).

References

1. Habib A, Desai K, Hickey R, Thornburg B, Lewandowski R, Salem R (2015) Transarterial approaches to primary and secondary hepatic malignancies. Nat Rev Clin Oncol 12:481–489
2. Mocellin S, Pilati P, Lise M, Nitti D (2007) Meta-analysis of hepatic arterial infusion for unresectable liver metastases from colorectal cancer: the end of an era? J Clin Oncol 25:5649–5654
3. McAuliffe JC, Qadan M, D'Angelica MI (2015) Hepatic resection, hepatic arterial infusion pump therapy, and genetic biomarkers in the management of hepatic metastases from colorectal cancer. J Gastrointest Oncol 6:699–708

4. Fiorentini G, Sarti D, Aliberti C, Carandina R, Mambrini A, Guadagni S (2017) Multidisciplinary approach of colorectal cancer liver metastases. World J Clin Oncol 8:190–202
5. Cercek A, Boucher TM, Gluskin JS, Aguiló A, Chou JF, Connell LC et al (2016) Response rates of hepatic arterial infusion pump therapy in patients with metastatic colorectal cancer liver metastases refractory to all standard chemotherapies. J Surg Oncol 114:655–663
6. D'Angelica MI, Correa-Gallego C, Paty PB, Cercek A, Gewirtz AN, Chou JF et al (2015) Phase II trial of hepatic artery infusional and systemic chemotherapy for patients with unresectable hepatic metastases from colorectal cancer: conversion to resection and long-term outcomes. Ann Surg 261:353–360
7. Martin RC III, Scoggins CR, Schreeder M, Rilling WS, Laing CJ, Tatum CM et al (2015) Randomized controlled trial of irinotecan drug-eluting beads with simultaneous FOLFOX and bevacizumab for patients with unresectable colorectal liver-limited metastasis. Cancer 121:3649–3658
8. Groot Koerkamp B, Sadot E, Kemeny NE, Gönen M, Leal JN, Allen PJ et al (2017) Perioperative hepatic arterial infusion pump chemotherapy is associated with longer survival after resection of colorectal liver metastases: a propensity score analysis. J Clin Oncol 35:1938–1944
9. Gruber-Rouh T, Marko C, Thalhammer A, Nour-Eldin NE, Langenbach M, Beeres M et al (2016) Current strategies in interventional oncology of colorectal liver metastases. Br J Radiol 26:20151060
10. Fujita K, Kubota Y, Ishida H, Sasaki Y (2015) Irinotecan, a key chemotherapeutic drug for metastatic colorectal cancer. World J Gastroenterol 21:12234–12248
11. Mathijssen RH, van Alphen RJ, Verweij J, Loos WJ, Nooter K, Stoter G, Sparreboom A (2001) Clinical pharmacokinetics and metabolism of irinotecan (CPT-11). Clin Cancer Res 7:2182–2194
12. Xie R, Mathijssen RH, Sparreboom A, Verweij J, Karlsson MO (2002) Clinical pharmacokinetics of irinotecan and its metabolites in relation with diarrhea. Clin Pharmacol Ther 72:265–275
13. Colucci G, Gebbia V, Paoletti G, Giuliani F, Caruso M, Gebbia N et al (2005) Phase III randomized trial of FOLFIRI versus FOLFOX4 in the treatment of advanced colorectal cancer: a multicenter study of the Gruppo Oncologico Dell'Italia Meridionale. J Clin Oncol 23:4866–4875
14. Benedict FG (1934) Die Oberflächenbestimmungen verschiedener Tiergattungen [Determination of body surface area in different animal species]. Ergeb Physiol Exp Pharmakol 36:300–346
15. Workman P, Aboagye EO, Balkwill F, Balmain A, Bruder G, Chaplin DJ et al (2010) Guidelines for the welfare and use of animals in cancer research. Br J Cancer 102:1555–1577
16. Institute of Laboratory Animal Resources, National Research Council (1996) Guide for the care and use of laboratory animals, 8th edn. NIH Guide, UK
17. Sperling J, Schäfer T, Ziemann C, Benz-Weiber A, Kollmar O, Schilling MK et al (2012) Hepatic arterial infusion of bevacizumab in combination with oxaliplatin reduces tumor growth in a rat model of colorectal liver metastases. Clin Exp Metastasis 29:91–99
18. Sperling J, Brandhorst D, Schäfer T, Ziemann C, Benz-Weißer A, Scheuer C et al (2013) Liver-directed chemotherapy of cetuximab and bevacizumab in combination with oxaliplatin is more effective to inhibit tumor growth of CC531 colorectal rat liver metastases than systemic chemotherapy. Clin Exp Metastasis 30:447–455
19. Sperling J, Schäfer T, Benz-Weißer A, Ziemann C, Scheuer C, Kollmar O et al (2013) Hepatic arterial infusion but not systemic application of cetuximab in combination with oxaliplatin significantly reduces growth of CC531 colorectal rat liver metastases. Int J Colorectal Dis 28:555–562
20. Eder I, Czejka M, Schueller J, Zeleny U (2000) Clinical pharmacokinetics (PHK) and metabolism of irinotecan (IRINO) during mono- and polychemotherapy with 5-Fluorouracil/Leucovorin (5FU/LV) and Docetaxel (DOCE). Eur J Pharm Sci 11:23
21. Slatter JG, Schaaf LJ, Sams JP, Feenstra KL, Johnson MG, Bombardt PA et al (2000) Pharmacokinetics, metabolism, and excretion of irinotecan (CPT-11) following I.V. infusion of [(14)C] CPT-11 in cancer patients. Drug Metab Dispos 28:423–433
22. Czejka M, Kiss A, Koessner C, Terkola R, Ettlinger D, Schueller J (2011) Metabolic activation of irinotecan during intra-arterial chemotherapy of metastatic colorectal cancer. Anticancer Res 31:3573–3578
23. Basu S, Zeng M, Yin T, Gao S, Hu M (2016) Development and validation of an UPLC-MS/MS method for the quantification of irinotecan, SN-38 and SN-38 glucuronide in plasma, urine, feces, liver and kidney: application to a pharmacokinetic study of irinotecan in rats. J Chromatogr B Analyt Technol Biomed Life Sci 1015–1016:34–41
24. Tanaka T, Nishiofuku H, Hukuoka Y, Sato T, Masada T, Takano M et al (2014) Pharmacokinetics and antitumor efficacy of chemoembolization using 40 μm irinotecan-loaded microspheres in a rabbit liver tumor model. J Vasc Interv Radiol 25:1037–1044
25. Gnutzmann DM, Mechel J, Schmitz A, Köhler K, Krone D, Bellemann N et al (2015) Evaluation of the plasmatic and parenchymal elution kinetics of two different irinotecan-loaded drug-eluting embolics in a pig model. J Vasc Interv Radiol 26:746–754
26. Baker DG, Kearney MT (2015) The need for econometric research in laboratory animal operations. Lab Anim (NY) 44:217–220
27. Thomas C, Nijenhuis AM, Timens W, Kuppen PJ, Daemen T, Scherphof GL (1993) Liver metastasis model of colon cancer in the rat: immunohistochemical characterization. Invasion Metastasis 13:102–112
28. White SB, Procissi D, Chen J, Gogineni VR, Tyler P, Yang Y et al (2016) Characterization of CC-531 as a rat model of colorectal liver metastases. PLoS ONE 11:e0155334
29. Eyol E, Boleij A, Taylor RR, Lewis AL, Berger MR (2008) Chemoembolisation of rat colorectal liver metastases with drug eluting beads loaded with irinotecan or doxorubicin. Clin Exp Metastasis 25:273–282
30. van Duijnhoven FH, Tollenaar RA, Terpstra OT, Kuppen PJ (2005) Locoregional therapies of liver metastases in a rat CC531 coloncarcinoma model results in increased resistance to tumour rechallenge. Clin Exp Metastasis 22:247–253
31. Seelig MH, Leible M, Sänger J, Berger MR (2004) Chemoembolization of rat liver metastasis with microspheres and gemcitabine followed by evaluation of tumor cell load by chemiluminescence. Oncol Rep 11:1107–1113
32. Hutteman M, Mieog JS, van der Vorst JR, Dijkstra J, Kuppen PJ, van der Laan AM et al (2011) Intraoperative near-infrared fluorescence imaging of colorectal metastases targeting integrin α(v)β(3) expression in a syngeneic rat model. Eur J Surg Oncol 37:252–257
33. Krause P, Flikweert H, Monin M, Seif Amir Hosseini A, Helms G, Cantanhede G et al (2013) Increased growth of colorectal liver metastasis following partial hepatectomy. Clin Exp Metastasis 30:681–693
34. Sperling J, Ziemann C, Gittler A, Benz-Weißer A, Menger MD, Kollmar O (2015) Tumour growth of colorectal rat liver metastases is inhibited by hepatic arterial infusion of the mTOR-inhibitor temsirolimus after portal branch ligation. Clin Exp Metastasis 32:313–321
35. Vollmar B, Menger MD (2009) The hepatic microcirculation: mechanistic contributions and therapeutic targets in liver injury and repair. Physiol Rev 98:1269–1339
36. Oda M, Yokomori H, Han JY (2003) Regulatory mechanisms of hepatic microcirculation. Clin Hemorheol Microcirc 29:167–182

37. Koo A, Liang IY, Cheng KK (1975) The terminal hepatic microcirculation in the rat. Q J Exp Physiol Cogn Med Sci 60:261–266
38. Gonda T, Ishida H, Yoshinaga K, Sugihara K (2000) Microvasculature of small liver metastases in rats. J Surg Res 94:43–48
39. Buck A, Halbritter S, Späth C, Feuchtinger A, Aichler M, Zitzelsberger H et al (2015) Distribution and quantification of irinotecan and its active metabolite SN-38 in colon cancer murine model systems using MALDI MSI. Anal Bioanal Chem 407:2107–2116
40. Martignoni M, Groothuis GM, de Kanter R (2006) Species differences between mouse, rat, dog, monkey and human CYP-mediated drug metabolism, inhibition and induction. Expert Opin Drug Metab Toxicol 2:875–894
41. Chabot GG (1997) Clinical pharmacokinetics of irinotecan. Clin Pharmacokinet 33:245–259
42. http://pharmacept.com/en/produkte/EmboCept-s-ubersicht/
43. Pieper CC, Meyer C, Vollmar B, Hauenstein K, Schild HH, Wilhelm KE (2015) Temporary arterial embolization of liver parenchyma with degradable starch microspheres (EmboCept® S) in a swine model. Cardiovasc Intervent Radiol 38:435–441
44. Bhutiani N, Akinwande O, Martin RC III (2016) Efficacy and toxicity of hepatic intra-arterial drug-eluting (irinotecan) bead (DEBIRI) therapy in irinotecan-refractory unresectable colorectal liver metastases. World J Surg 40:1178–1190

6.1.3 Selumetinib

Physiologically based pharmacokinetic modeling of the MEK 1/2 inhibitor selumetinib: impact of pharmaceutical formulation and co-variates on the plasma disposition.

Gruber A, Czejka M.

AAPS PharmSciTech. *Submitted 2019*

AAPS PharmSciTech

Physiologically based pharmacokinetic modeling of the MEK 1/2 inhibitor selumetinib: impact of pharmaceutical formulation and co-variates on the plasma disposition

--Manuscript Draft--

Manuscript Number:	
Full Title:	Physiologically based pharmacokinetic modeling of the MEK 1/2 inhibitor selumetinib: impact of pharmaceutical formulation and co-variates on the plasma disposition
Article Type:	Research Article
Section/Category:	NOT APPLICABLE (Choose this section if you have NOT been invited to submit a manuscript)
Keywords:	PBPK modeling, selumetinib, BCS class IV, formulation, co-variates
Corresponding Author:	Andrea Gruber, Mag. Universitat Wien Vienna, Vienna AUSTRIA
Corresponding Author Secondary Information:	
Corresponding Author's Institution:	Universitat Wien
Corresponding Author's Secondary Institution:	
First Author:	Andrea Gruber, Mag.
First Author Secondary Information:	
Order of Authors:	Andrea Gruber, Mag.
	Martin Czejka, Univ.-Prof Mag. Dr.
Order of Authors Secondary Information:	
Manuscript Region of Origin:	AUSTRIA
Abstract:	The MEK 1/2 inhibitor selumetinib has been administered to patients in a suspension and a capsule formulation, each containing an excipient to enhance the bioavailability of the drug. Resulting plasma-concentrations varied distinctly between the two formulations and additionally included a high interpatient variability. A physiologically-based pharmacokinetic (PBPK) model was created to analyze the impact of the applied bioavailability-enhancing excipients Captisol® and TPGS on the absorption of the drug. The pharmacokinetic profiles of the two formulations showed a superior plasma disposition for the TPGS formulation, with an increased dose normalized (DN) Cmax by 2.78- and 2.81-fold and DN AUCinf by 1.97- and 1.84-fold, respectively in patients and simulation, compared to the Captisol® formulation. A parameter sensitivity analysis of the absorption parameters revealed an increased solubilization and permeability for selumetinib in the TPGS formulation and an increased intestinal solubility for the combination with Captisol®, resulting in an improved bioavailability for both formulations, compared to the application without excipients. Furthermore, the impact of physiological influences was evaluated in the model, to investigate the observed variability in the selumetinib plasma disposition. Changes in the plasma protein binding rate and hepatic clearance both significantly influenced the plasma concentration of selumetinib and are thus responsible for a basic variation in patients, depending on the physiological condition, state of disease or co-medication of the patient. PBPK modelling is a potent tool to understand the mechanisms responsible for highly variable plasma concentrations and can therefore provide support in both drug development and clinical practice.
Suggested Reviewers:	
Opposed Reviewers:	

Research Article

Physiologically based pharmacokinetic modeling of the MEK 1/2 inhibitor selumetinib: impact of pharmaceutical formulation and co-variates on the plasma disposition

Andrea Gruber[1] • Martin Czejka[1]

A. Gruber (0000-0001-8298-5090, ✉)• M. Czejka (0000-0002-9754-0921)

[1]Division of Clinical Pharmacy and Diagnostics, Faculty of Life Sciences, University of Vienna, Althanstrasse 14, A-1090 Vienna, Austria

Phone: +43-1-4277-55581

e-mail: andrea.gruber@univie.ac.at

Running head: Selumetinib PBPK model– formulation + co-variates

Abstract

The MEK 1/2 inhibitor selumetinib has been administered to patients in a suspension and a capsule formulation, each containing an excipient to enhance the bioavailability of the drug. Resulting plasma-concentrations varied distinctly between the two formulations and additionally included a high interpatient variability. A physiologically-based pharmacokinetic (PBPK) model was created to analyze the impact of the applied bioavailability-enhancing excipients Captisol® and TPGS on the absorption of the drug. The pharmacokinetic profiles of the two formulations showed a superior plasma disposition for the TPGS formulation, with an increased dose normalized (DN) C_{max} by 2.78- and 2.81-fold and DN AUC_{inf} by 1.97- and 1.84-fold, respectively in patients and simulation, compared to the Captisol® formulation. A parameter sensitivity analysis of the absorption parameters revealed an increased solubilization and permeability for selumetinib in the TPGS formulation and an increased intestinal solubility for the combination with Captisol®, resulting in an improved bioavailability for both formulations, compared to the application without excipients. Furthermore, the impact of physiological influences was evaluated in the model, to investigate the observed variability in the selumetinib plasma disposition. Changes in the plasma protein binding rate and hepatic clearance both significantly influenced the plasma concentration of selumetinib and are thus responsible for a basic variation in patients, depending on the physiological condition, state of disease or co-medication of the patient. PBPK modelling is a potent tool to understand the mechanisms responsible for highly variable plasma concentrations and can therefore provide support in both drug development and clinical practice.

Introduction

Physiologically based pharmacokinetic (PBPK) modeling has become an increasingly important method in drug development to predict and visualize the performance of a drug candidate in their respective formulation and physiological environment. PBPK models can help to better understand the pharmacokinetic (PK) profile of a drug, including underlying mechanisms, to identify problems for the intended clinical use, based on the physicochemical properties of the compound and the physiological parameters of the target population (1-8). This is especially useful for drugs with a high variability in their plasma concentration-time profile. Additionally, the biopharmaceutics classification system (BCS) has proven to be a useful scientific framework for an assessment of the absorption process, based on the solubility and permeability characteristics of the compound. It has been introduced by Amidon et al and was originally intended for regulatory bioequivalence issues (9), however it is now also commonly used in drug discovery and development (10-11). It classifies orally administered drugs into four different classes, depending on the magnitude of their key absorption parameters aqueous solubility and intestinal permeability (12-14). However, also physiological parameters, as well as dosage forms and formulations of a drug can influence the absorption rate and consequently the characteristics and BCS classification as well as the bioavailability of the compound (15). Dealing with low solubility and low permeability drugs is becoming an increasingly pressing issue, since many of the pipeline drugs exhibit these characteristics (16). Therefore, various strategies have emerged to enhance the absorption rate of a compound, such as particle size reduction, nano-formulations, crystal engineering or the use of excipients for inclusion-complexes, lipid-based technologies or self-emulsifying systems (17-22). Excipients are inactive additives, used to modify the solubility and hence increase the absorption and bioavailability of a drug. Additionally, some excipients have shown to inhibit the P-glycoprotein (P-gp) transporter and thus drug efflux from enterocytes, which can also lead to a higher effective intestinal permeability and therefore a higher bioavailability of the compound (23-24). However, modifying the physicochemical properties of a compound and therefore altering the balance between solubility and permeability is delicate and may result in a tradeoff. Improving the solubility and hydrophilicity might at the same time decrease the permeability through the intestinal membrane and thus lead to an unwanted effect of an overall reduced bioavailability (25). To assess the effect of an excipient on the absolute bioavailability of the compound, changes to both, solubility and permeability should be considered.

In this study, a PBPK model of selumetinib (AZD6244, Astra Zeneca), an orally administered MEK 1/2 inhibitor (26) was used to demonstrate the effect of different formulations on the absorption and bioavailability of the drug as well as to identify additional parameters responsible for the high variability in the plasma disposition of patients. In vitro and in vivo literature data of two formulations, including different dose strengths was used to establish the PBPK model with the software GastroPlus™ (Simulations Plus Inc., CA.) and validate the simulated plasma concentration-time profile. Selumetinib is a lipophilic compound with low aqueous solubility and low to moderate permeability and is therefore

classified as BCS class IV drug (27). It has a considerably high protein binding rate and is eliminated hepatically (28). It has been administered to patients in two formulations each containing a different excipient, to enhance its absorption rate. Variations in plasma concentration were therefore expected from the formulation differences. The impact of the excipients on the absorption and bioavailability of selumetinib can be demonstrated in a PBPK model as well as additional influences in absorption, distribution, metabolism and excretion (ADME) parameters. Some co-variates have already been identified by previous studies (27-32), but their effect on the plasma concentration has not been evaluated in a PBPK model yet. Several physiological and pharmacokinetic co-variates were therefore selected for assessment, such as administration to a fed state, pH changes in the stomach due to a possible co-medication of acid reducing agents (ARAs), changes in protein binding, body weight or age and impairment of hepatic or renal function.

Materials and methods

Data evaluation

Table I

In vivo PK data of selumetinib was assessed from 11 clinical phase I-III trials, published between 2010-2017, for comparison and validation of the PBPK model. The evaluated studies are listed in Table I (27,32-41). The first in human studies of selumetinib were conducted with a “mix and drink” suspension of 100 mg selumetinib free base, formulated in 30 ml 25% (v/w) aqueous solution of Captisol®, a substituted cyclodextrin, as excipient. In further studies, the suspension was replaced by a capsule formulation of 75 mg selumetinib hydrogen sulfate, formulated with Tocophersolan, a water-soluble vitamin E derivative, as excipient. The PK parameters C_{max}, AUC_{inf} and T_{max} as well as clearance (Cl), volume of distribution (Vd) and elimination half-life ($T_{1/2el}$) were evaluated from single dose administrations of selumetinib monotherapy. The capsule formulation has been further investigated in patients regarding food effect and hepatic and renal impairment (27-28,32).

Excipients

Captisol®, a sulfobutylether-β-cyclodextrin (SBE-βCD), is used to enhance the solubility of poorly soluble compounds (42-45). The cyclodextrin structure consists of a hydrophilic surface and a lipophilic central cavity and can thus form water-soluble inclusion complexes with lipophilic compounds, such as selumetinib. In an aqueous solution, the complex and the free fraction of the drug are in dynamic equilibrium. Although the solubility strongly increases through the complexation, the permeability has been observed to decrease for many compounds when combined with cyclodextrins (46-50). Literature revealed various effects of cyclodextrin complexation on the overall bioavailability of compounds, from decreased or unchanged to increased bioavailability (25). An increase in bioavailability can result from

71 an enhanced availability of drug in solution and reduced precipitation at the absorption site, due to the
72 constant release of drug from the complex and its stabilizing effects (42,51). However, the
73 bioavailability can also decrease through the complexation, when a major fraction of the drug is bound
74 and consequently unavailable for permeation, therefore an excess of cyclodextrin is not recommended
75 for a drug formulation (51). Although the mechanistic understanding of the excipient-drug-reaction has
76 advanced, it still underlies many compound-individual variations.

77 Tocophersolan, D-α-tocopheryl polyethylene glycol 1000 succinate (TPGS), is used as solubility and
78 permeability enhancer for poorly performing compounds (52-54). It has an amphiphilic structure with a
79 hydrophilic head and lipophilic tail and assembles to stable micelles in aqueous environment. It can
80 incorporate lipophilic molecules into the micelles to increase their solubility and further the permeation
81 through the intestinal membrane. Its ability as surfactant is also important to prevent nucleation and
82 subsequent precipitation of poorly soluble drugs at the absorption site (55). Moreover, TPGS also
83 showed effective inhibitory function to P-gp (56) and has been hence described to further increase the
84 permeability and overall bioavailability in many drugs susceptible to P-gp efflux. TPGS can be
85 formulated in self-emulsifying/micro-emulsifying drug delivery systems (SEDDs/SMEDDs) as solid
86 dispersions (17,19), which can be then encapsulated for an easier drug administration and higher
87 compliance.

88 *PBPK modeling*

89 Table II

90 The software GastroPlus™ 9.6 (Simulations Plus Inc., Lancaster, CA) was used to build the PBPK
91 model of selumetinib, based on literature data and predictions from the ADMET Predictor™ module of
92 the software. The input parameters are summarized in Table II. Values for the physicochemical
93 parameters lipophilicity (logP), ionization constant (pKa) and solubility, the distribution parameters
94 protein binding (fraction unbound in plasma) and blood/plasma ratio as well as the hepatic clearance
95 were included according to literature (27-29,37). The permeability was estimated for a low to moderately
96 permeable compound (8,27). The total body clearance of the in vivo studies was integrated as hepatic
97 clearance in the model, since selumetinib has not shown significant gut metabolism or renal excretion.
98 The gut physiology was set to a fasted state. This basic model was used to assess the impact of a
99 simultaneous change of the main absorption related parameters permeability and solubility on the
100 bioavailability of selumetinib in a 3D parameter sensitivity analysis (PSA). However, the absorption
101 process for a highly lipophilic compound with low aqueous solubility can also depend on further
102 parameters, such as the solubilization ratio, which describes the solubility increase through bile salt
103 solubilization in the intestine, as well as the particle size of the formulation or the precipitation time in
104 the intestine. Therefore, the absorption related parameters were optimized for each formulation, using
105 the Optimization module of GastroPlus™ and a population simulation was conducted to subsequently
106 compare and validate the simulations with the respective reported plasma concentration-time data.

Influences of formulation and co-variates

The models of both formulations were used to describe the influence of the excipients from the two formulations on the absorption and pharmacokinetic profile of selumetinib by PSA. Additionally, the simulation of the TPGS-selumetinib capsule was used to demonstrate the effect of further co-variates on the plasma concentration of the compound. Possible influences of seven co-variates on the variability of selumetinib plasma concentration were considered. The absorption of BCS class IV compounds can be altered by concomitant food intake (27,32). Usually in a fed state, the stomach pH increases from about 1-2 to 4-5 and the transit time prolongs from 15 min to about 1 h, which often results in varied absorption kinetics compared to a fasted state administration (57). ARAs are frequently combined with oral chemotherapeutic agents because of a prevalent appearance of gastrointestinal side effects of these drugs. The triggered increase in stomach pH can alter the solubility and consequently the absorption of the chemotherapeutic agent, if the solubility of the drug is low and pH-dependent (58). As a lipophilic drug, selumetinib is considerably distributed into tissues, therefore age and body weight were assumed to be a likely co-variate (29). Since selumetinib is highly bound to plasma proteins, it was expected that even a minor variation of the unbound fraction would result in a significantly altered plasma concentration (28). The hepatic clearance is the major elimination route and the plasma concentration of selumetinib is therefore presumably sensitive to changes in this parameter, whereas changing the renally eliminated fraction should not result in significant changes (28).

Results

Analysis of literature data

Table III

The selumetinib PK parameters evaluated from literature are listed in Table III, of both, the suspension and the capsule formulation. It comprises PK data from published clinical trials (see Table I) of 68 patients receiving the “mix and drink” suspension with 100 mg selumetinib free base and 484 patients receiving the capsule formulation with 75 mg selumetinib hydrogen sulfate salt. Since the composition of phase II and phase III capsule shells differ by minor qualitative changes, a bioavailability trial was conducted, but concluded a similar exposure for both formulations, even though the phase III formulation resulted in a marginally reduced C_{max}, compared to the phase II capsule (32). However, the reported variation is still within the C_{max} range of the evaluated literature data of the capsule formulation, therefore the PK results of phase II and III capsules were combined in this data analysis. The reported mean C_{max} values for the suspension ranged from 486-807 ng/ml and from 1150-1537 ng/ml for the capsule. AUC_{inf} mean values ranged from 2700-3299 ng-h/ml and 3680-6335 ng-h/ml in the respective groups. T_{max} median values were between 1-1,5 h for both formulations. To enable a better comparison of the two formulations, dose normalized (DN) values were calculated. Values increased by 2.78-fold

142 for DN C_{max} and 1.97-fold for DN AUC_{inf} from the suspension to the capsule formulation. The absolute
143 bioavailability of the capsule formulation was calculated to be 62% (39) and the reported relative
144 increase of bioavailability from the suspension to the capsule formulation, based on DN AUC_{0-24}, was
145 calculated to be 263% (36). Both, Cl and Vd appeared to be higher in the suspension group with 29.0-
146 44.4 l/h and 365.0-415.0 l respectively, compared to the capsule group with 12.1-21.5 l/h and 89.3-
147 175.2 l. $T_{1/2el}$ was observed in all trials in a similar range of 4.5-13.7 h and therefore remained unaffected
148 from the galenic formulation.

149 *PBPK simulations*

150 Fig. 1.

151 The basic model, built from ADMET Predictor™ calculations and literature data resulted in a low
152 fraction absorbed of 12.5%, as well as a low bioavailability of 7.6%, as expected for a BCS class IV
153 compound. The model was used to demonstrate the effect of increased absorption parameters on the
154 bioavailability of selumetinib. The 3D PSA (Fig. 1) showed the sensitivity of the absolute bioavailability
155 towards increasing values of the absorption parameters solubility and permeability. A distinct
156 augmentation in solubility could improve the bioavailability up to approximately 40%. Any further
157 increase in bioavailability to the reported 62% for the capsule formulation involved an additional
158 enhancement of the compound's intestinal permeability. The model can be used to evaluate the potential
159 risk of a tradeoff between solubility and permeability and its effect on the bioavailability and plasma
160 disposition of the compound, thus facilitating the process of formulation development.

161 Table IV

162 Fig. 2.

163 The models of the two selumetinib formulations were generated by optimizing the absorption related
164 parameters to fit the evaluated literature data for further investigation. The resulting PK parameters and
165 plasma concentration-time profiles of the respective population simulations are shown in Table IV and
166 Fig. 2. Plasma concentration-time data has also been transformed into logarithmic values to illustrate
167 the biphasic course of the curve, indicating a two-compartment model; 2-3 h after administration, the
168 distribution phase terminates, and the elimination phase predominates. The optimization of the
169 suspension formulation resulted in a strong increase of the solubilization ratio (SR), highlighting the
170 importance of the solubility of the compound in the intestinal fluid and only a modest change in
171 permeability. Due to the increased SR there was no further change in the intrinsic solubility. The
172 resulting mean C_{max} of the population simulation for the suspension was 484 ng/ml in a 90% CI range
173 of 401-566 ng/ml and the mean AUC_{inf} value was 3019 ng-h/ml in a 90% CI range of 2771-3814 ng-
174 h/ml. T_{max} was reached after 1.44 h (1.37-1.56 h) and the calculated bioavailability (F%) of the
175 population simulation was 47.8%. The optimization of the capsule formulation included a strong
176 increase in both, permeability and SR, compared to the basic model as well as a prolonged precipitation

177 time, indicating a higher stability of the compound in the intestine. The resulting mean C_{max} of the
178 population simulation for the capsule formulation was 1014 ng/ml in a 90% CI range of 933-1095 ng/ml
179 and the corresponding mean AUC_{inf} value was 4171 ng-h/ml in a 90% CI range of 3721-4623 ng-h/ml.
180 The mean T_{max} was reached after 0.74 h (0.7-0.83 h) and the calculated absolute bioavailability of the
181 simulation was 65.7%. To compare the simulated PK parameters of the different formulations and dose
182 strengths, DN values were calculated and resulted in similar values as the reported literature data, with
183 an increase from the suspension to the capsule formulation for DN C_{max} by 2.81-fold and for DN AUC_{inf}
184 by 1.84-fold. However, even though the simulations achieved a good fit with the reported PK profiles,
185 the relative increase in simulated bioavailability resulted in only 137%, and thus differed significantly
186 from the value described in literature (36). Therefore, additional parameters influencing the plasma
187 disposition of the compound were evaluated.

188 *Impact of formulation and physiological co-variates on the plasma disposition*

189 Fig. 3.

190 To evaluate the influence of the optimized absorption values on the PBPK models, PSAs were conducted
191 for both formulations. Fig. 3 shows the sensitivity of the PK parameters C_{max} (Fig. 3a) AUC (Fig. 3b),
192 T_{max} (Fig. 3c) and bioavailability (F%) (Fig. 3d) in the Captisol® suspension model of selumetinib
193 towards the permeability and SR of the compound. All four parameters were strongly influenced by the
194 enhanced SR and only to a minor extent by the permeability. Optimizing the SR value in the PBPK
195 model increased C_{max} by 6.3-fold, the AUC by 2.7-fold and the F% by 2.9-fold compared to the basic
196 model. This enhancement shows that a higher availability of dissolved drug in the intestine has a distinct
197 effect on the plasma disposition of the drug. The higher solubility in the intestinal fluids also reduced
198 T_{max} by 2.8-fold, indicating a quicker uptake from the intestine. Since the optimization of the
199 permeability resulted in only a small change compared to the basic model, its contribution to the
200 enhanced plasma disposition of selumetinib in the suspension formulation is limited. C_{max} increased by
201 1.25-fold through optimizing the permeability, AUC by 1.23-fold, F% by 1.2-fold and T_{max} was reduced
202 by 2.25-fold. However, even though the effect of permeability within the range of the optimization on
203 the plasma disposition was small, the PSA indicates that an onward rise in permeability can further
204 increase C_{max}, AUC and F%, contrarily to an additional enhancement of SR. Based on literature, the
205 expected effect of Captisol® was an increased solubility and therefore an increased bioavailability,
206 matching the outcome of the PSA and the GastroPlus™ optimization. The excipient was not associated
207 with an enhanced intestinal permeability (44,48).

208 Fig. 4.

209 Fig. 4 depicts the sensitivity of C_{max} (Fig. 4a), AUC (Fig. 4b), T_{max} (Fig. 4c) and F% (Fig. 4d) in the
210 TPGS capsule simulation of selumetinib towards the optimized absorption parameters permeability and
211 SR. On the contrary to the suspension model, the capsule simulation is considerably dependent on both

212 parameters. Optimizing SR enhanced C_{max} by 2.3-fold and reduced T_{max} by 1.75-fold, compared to a
213 2.7-fold increase of C_{max} and 2.8-fold decrease of T_{max} by optimizing the permeability. Although the
214 effect of both parameters on C_{max} is similar in the optimized range, only an additional increase of
215 intestinal permeability has the potential to further enhance C_{max}, in opposition to the intestinal solubility,
216 which shows a limited effect on the peak plasma concentration. However, altering the absorption
217 parameters showed minimal effect on the plasma disposition of the selumetinib capsule simulation, with
218 an increase of 4% by SR and 14% by permeability for the AUC as well as 2% and 11% respectively for
219 the F%. Moreover, a further enhancement of both absorption parameters did not result in an additional
220 growth of AUC and F%. As described in literature, TPGS was expected to enhance both, solubility and
221 permeability of selumetinib, due to its stabilizing and solubilizing effects and surfactant characteristics
222 (55).

223 The PSAs showed that the optimization of the absorption parameters produced similar results for the
224 characterization of the excipients Captisol® and TPGS as reported in literature. However, the PBPK
225 model also demonstrated, that the high variations in the patient plasma profiles of selumetinib not only
226 derived from formulation differences and varying absorption parameters. The PBPK model of the
227 capsule formulation was therefore used to illustrate the impact of several physiological co-variates on
228 the selumetinib plasma concentration, to better explain the high variability in the data obtained from
229 patients. The influences of selected clinically relevant co-variates are displayed in Fig. 5.

230 Fig. 5.

231 The absorption of a BCS class IV compound is usually altered positively by concomitant food intake,
232 resulting in an increase in AUC and bioavailability. However, in this case the excipient TPGS changed
233 the properties and BCS classification of the compound and consequently the food effect. It has been
234 shown in patients that concomitant food intake negatively affected the absorption of selumetinib,
235 resulting in a reduced C_{max} by 50-62% and a minimal decrease in AUC_{inf} by 16-19% (27,32). T_{max} was
236 delayed by 1.5-2.5 h. Simulating a fed state in the model decreased C_{max} by 32%, whereas AUC_{inf}
237 remained unchanged and T_{max} increased by 0.2 h, which does not correspond to the reported data. Yet,
238 by additionally prolonging the transit time in the stomach, C_{max} was reduced by 58%, AUC_{inf} by 19%
239 and T_{max} was prolonged by 2.5-fold (Fig. 5a). Otherwise, eliminating the positive effect of TPGS on the
240 permeability reduced C_{max} by 50% and prolonged T_{max} by 2-fold thus suggesting either an altered
241 transportation of the capsule through the intestine when administered with food, or an instability of the
242 TPGS micelles in the presence of food. In both cases, the calculated F% was only reduced
243 insignificantly. Another possible co-variate could be the concomitant administration of ARAs, which
244 are used to reduce the frequently occurring gastrointestinal side effects of many chemotherapeutic agents
245 through elevating the stomach pH. A weakly acidic environment can significantly decline the solubility
246 of a weak base such as selumetinib and might result in an inferior absorption and plasma concentration
247 (57-59). The combination of ARAs with selumetinib has not yet been reported in patients. The model

248 displayed no significant effect of a gastric pH elevation on the plasma disposition, as shown in Fig. 5b,
249 only T_{max} was minimally extended, due to a prolonged gastric emptying time, indicating a stable
250 solubility of the TPGS formulation over the physiological pH range (52). The elevated lipophilicity of
251 selumetinib correlates with a high protein binding rate, with a small unbound fraction of 0.35%. The
252 plasma concentration is therefore sensitive to small changes in the protein binding rate, which could be
253 demonstrated in Fig. 5c. Increasing the unbound fraction to 0.6% (+71%) resulted in a decreased C_{max}
254 and AUC_{inf} by 27% and 35% respectively and reducing it to 0.2% (-43%) led to higher C_{max} and AUC_{inf}
255 by 44% and 68%. The deviation from 0.2%-0.6% used in this example was measured in patients and
256 thus accounts for a basic variation in the plasma concentration (28). An equally important co-variate
257 responsible for a high variability is the hepatic clearance. Selumetinib is metabolized mainly by CYP
258 enzymes in the liver, only a small percentage is eliminated renally, therefore any changes in the hepatic
259 clearance were expected to impact the plasma concentration of selumetinib. As demonstrated in Fig. 5d,
260 elevating the hepatic clearance from 12 to 16 l/h, decreased C_{max} and AUC_{inf} by 20% and 19%
261 respectively and reducing it to 8 l/h yielded an increase in C_{max} and AUC_{inf} by 23% and 62%
262 respectively. The applied range of hepatic clearance values in the simulation was within the range of the
263 reported patient data. Both parameters, protein binding and hepatic clearance resulted in a deviation of
264 ± 15% for the calculated F% in the investigated range of variation. The impact of the physiological
265 parameters age and body weight was minimal and a reduction of the already low renal clearance did not
266 affect the plasma profile of selumetinib, as anticipated.

267

268 **Discussion**

269 The PBPK model of selumetinib was used to evaluate the PK profile of the compound and investigate
270 the potential mechanisms responsible for the high variability in plasma concentrations, observed in
271 patients. Based on the low solubility and low to moderate permeability of the compound, variations were
272 expected mainly during the absorption process. However, selumetinib was administered to patients in
273 formulations containing excipients to increase the absorption and bioavailability of the drug for an
274 effective treatment. The utilized excipients were Captisol® in a suspension and TPGS in a capsule
275 formulation, both increasing the absorption of selumetinib. The TPGS formulation was subsequently
276 selected for further development and investigation, due to the better performance concerning absorption
277 rate and bioavailability, compared to the suspension. The detailed mechanisms behind the absorption-
278 increasing effects of both excipients on the PK profile of selumetinib have however not been further
279 examined. Even though excipients can be generally characterized, they often exhibit compound-
280 individual and concentration-dependent effects. Captisol® has been described in literature as solubility
281 enhancer, but also showed the potential of decreasing the permeability of compound, presumably
282 through increased complexation and therefore reduced availability of unbound drug for absorption in
283 the intestine (46-50). The GastroPlus™ optimization as well as the PSA of selumetinib in the suspension

284 formulation showed a distinct increase in solubilization due to the cyclodextrin completion, but no
285 tradeoff in permeability. TPGS was associated with increased solubilization and stabilization through
286 micelle formation with the compound in the intestinal fluids. Consequently, a higher permeability can
287 be achieved, resulting in enhanced absorption and bioavailability of the drug. TPGS also inhibits the P-
288 gp transporter and is therefore often used in formulations of drugs susceptible to the drug efflux of P-gp
289 (56). Selumetinib possesses a high lipophilicity, which suggests adequate permeability, since lipophilic
290 molecules are likely to permeate well through membranes via passive transport, except for very large
291 molecules or a high activity of efflux transporters (19). In the case of selumetinib, the molecular weight
292 is still within the range of drug-like compounds (17), therefore the possibility of efflux transporters
293 should be further investigated to explain the low permeability. The absorption related parameters of both
294 formulation models were optimized using the GastroPlus™ Optimization module. It can calculate
295 simulation parameters to fit available plasma concentration-time data and was therefore applicable and
296 useful in the presented model. However, to describe the absorption process more detailed, in vitro-in
297 vivo correlations (IVIVC) could be performed, by implementing data on dissolution, solubility and
298 permeability of the compound in the respective formulations into the model. The model was able to
299 produce plasma concentration-time simulations in a similar range as observed in patients. DN C_{max} and
300 DN AUC_{inf} values showed a distinct increase from the suspension to the capsule formulation in both
301 data sets, with an increase by 2.78- and 2.81-fold for DN C_{max} and 1.97- and 1.84-fold for DN AUC_{inf}
302 in literature and simulation respectively. The reported relative increase in bioavailability by 263% from
303 the suspension to the capsule formulation was however not reproducible to this extent by only changing
304 the formulation dependent absorption parameters in the model. A broader evaluation of co-variates
305 responsible for variations in plasma disposition revealed the hepatic clearance and protein binding rate
306 as parameters with significant influence on the plasma profile of selumetinib. Values for both parameters
307 have been fluctuating in patients due to their physiology, different stages of the respective diseases and
308 the overall performance as well as co-medication. Even small changes in these parameters resulted in
309 relevant changes in the corresponding plasma concentration. Given, that the simulations considered just
310 one parameter at the time, the probability for higher variations strongly increases when two or more
311 parameters vary simultaneously, as will be the case in a physiological environment. Body weight and
312 age were thought to have a larger effect on the plasma concentration, however the actual effect remained
313 minimal in the tested range. The renal elimination of selumetinib is low, therefore changes in plasma
314 concentration were not expected. Patients with end-stage renal disease undergoing hemodialysis showed
315 an altered selumetinib plasma disposition, depending on the timing of drug administration and dialysis
316 (28). It was however not possible to display the impact of hemodialysis in the current model. As BCS
317 class IV drug, selumetinib was expected to exhibit an increased absorption when administered with food,
318 due to the bile salt solubilization effect (17). A higher concentration of bile salts in the intestine can
319 incorporate lipophilic molecules and therefore enhance their solubility further the permeation through
320 the intestinal membrane. However, excipients such as TPGS can change those characteristics, hence the

expected positive food effect for selumetinib resulted in a negative effect in the formulation with TPGS. This effect has already been observed in a similar case of a BCS class II compound with low solubility and high lipophilicity where an alteration of relevant absorption properties by TPGS resulted in a reduced absorption at a fed state, compared to a fasted state (2). Furthermore, drugs with weakly basic properties have often shown a significantly reduced absorption rate when co-administered with ARAs, because of a decreased solubility at a higher pH (57-62). However, due to the stable intestinal solubility of selumetinib with TPGS over the physiological pH range, the malabsorption effect through commonly co-administered ARAS is negligible.

Conclusion

The PBPK model shows the PK profile of selumetinib and the impact of two excipients on the absorption of the BCS class IV compound. The model additionally demonstrates the influence of several physiological co-variates on the plasma disposition of selumetinib and thus reveals parameters responsible for the high variability observed in plasma concentrations of patients. The goal of this study was to emphasize the potential of PBPK modeling in drug development to identify co-variates and gain understanding of the underlying mechanisms, to ensure an efficient and safe treatment for patients.

Acknowledgements

The open access funding was provided by University of Vienna.

Compliance with Ethical Standards

Conflict of interest

The authors declare that they have no conflict of interest.

References

1. Chow EC, Talattof A, Tsakalozou E, Fan J, Zhao L, Zhang X. Using Physiologically Based Pharmacokinetic (PBPK) Modeling to Evaluate the Impact of Pharmaceutical Excipients on Oral Drug Absorption: Sensitivity Analyses. AAPS J. 2016;18:1500-1511.

2. Pandey P, Hamey R, Bindra DS, Huang Z, Mathias N, Eley T et al. From bench to humans: formulation development of a poorly water soluble drug to mitigate food effect. AAPS PharmSciTech. 2014 ;15:407-416. doi: 10.1208/s12249-013-0069-4.

3. Xia B, Heimbach T, Lin TH, Li S, Zhang H, Sheng J, et al. Utility of physiologically based modeling and preclinical in vitro/in vivo data to mitigate positive food effect in a BCS class 2 compound. AAPS PharmSciTech. 2013;14:1255-1266. doi: 10.1208/s12249-013-0018-2.

4. Honório Tda S, Pinto EC, Rocha HV, Esteves VS, dos Santos TC, Castro HC, et al. In vitro-in vivo correlation of efavirenz tablets using GastroPlus®. AAPS PharmSciTech. 2013;14:1244-1254. doi: 10.1208/s12249-013-0016-4.

5. Zhang H, Xia B, Sheng J, Heimbach T, Lin TH, He H, et al. Application of physiologically based absorption modeling to formulation development of a low solubility, low permeability weak base: mechanistic investigation of food effect. AAPS PharmSciTech. 2014;15:400-406. doi: 10.1208/s12249-014-0075-1.

6. Sager JE, Yu J, Ragueneau-Majlessi I, Isoherranen N. Physiologically Based Pharmacokinetic (PBPK) Modeling and Simulation Approaches: A Systematic Review of Published Models, Applications, and Model Verification. Drug Metab Dispos. 2015;43:1823-1837. doi: 10.1124/dmd.115.065920.

7. Willmann S, Edginton AN, Kleine-Besten M, Jantratid E, Thelen K, Dressman JB. Whole-body physiologically based pharmacokinetic population modelling of oral drug administration: inter-individual variability of cimetidine absorption. J Pharm Pharmacol. 2009;61:891-899. doi: 10.1211/jpp/61.07.0008.

8. Hansmann S, Darwich A, Margolskee A, Aarons L, Dressman J. Forecasting oral absorption across biopharmaceutics classification system classes with physiologically based pharmacokinetic models. J Pharm Pharmacol. 2016;68:1501-1515. doi: 10.1111/jphp.12618.

9. Shah VP, Amidon GL. G.L. Amidon, H. Lennernas, V.P. Shah, and J.R. Crison. A theoretical basis for a biopharmaceutic drug classification: the correlation of in vitro drug product dissolution and in vivo bioavailability, Pharm Res 12, 413-420, 1995-backstory of BCS. AAPS J. 2014;16:894-898. doi: 10.1208/s12248-014-9620-9.

10. Benet LZ. The role of BCS (biopharmaceutics classification system) and BDDCS (biopharmaceutics drug disposition classification system) in drug development. J Pharm Sci. 2013;102:34-42. doi: 10.1002/jps.23359.

11. Larregieu CA, Benet LZ. Distinguishing between the permeability relationships with absorption and metabolism to improve BCS and BDDCS predictions in early drug discovery. Mol Pharm. 2014;11:1335-1344. doi: 10.1021/mp4007858.

12. Amidon GL, Lennernäs H, Shah VP, Crison JR. A theoretical basis for a biopharmaceutic drug classification: the correlation of in vitro drug product dissolution and in vivo bioavailability. Pharm Res. 1995;12:413-420.

13. Dahan A, Miller JM, Amidon GL. Prediction of solubility and permeability class membership: provisional BCS classification of the world's top oral drugs. AAPS J. 2009;11:740-746. doi: 10.1208/s12248-009-9144-x.

14. Lennernäs H, Abrahamsson B. The use of biopharmaceutic classification of drugs in drug discovery and development: current status and future extension. J Pharm Pharmacol. 2005;57:273-285.

15. Dahan A, Miller JM, Hoffman A, Amidon GE, Amidon GL. The solubility-permeability interplay in using cyclodextrins as pharmaceutical solubilizers: mechanistic modeling and application to progesterone. J Pharm Sci. 2010;99:2739-2749. doi: 10.1002/jps.22033.

395 16. Lipinski CA1, Lombardo F, Dominy BW, Feeney PJ. Experimental and computational approaches
396 to estimate solubility and permeability in drug discovery and development settings. Adv Drug Deliv
397 Rev. 2001;46:3-26.

398 17. Ghadi R, Dand N. BCS class IV drugs: Highly notorious candidates for formulation development. J
399 Control Release. 2017;248:71-95. doi: 10.1016/j.jconrel.2017.01.014.

400 18. Zheng W, Jain A, Papoutsakis D, Dannenfelser RM, Panicucci R, Garad S. Selection of oral
401 bioavailability enhancing formulations during drug discovery. Drug Dev Ind Pharm. 201;38:235-247.
402 doi: 10.3109/03639045.2011.602406.

403 19. Gupta S, Kesarla R, Omri A. Formulation strategies to improve the bioavailability of poorly
404 absorbed drugs with special emphasis on self-emulsifying systems. ISRN Pharm. 2013;2013:848043.
405 doi: 10.1155/2013/848043.

406 20. Savjani KT1, Gajjar AK, Savjani JK. Drug solubility: importance and enhancement techniques.
407 ISRN Pharm. 2012;2012:195727. doi: 10.5402/2012/195727.

408 21. B Shekhawat P, B Pokharkar V. Understanding peroral absorption: regulatory aspects and
409 contemporary approaches to tackling solubility and permeability hurdles. Acta Pharm Sin B.
410 2017;7:260-280. doi: 10.1016/j.apsb.2016.09.005.

411 22. Kollipara S, Gandhi RK. Pharmacokinetic aspects and in vitro-in vivo correlation potential for lipid-
412 based formulations. Acta Pharm Sin B. 2014;4:333-49. doi: 10.1016/j.apsb.2014.09.001.

413 23. Hetal PT, Jagruti LD. Influence of excipients on drug absorption via modulation of intestinal
414 transporters activity. Asian J Pharmaceutics. 2015;9:69-82. doi: 10.4103/0973-8398.154688

415 24. de Gooijer MC, Zhang P, Weijer R, Buil LCM, Beijnen JH, van Tellingen O. The impact of P-
416 glycoprotein and breast cancer resistance protein on the brain pharmacokinetics and pharmacodynamics
417 of a panel of MEK inhibitors. Int J Cancer. 2018;142:381-391. doi: 10.1002/ijc.31052.

418 25. Avdeef A, Kansy M, Bendels S, Tsinman K. Absorption-excipient-pH classification gradient maps:
419 sparingly soluble drugs and the pH partition hypothesis. Eur J Pharm Sci. 2008;33:29-41.

420 26. Ciombor KK, Bekaii-Saab T. Selumetinib for the treatment of cancer. Expert Opin Investig Drugs.
421 2015;24:111-123.

422 27. Leijen S, Soetekouw PM, Jeffry Evans TR, Nicolson M, Schellens JH, Learoyd M, et al. A phase I,
423 open-label, randomized crossover study to assess the effect of dosing of the MEK 1/2 inhibitor
424 Selumetinib (AZD6244; ARRY-142866) in the presence and absence of food in patients with advanced
425 solid tumors. Cancer Chemother Pharmacol. 2011;68:1619-1628. doi: 10.1007/s00280-011-1732-7.

426 28. Dymond AW, Martin P, So K, Huang Y, Severin P, Holmes V, et al. Pharmacokinetics of a Single
427 Oral Dose of the MEK1/2 Inhibitor Selumetinib in Subjects With End-Stage Renal Disease or Varying
428 Degrees of Hepatic Impairment Compared With Healthy Subjects. J Clin Pharmacol. 2017;57:592-605.
429 doi: 10.1002/jcph.848.

430 29. Patel P, Howgate E, Martin P, Carlile DJ, Aarons L, Zhou D. Population pharmacokinetics of the
431 MEK inhibitor selumetinib and its active N-desmethyl metabolite: data from 10 phase I trials. Br J Clin
432 Pharmacol. 2018;84:52-63. doi: 10.1111/bcp.13404.

433 30. Patel YT, Daryani VM, Patel P, Zhou D, Fangusaro J, Carlile DJ et al. Population Pharmacokinetics
434 of Selumetinib and Its Metabolite N-desmethyl-selumetinib in Adult Patients With Advanced Solid
435 Tumors and Children With Low-Grade Gliomas. CPT Pharmacometrics Syst Pharmacol. 2017;6:305-
436 314. doi: 10.1002/psp4.12175.

437 31. Seto T, Hirai F, Saka H, Kogure Y, Yoh K, Niho S, et al. Safety and tolerability of selumetinib as a
438 monotherapy, or in combination with docetaxel as second-line therapy, in Japanese patients with
439 advanced solid malignancies or non-small cell lung cancer. Jpn J Clin Oncol. 2018;48:31-42. doi:
440 10.1093/jjco/hyx144.

441 32. Tomkinson H, McBride E, Martin P, Lisbon E, Dymond AW, Cantarini M, et al. Comparison of the
442 Pharmacokinetics of the Phase II and Phase III Capsule Formulations of Selumetinib and the Effects of
443 Food on Exposure: Results From Two Randomized Crossover Trials in Healthy Male Subjects. Clin
444 Ther. 2017;39:2260-2275.e1. doi: 10.1016/j.clinthera.2017.08.022.

445 33. Adjei AA, Cohen RB, Franklin W, Morris C, Wilson D, Molina JR, et al. Phase I pharmacokinetic
446 and pharmacodynamic study of the oral, small-molecule mitogen-activated protein kinase kinase 1/2
447 inhibitor AZD6244 (ARRY-142886) in patients with advanced cancers. J Clin Oncol. 2008;26:2139-
448 2146. doi: 10.1200/JCO.2007.14.4956.

449 34. Banerji U, Camidge DR, Verheul HM, Agarwal R, Sarker D, Kaye SB, et al. The first-in-human
450 study of the hydrogen sulfate (Hyd-sulfate) capsule of the MEK1/2 inhibitor AZD6244 (ARRY-
451 142886): a phase I open-label multicenter trial in patients with advanced cancer. Clin Cancer Res.
452 2010;16:1613-1623. doi: 10.1158/1078-0432.CCR-09-2483.

453 35. O'Neil BH, Goff LW, Kauh JS, Strosberg JR, Bekaii-Saab TS, Lee RM, et al. Phase II study of the
454 mitogen-activated protein kinase 1/2 inhibitor selumetinib in patients with advanced hepatocellular
455 carcinoma. J Clin Oncol. 2011;29:2350-2356. doi: 10.1200/JCO.2010.33.9432.

456 36. Bridgewater J, Lopes A, Beare S, Duggan M, Lee D, Ricamara M, et al. A phase 1b study of
457 Selumetinib in combination with Cisplatin and Gemcitabine in advanced or metastatic biliary tract
458 cancer: the ABC-04 study. BMC Cancer. 2016;16:153. doi: 10.1186/s12885-016-2174-8.

459 37. Dymond AW, Howes C, Pattison C, So K, Mariani G, Savage M, et al. Metabolism, Excretion, and
460 Pharmacokinetics of Selumetinib, an MEK1/2 inhibitor, in Healthy Adult Male Subjects. Clin Ther.
461 2016;38:2447-2458. doi: 10.1016/j.clinthera.2016.09.002.

462 38. Zhou D, So K, Dymond AW, Vik T, Al-Huniti N, Mariani G, et al. Evaluation of the Effect of
463 Selumetinib on Cardiac Repolarization: A Randomized, Placebo- and Positive-controlled Crossover
464 QT/QTc Study in Healthy Subjects. Clin Ther. 2016;38:2555-2566. doi:
465 10.1016/j.clinthera.2016.10.004.

466 39. Dymond AW, So K, Martin P, Huang Y, Severin P, Mathews D, et al. Effects of cytochrome P450
467 (CYP3A4 and CYP2C19) inhibition and induction on the exposure of selumetinib, a MEK1/2 inhibitor,
468 in healthy subjects: results from two clinical trials. Eur J Clin Pharmacol. 2017;73:175-184. doi:
469 10.1007/s00228-016-2153-7.

470 40. Dymond AW, Elks C, Martin P, Carlile DJ, Mariani G, Lovick S, et al. Pharmacokinetics and
471 pharmacogenetics of the MEK1/2 inhibitor, selumetinib, in Asian and Western healthy subjects: a
472 pooled analysis. Eur J Clin Pharmacol. 2017;73:717-726. doi: 10.1007/s00228-017-2217-3.

473 41. LoRusso PM, Infante JR, Kim KB, Burris HA 3rd, Curt G, Emeribe U, et al. A phase I dose-
474 escalation study of selumetinib in combination with docetaxel or dacarbazine in patients with advanced
475 solid tumors. BMC Cancer. 2017;17:173. doi: 10.1186/s12885-017-3143-6.

476 42. Loftsson T, Jarho P, Másson M, Järvinen T. Cyclodextrins in drug delivery. Expert Opin Drug Deliv.
477 2005;2:335-351.

478 43. Rao VM, Stella VJ. When can cyclodextrins be considered for solubilization purposes? J Pharm Sci.
479 2003;92:927-932.

480 44. Gidwani B, Vyas A. A Comprehensive Review on Cyclodextrin-Based Carriers for Delivery of
481 Chemotherapeutic Cytotoxic Anticancer Drugs. Biomed Res Int. 2015;2015:198268. doi:
482 10.1155/2015/198268.

483 45. Fukuda M, Miller DA, Peppas NA, McGinity JW. Influence of sulfobutyl ether beta-cyclodextrin
484 (Captisol) on the dissolution properties of a poorly soluble drug from extrudates prepared by hot-melt
485 extrusion. Int J Pharm. 2008;350:188-196.

486 46. Dahan A, Miller JM, Hoffman A, Amidon GE, Amidon GL. The solubility-permeability interplay
487 in using cyclodextrins as pharmaceutical solubilizers: mechanistic modeling and application to
488 progesterone. J Pharm Sci. 2010;99:2739-2749. doi: 10.1002/jps.22033.

489 47. Beig A, Agbaria R, Dahan A. Oral delivery of lipophilic drugs: the tradeoff between solubility
490 increase and permeability decrease when using cyclodextrin-based formulations. PLoS One.
491 2013;8:68237. doi: 10.1371/journal.pone.0068237.

492 48. Beig A, Agbaria R, Dahan A. The use of captisol (SBE7-β-CD) in oral solubility-enabling
493 formulations: Comparison to HPβCD and the solubility-permeability interplay. Eur J Pharm Sci.
494 2015;77:73-78. doi: 10.1016/j.ejps.2015.05.024.

495 49. Miller JM, Dahan A. Predicting the solubility-permeability interplay when using cyclodextrins in
496 solubility-enabling formulations: model validation. Int J Pharm. 2012;430:388-391. doi:
497 10.1016/j.ijpharm.2012.03.017.

498 50. Beig A, Miller JM, Dahan A. The interaction of nifedipine with selected cyclodextrins and the
499 subsequent solubility-permeability trade-off. Eur J Pharm Biopharm. 2013;85:1293-1299. doi:
500 10.1016/j.ejpb.2013.05.018.

501 51. Loftsson, T. Cyclodextrins and the Biopharmaceutics Classification System of Drugs. Journal of
502 Inclusion Phenomena 2002;44:63-67. https://doi.org/10.1023/A:1023088423667

503 52. Guo Y, Luo J, Tan S, Otieno BO, Zhang Z. The applications of Vitamin E TPGS in drug delivery.
504 Eur J Pharm Sci. 2013;49:175-186. doi: 10.1016/j.ejps.2013.02.006.

505 53. Argao EA, Heubi JE, Hollis BW, Tsang RC. d-Alpha-tocopheryl polyethylene glycol-1000 succinate
506 enhances the absorption of vitamin D in chronic cholestatic liver disease of infancy and childhood.
507 Pediatr Res. 1992;31:146-150.

508 54. Chen W, Miao YQ, Fan DJ, Yang SS, Lin X, Meng LK, et al. Bioavailability study of berberine and
509 the enhancing effects of TPGS on intestinal absorption in rats. AAPS PharmSciTech. 2011;12:705-711.
510 doi: 10.1208/s12249-011-9632-z.

511 55. Yang C, Wu T, Qi Y, Zhang Z. Recent Advances in the Application of Vitamin E TPGS for Drug
512 Delivery. Theranostics. 2018;8:464-485. doi: 10.7150/thno.22711.

513 56. Bittner B., Bravo González RB, Bohrmann B, Kuentz M, Huwyler J. Drug-excipient interactions by
514 Vitamin E-TPGS: *in vitro* studies on inhibition of P-glycoprotein and colonic drug absorption. J Drug
515 Deliv Sci Technol. 2008;18:145-148 https://doi.org/10.1016/S1773-2247(08)50023-2.

516 57. Willemsen AE, Lubberman FJ, Tol J, Gerritsen WR, van Herpen CM, van Erp NP. Effect of food
517 and acid-reducing agents on the absorption of oral targeted therapies in solid tumors. Drug Discov
518 Today. 2016;21:962-976. doi: 10.1016/j.drudis.2016.03.002.

519 58. Zhang L, Wu F, Lee SC, Zhao H, Zhang L. pH-dependent drug-drug interactions for weak base
520 drugs: potential implications for new drug development. Clin Pharmacol Ther. 2014;96:266-277. doi:
521 10.1038/clpt.2014.87.

522 59. Budha NR, Frymoyer A, Smelick GS, Jin JY, Yago MR, Dresser MJ, et al. Drug absorption
523 interactions between oral targeted anticancer agents and PPIs: is pH-dependent solubility the Achilles
524 heel of targeted therapy? Clin Pharmacol Ther. 2012;92:203-213. doi: 10.1038/clpt.2012.73.

525 60. Parrott NJ, Yu LJ, Takano R, Nakamura M, Morcos PN. Physiologically Based Absorption
526 Modeling to Explore the Impact of Food and Gastric pH Changes on the Pharmacokinetics of Alectinib.
527 AAPS J. 2016;18:1464-1474.

528 61. Gruber A, Czejka M, Buchner P, Kitzmueller M, Kirchbaumer Baroian N, Dittrich C, et al.
529 Monitoring of erlotinib in pancreatic cancer patients during long-time administration and comparison to
530 a physiologically based pharmacokinetic model. Cancer Chemother Pharmacol. 2018;81:763-771. doi:
531 10.1007/s00280-018-3545-4.

532 62. Lu T, Fraczkiewicz G, Salphati L, Budha N, Dalziel G, Smelick GS, et al. Combining "Bottom-up"
533 and "Top-down" Approaches to Assess the Impact of Food and Gastric pH on Pictilisib (GDC-0941)
534 Pharmacokinetics. CPT Pharmacometrics Syst Pharmacol. 2017;6:747-755. doi: 10.1002/psp4.12228.

Table I. List of studies contributing to the pooled pharmacokinetic analysis.

Table II. GastroPlus™ model input parameters.

Table III. Literature pharmacokinetic parameters for selumetinib in the suspension and capsule formulation.

Table IV. Pharmacokinetic key parameters for selumetinib in the suspension and capsule formulation, calculated in a GastroPlus™ population simulation.

Table I. List of studies contributing to the pooled pharmacokinetic analysis.

Formulation	Dosage	N	Reference	Year	Lit.
Suspension	100 mg	26	Adjei A. et al.	2008	33
		28	Banerji U. et al.	2010	34
		14	O'Neil B. et al.	2011	35
Capsule	75 mg	34	Banerji U. et al.	2010	34
		21	Leijen S. et al.	2011	27
		11	Bridgewater J. et al.	2016	36
		6	Dymond A. et al.	2016	37
		50	Zhou D. et al.	2016	38
		22	Dymond A. et al.	2017	39
		190	Dymond A. et al.	2017	40
		37	LoRusso P. et al.	2017	41
		113	Tomkinson H. et al.	2017	32

Table II. GastroPlus™ model input parameters.

Parameters	Basic model	Suspension	Capsule
Molecular weight [g/mol]	457.69	457.69	457.69
pKa acidic (a), basic (b)	8.2 (a), 2.7 (b)	8.2 (a), 2.7 (b)	8.2 (a), 2.7 (b)
logP	3.88	3.88	3.88
Solubility [mg/ml]	0.0034 at pH 7.4	0.0034 at pH 7.4	0.0034 at pH 7.4
Permeability [cm/s x 10^4]	0.5	0.7	4.0
Solubilization ratio	6.54 E4	1.94 E6	3.18 E6
Particle radius [µm]	25.0	5.0	5.0
Mean precipitation time [sec]	900	100	2000
Fraction unbound in plasma [%]	0.35	0.35	0.35
Blood/plasma ratio	0.6	0.6	0.6
Hepatic clearance [l/h]	14.0	16.0	12.0

Table III. Literature pharmacokinetic parameters for selumetinib in the suspension and capsule formulation.

Parameters	Suspension – 100 mg	Capsule – 75 mg
	Mean range *	Mean range *
	(n=68)	(n=484)
C_{max} [ng/ml]	486-807	1150-1537
AUC_{inf} [ng-h/ml]	2700-3299	3680-6335
T_{max} [h]	1.0-1.08	1.0-1.55
Cl/F [l/h]	29.0-44.4	12.1-21.5
Vd/F [l]	365.0-415.0	89.3-175.2
$T_{1/2\ el}$ [h]	4.5-11.1	5.33-13.7

* Values were obtained as geometric mean. only T_{max} as median

Table IV. Pharmacokinetic key parameters for selumetinib in the suspension and capsule formulation, calculated in a GastroPlus™ population simulation.

Parameters	Suspension – 100 mg		Capsule – 75 mg	
	Mean *	90% CI	Mean *	90% CI
	(n=25)		(n=25)	
C_{max} [ng/ml]	484	401-566	1014	933-1095
AUC_{inf} [ng-h/ml]	3019	2771-3814	4171	3721-4623
T_{max} [h]	1.44	1.37-1.56	0.74	0.7-0.83
Cl [l/h]	16.02	n.c.	12.34	n.c.
Vd [l]	69.13	n.c.	69.26	n.c.
$T_{1/2\ el}$ [h]	2.99	n.c.	3.89	n.c.

* All simulated values were calculated as geometric mean

n.c. not calculable

Fig. 1. 3D PSA surface plot of solubility and permeability on the bioavailability of selumetinib.

Fig. 2. Plasma concentration-time profile of selumetinib (linear + log scale), calculated in a GastroPlus™ population simulation (± 90% CI), in the suspension (triangles) and capsule (squares) formulation.

Fig. 3. Parameter sensitivity analyses of the selumetinib suspension formulation: impact of permeability and solubilization ratio on C_{max} (**a**), AUC (**b**), T_{max} (**c**) and bioavailability (F%) (**d**).

Fig. 4. Parameter sensitivity analyses of the selumetinib capsule formulation: impact of permeability and solubilization ratio on C_{max} (**a**), AUC (**b**), T_{max} (**c**) and bioavailability (F%) (**d**).

Fig. 5. Simulation of physiological influences on the plasma concentration of selumetinib. Fasted vs fed state administration (**a**), influence of gastric pH-changes due to co-administered acid reducing agents (ARAs) (**b**), changes in the protein binding rate (unbound fraction – FuP%) (**c**), changes in hepatic clearance (Cl_{hep}) (**d**).

Figure 1

Click here to access/download;Figure;Fig. 1.jpg

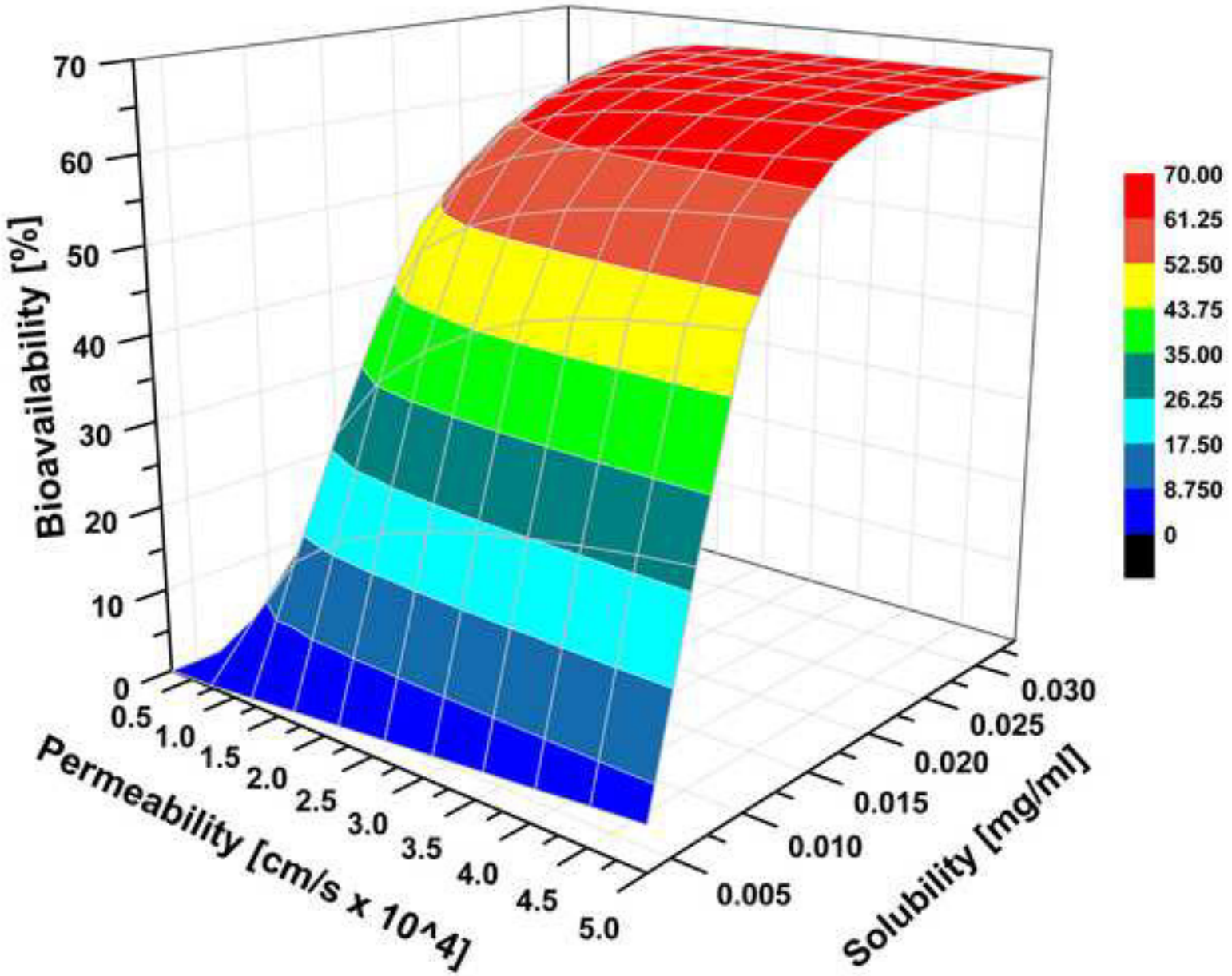

Figure 2

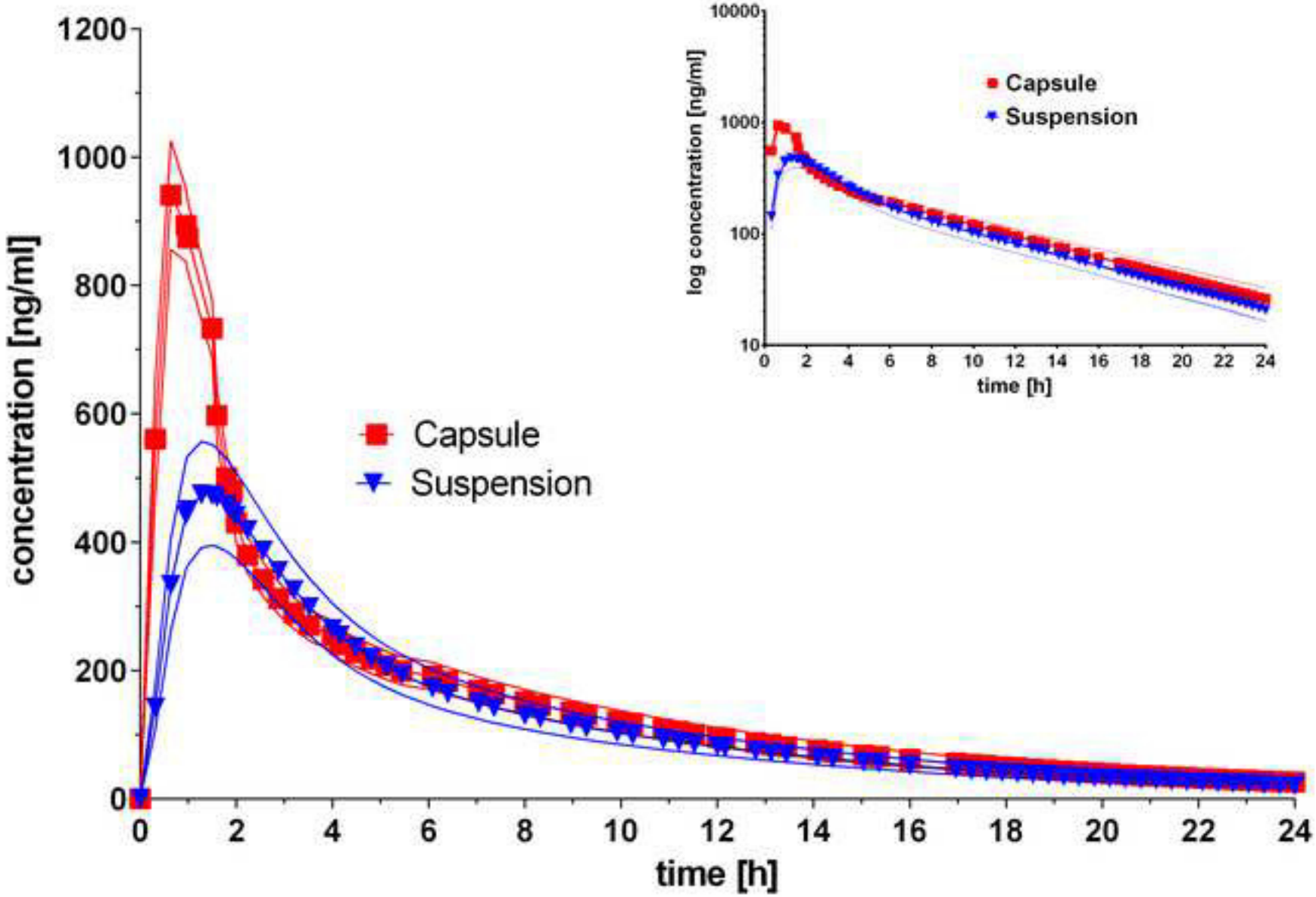

Figure 3

Click here to access/download;Figure;Fig. 3.jpg

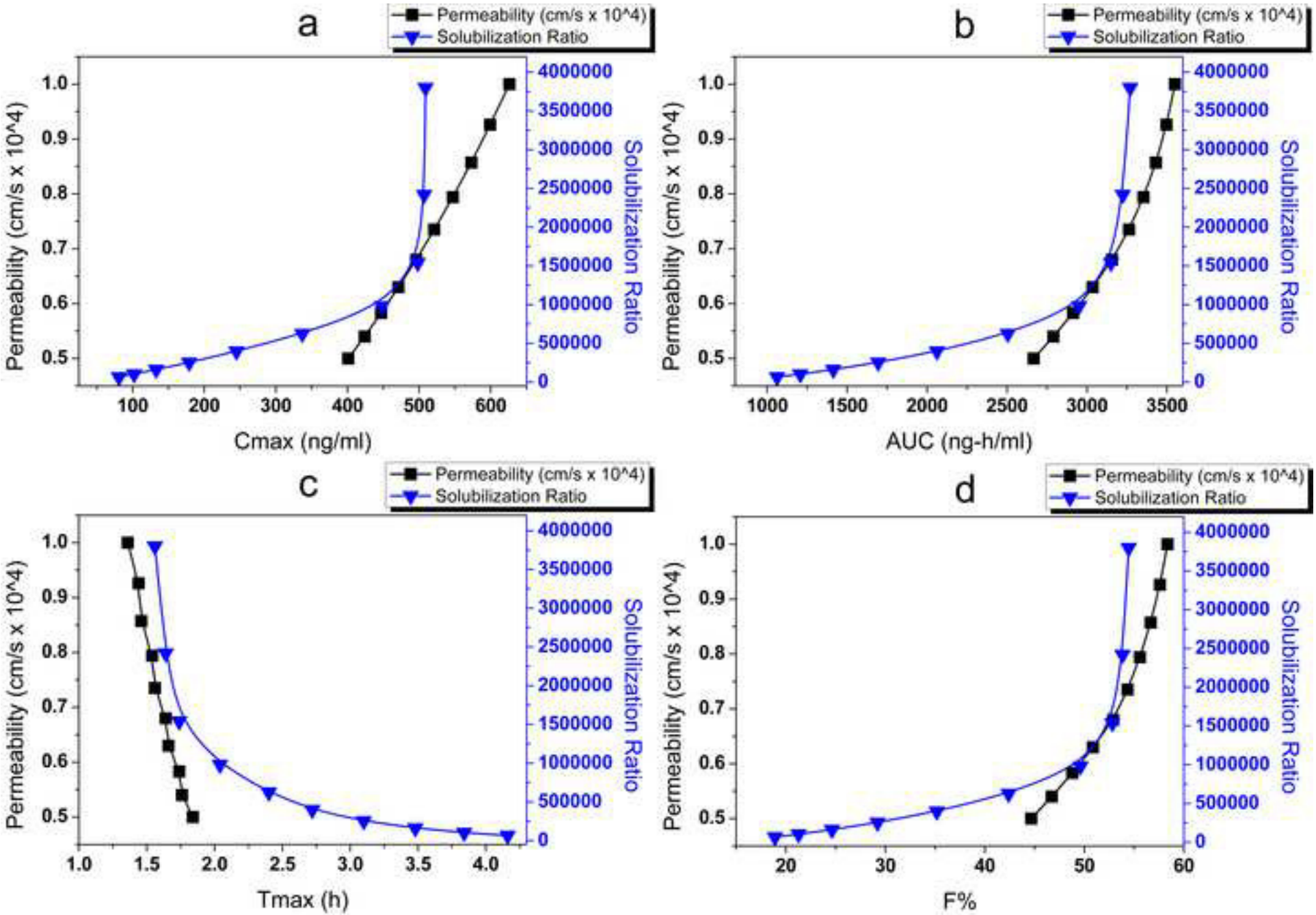

Figure 4

Click here to access/download;Figure;Fig. 4.jpg

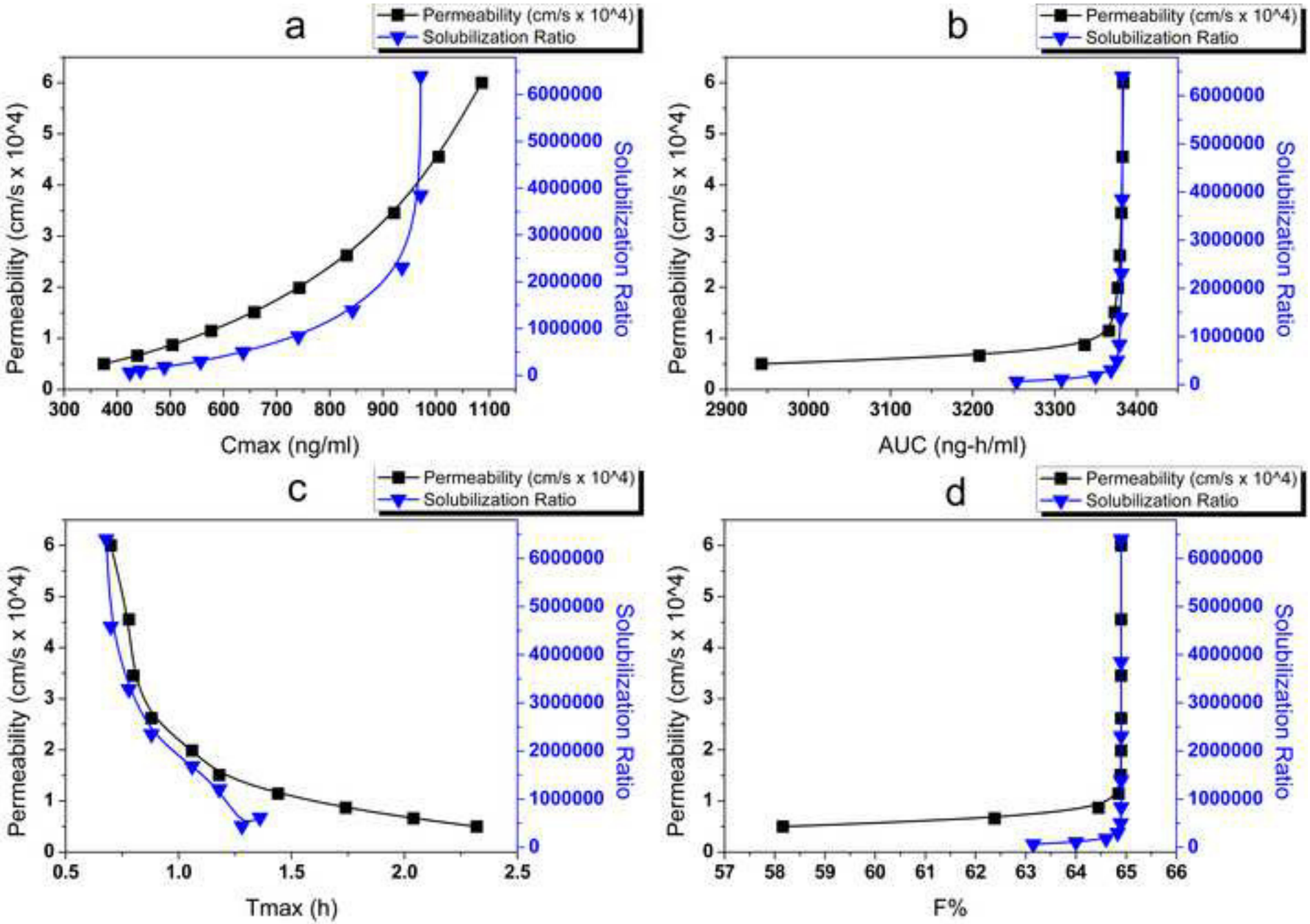

Figure 5

Click here to access/download;Figure;Fig. 5.jpg

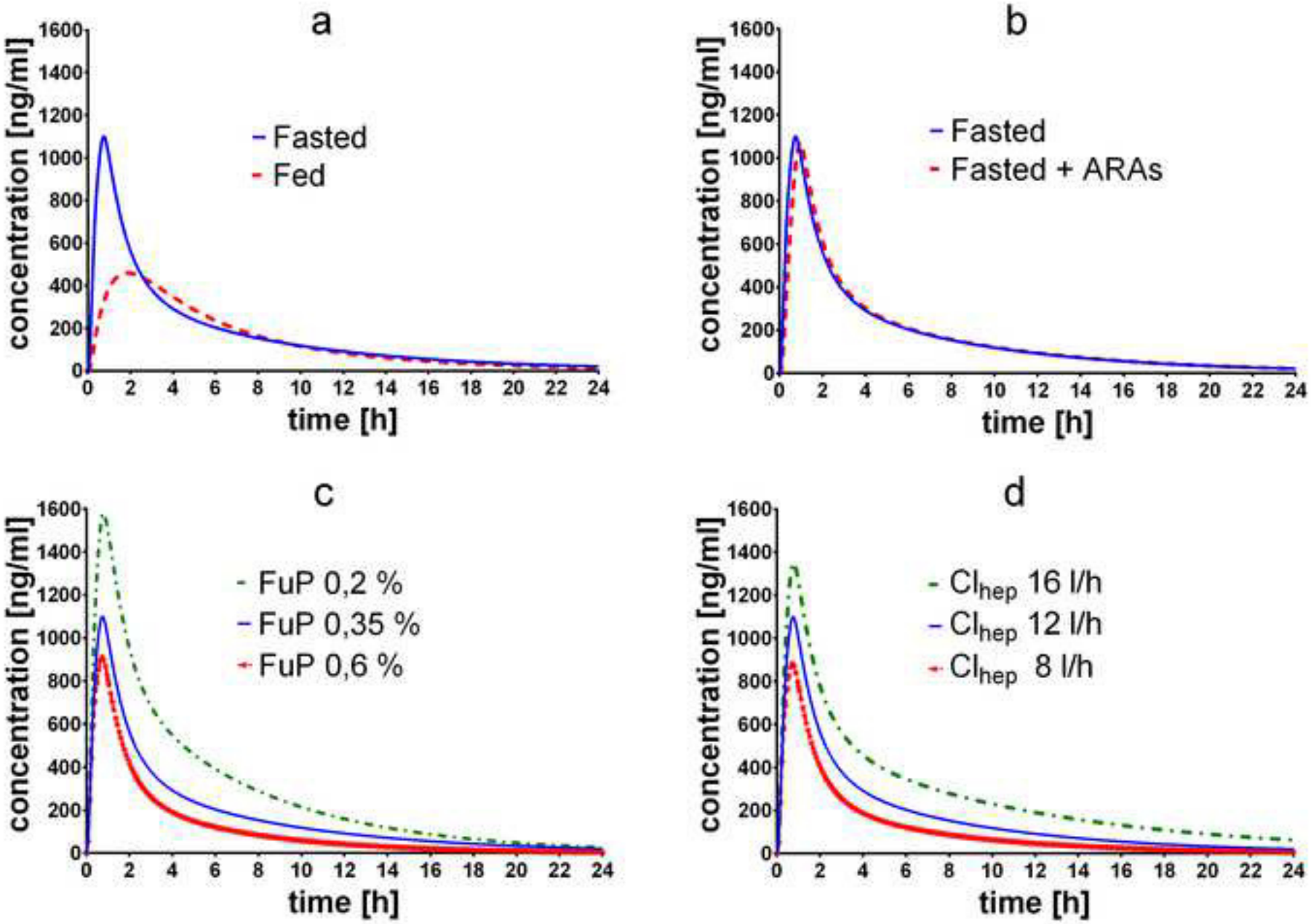

6.1.4 Capecitabine

Pharmacokinetic modeling of the sequential metabolism of capecitabine to 5-fluorouracil (5FU) for evaluation of influencing factors on 5FU disposition in plasma, liver and tumor tissue and assessment of related toxicities.

Gruber A, Czejka M, Dittrich C.

Cancer Chemother Pharmacol. *Submitted 2019*

Cancer Chemotherapy and Pharmacology

Pharmacokinetic modeling of the sequential metabolism of capecitabine to 5-fluorouracil (5FU) for evaluation of influencing factors on 5FU disposition in plasma, liver and tumor tissue and assessment of related toxicities

--Manuscript Draft--

Manuscript Number:	
Full Title:	Pharmacokinetic modeling of the sequential metabolism of capecitabine to 5-fluorouracil (5FU) for evaluation of influencing factors on 5FU disposition in plasma, liver and tumor tissue and assessment of related toxicities
Article Type:	Original Article
Funding Information:	Merck Austria — Not applicable
Abstract:	Purpose This study evaluated the pharmacokinetic (PK) profile and toxicities of the combination therapy of capecitabine (CCB) with oxaliplatin and cetuximab and used a physiologically-based pharmacokinetic (PBPK) model to assess the impact of physiological changes on the concentration of CCB and its metabolites in plasma, liver and tumor. Methods Plasma concentrations of 24 patients receiving the triple therapy were assessed as well as treatment-emergent adverse events (TEAEs), graded according to CTCAE. The PBPK model was developed based on CCB, 5'-deoxy-5-fluorocytidine, 5'-deoxy-5-fluorouridine and 5-fluorouracil (5FU) and the enzymatic steps involved in the activation of CCB to 5FU in liver and tumor tissue. Results Plasma PK data of CCB and its metabolites was in a similar range as reported for CCB monotherapy, hence ruling out an underlying drug-drug interaction in the triple-therapy. In two patients TEAEs grade (G) 3 and in 18 patients 52 TEAEs G 2 were observed. The PBPK model showed the impact of physiological co-variates and variations in the metabolic conversion on the disposition of CCB and its metabolites. As anticipated, the highest influence on the 5FU tumor disposition derived from the enzymes directly involved in formation and inactivation of 5FU, with significantly higher influence of the liver enzymes compared to the tumor enzymes, indicating that the tumor blood flow is relevant in the 5FU tumor disposition. Conclusion PBPK models can illustrate underlying mechanisms of TEAEs and physiological consequences of co-variate influences on drug disposition, thus enabling a more rational treatment and a decrease of unexpected toxicities.
Corresponding Author:	Andrea Gruber, Mag. University of Vienna Vienna, Vienna AUSTRIA
Corresponding Author Secondary Information:	
Corresponding Author's Institution:	University of Vienna
Corresponding Author's Secondary Institution:	
First Author:	Andrea Gruber, Mag.
First Author Secondary Information:	

ORIGINAL ARTICLE

Pharmacokinetic modeling of the sequential metabolism of capecitabine to 5-fluorouracil (5FU) for evaluation of influencing factors on 5FU disposition in plasma, liver and tumor tissue and assessment of related toxicities

Andrea Gruber[1] • Martin Czejka[1] • Christian Dittrich[2]

A. Gruber (0000-0001-8298-5090, ✉)• M. Czejka (0000-0002-9754-0921)

[1]Division of Clinical Pharmacy and Diagnostics, Faculty of Life Sciences, University of Vienna, Althanstrasse 14, A-1090 Vienna, Austria

Phone: +43-1-4277-55581

e-mail: andrea.gruber@univie.ac.at

C. Dittrich

[2]Applied Cancer Research - Institution for Translational Research, Vienna (ACR-ITR VIEnna), Bernardgasse 24/2, A-1070 Vienna, Austria

Acknowledgements

The authors would like to thank Veronika Rachar for providing the pharmacokinetic patient data as well as Nicole Weissenboeck and Maria Lichteneckert for clinical data management. The authors would further like to acknowledge the valuable contributions of Daniela Wolkersdorfer and Richard Greil to the study organization and administration in the frame of the AGMT, Arbeitsgemeinschaft Medikamentöse Tumortherapie gemeinnützige GmbH, the sponsor of the clinical study (Protocol # AGMT_Capecet_PK). The open access funding is provided by University of Vienna.

Abstract

Purpose

This study evaluated the pharmacokinetic (PK) profile and toxicities of the combination therapy of capecitabine (CCB) with oxaliplatin and cetuximab and used a physiologically-based pharmacokinetic (PBPK) model to assess the impact of physiological changes on the concentration of CCB and its metabolites in plasma, liver and tumor.

Methods

Plasma concentrations of 24 patients receiving the triple therapy were assessed as well as treatment-emergent adverse events (TEAEs), graded according to CTCAE. The PBPK model was developed based on CCB, 5'-deoxy-5-fluorocytidine, 5'-deoxy-5-fluorouridine and 5-fluorouracil (5FU) and the enzymatic steps involved in the activation of CCB to 5FU in liver and tumor tissue.

Results

Plasma PK data of CCB and its metabolites was in a similar range as reported for CCB monotherapy, hence ruling out an underlying drug-drug interaction in the triple- therapy. In two patients TEAEs grade (G) 3 and in 18 patients 52 TEAEs G 2 were observed. The PBPK model showed the impact of physiological co-variates and variations in the metabolic conversion on the disposition of CCB and its metabolites. As anticipated, the highest influence on the 5FU tumor disposition derived from the enzymes directly involved in formation and inactivation of 5FU, with significantly higher influence of the liver enzymes compared to the tumor enzymes, indicating that the tumor blood flow is relevant in the 5FU tumor disposition.

Conclusion

PBPK models can illustrate underlying mechanisms of TEAEs and physiological consequences of co-variate influences on drug disposition, thus enabling a more rational treatment and a decrease of unexpected toxicities.

Keywords: Capecitabine, metabolism, toxicities, PBPK modeling, 5FU disposition

Introduction

Capecitabine (CCB), a triple prodrug of the antimetabolite 5-fluorouracil (5FU), is used in mono- or combination therapy with several cytotoxic or cytostatic agents for the treatment of various solid cancers such as colorectal and breast cancer [1-6]. The efficacy of the treatment is dependent upon the tumor specific activation of CCB to 5FU by enzymes predominantly expressed in tumor tissue and liver [7-11]. The therapy with the orally administrable CCB is considered equivalent to 5FU regarding efficacy, however the toxicity profiles of the two drugs differ. The main side effects associated with CCB include gastrointestinal toxicities and hand-foot syndrome [12], which in severe cases can require dose reductions. An increase in treatment-emergent adverse events (TEAEs) was observed for CCB when combined with other cytotoxic compounds in a therapeutic regimen, which can derive from drug-drug interactions or an accumulation of side effects.

The treatment combination of 5FU or CCB with oxaliplatin (OX) and the monoclonal antibody cetuximab (CTX) in patients with advanced colorectal cancer was investigated in the COIN trial [13] and reported a significantly increased incidence of gastrointestinal toxicities in the CCB-based therapy, compared to the 5FU-based combination. Treatment-related deaths were predominantly connected to gastrointestinal toxic effects in the CCB-based therapy and the progression-free survival only improved in in the 5FU- based therapy with OX and CTX, but not in patients receiving the CCB-based treatment. Additionally, the negative influence of the combination CCB, OX, and CTX was reflected by a shorter overall median duration of therapy compared to the 5FU-based treatment. In this context, a PK study was conducted to elucidate possible drug-drug interactions of the chemotherapeutic agents CCB and OX and the monoclonal antibody CTX in metastatic colorectal cancer patients [14] to explain the detrimental effect described by Maughan et al [13] when using CCB instead of 5FU in the combination with CTX and OX. However, Rachar et al [14] detected no PK interaction between the investigated drugs CCB, CTX and OX. Since toxicities are often linked to a higher exposure of cytotoxic compounds and thus higher plasma concentrations of the respective compounds, adverse events in a chemotherapeutic treatment can be partly anticipated based on a patient's PK profile. Variabilities in the PK profile can furthermore be predicted by in silico tools, to illustrate if changes, derived from age, gender, dosage, tumor entity or other sensitive parameters, such as genetic variations in the case of CCB [15], impact the disposition of chemotherapeutic drugs in the tumor compartment or are responsible for a generally high interpatient variability. Additionally, pharmacogenetic tests to predict CCB related toxicities by analyzing genetic polymorphisms responsible for alterations in metabolic pathways have emerged. However, the detailed impact of critical polymorphisms on the PK profile of CCB and its metabolites in physiological environment has not yet been determined [15-18].

PBPK modeling facilitates risk assessment concerning dosage, physiology or co-medication by demonstrating the influence of co-variates on the disposition of drugs in various compartments [19-21] and can thus increase treatment safety. The current study presents a GastroPlus™ PBPK model of CCB and its sequential metabolism to 5'-deoxy-5-fluorocytidine (DFCR), 5'-deoxy-5-fluorouridine (5'-DFUR) and 5FU. It furthermore contains the metabolic steps involved in the activation and inactivation process of 5FU, characterized by enzyme expression and enzymatic activity, to identify sensitive parameters responsible for the high interpatient variability observed in patient data.

Materials and Methods

PK study

Study population

Patients eligible for this PK study were diagnosed with histologically confirmed KRAS wild type adenocarcinoma of the colon or rectum in the metastatic setting. Inclusion criteria were ECOG performance status ≤ 2, age ≥ 18 years, absolute neutrophil count (ANC) ≥ 1.5 x 10^9/L, platelet count ≥ 100 x 10^9/L, hemoglobin (Hb) ≥ 8 g/dl), serum (total) bilirubin ≤ 1.5 x upper limit of normal (ULN), aspartate aminotransferase (AST), alanine aminotransferase (ALT) ≤ 2.5 ULN (≤ 5 x ULN if liver metastases were present) and serum creatinine ≤ 2 x ULN. Patients must not have had previous chemotherapy for metastatic disease, except for prior adjuvant chemotherapy if the chemotherapy treatment free interval was > 6 months, or administration of any of the investigational agents within 4 weeks prior to the study entry as well as previous exposure to epidermal growth factor receptor (EGFR)-pathway targeting therapy. Further exclusion criteria were grade (G) 3/4 allergic reaction to any of the investigated chemotherapeutic agents, known or suspected brain metastases, New York Heart Association (NYHA) grade 3/4 heart failure or uncontrolled angina, pregnancy or lactation. The intake of drugs specifically contraindicated to one of the three study drugs was prohibited and all concomitant medication was reported. All patients were asked to keep a diary during their treatment and were checked upon once a week to retrace possible adverse events (AEs), interactions and treatment failures.

Study design

The study was designed as multicenter, randomized phase II trial with each 12 patients assigned to arm A and B, allowing the exclusion of potential carry-over effects. The study schedule of the two arms was characterized by a difference in the sequence of administration of the antitumoral agents CCB, OX and CTX in the three treatment cycles of each three weeks [14]. This procedure should minimize potential effects associated with inter-patient variability. A possible influence of CTX on the PK profile of CCB has been assessed in treatment cycles 1 and 2 with varying sequences of CCB and CTX [14]. The third treatment cycle was designed to assess the impact of CTX on the PK profile of CCB in the triple therapy with CCB, OX and CTX, compared to an administration of CCB and OX. CCB was administered at a dose of 1000 mg/m² bid for two consecutive weeks, OX was applied as 130 mg/m² iv on day 1 of cycle 3 and CTX was given as 400 mg/m² iv loading dose followed by 250 mg/m² iv maintenance dose weekly on day 1 of cycle 3 in arm A and on day 8 of cycle 3 in arm B, respectively. Safety assessments were including analyses of AEs, laboratory data and vital signs. TEAEs/toxicities which were at least possibly related to study treatment were graded according to U.S.-NCI Common Terminology Criteria for Adverse Events (CTCAE), version 4.0. TEAEs were coded using the MeDRA coding dictionary, version 17.0, and classified by the System Organ Class (SOC) Preferred Terms (PT). The study was approved by the Ethical Committee of the City of Vienna (EudraCT number 2011-002921-23). Patients had been informed about the aim of the investigation and had given their written consent. All procedures performed in studies involving human participants were in accordance with the ethical standards of the institutional and/or national research committee and with the 1964 Helsinki declaration and its later amendments or comparable ethical standards.

PBPK modeling

Fig. 1 PBPK model concept for CCB and its metabolites DFCR, DFUR and 5FU, including the involved enzymes carboxylesterases (CES) 1 and 2, cytidine deaminase (CDA), thymidine phosphorylase (TP) and dihydropyrimidine dehydrogenase (DPD) for the metabolic conversion in the respective compartments

The PBPK model was created using GastroPlus™ 9.6. (Simulations Plus Inc., Lancaster, CA, USA). Fig. 1 shows the PBPK model concept of CCB and its metabolites DFCR, DFUR and 5FU. The simulation is based on a single CCB dose of 1000 mg/m², calculated for a patient of 65 years and 75 kg and a body surface area of 1.9 m², thus matching the patient characteristics of the PK study from which patient data of CCB monotherapy was used for validation of the model [14]. A tumor compartment was added to the PBPK model to include the enzymatic activity of involved enzymes in the tumor itself as well as to monitor the concentrations of the active moiety 5FU in the tumor tissue and to evaluate the impact of possible influences on the tumor concentration. The relevant parameters for the additional compartment, tumor blood flow and volume, were based on literature data [22]. Furthermore, the basic physicochemical parameters for all compounds have been obtained from literature, as well as distribution and elimination data. The absorption parameters solubility and permeability have been included only for CCB to determine the absorption from the intestine and consequently the plasma disposition of the parent compound. The plasma protein binding rate is 54%, 10%, 62% and 10% for CCB, DFCR, DFUR and 5FU respectively and diffusion into red blood cells has been reported to be minimal [23-24]. The involvement of the enzymes carboxylesterases (CES), cytidine deaminase (CDA), thymidine phosphorylase (TP) and dihydropyrimidine dehydrogenase (DPD) in the metabolic conversion of CCB to 5FU and inactivation and elimination of 5FU was included in the model. The first conversion step from CCB to DFCR is performed by the carboxylesterases CES 1 and CES 2. Due to the main activity of CES 1 and CES 2 in the liver, the metabolic activity of both enzymes was determined in microsomal and cytosolic fractions of liver homogenates [25-27]. Even though the reported affinity of CCB to CES 2 is higher than to CES 1, the excessive predominance of CES 1 by 50-fold compared to CES 2 in liver microsomes [38-31] leads to an enzymatic conversion of CCB to DFCR by both enzymes. CES also occur to a minor extent in the intestine, yet the activity of the intestinal CES 1 and 2 show distinctly lower values than the hepatic CES 1 and 2 [32-33], hence its influence on the disposition of CCB and its metabolites is minimal and will not be regarded in the current PBPK model. The metabolic conversion of the first metabolite DFCR to the second metabolite DFUR is performed by CDA, which predominately occurs in liver and tumor tissue. Similarly, also the conversion from DFUR to 5FU occurs in both liver and tumor tissue and is performed by TP. Both enzyme activities have been determined in vitro in the cytosolic fraction of liver and tumor homogenates [8,25,34]. The elimination of CCB, DFCR and DFUR from the central compartment mainly takes place through metabolic conversion, however a small part of each metabolite is also excreted renally [35-36]. The elimination of 5FU and thus the inactivation of the drug is executed by the DPD, which transforms 5FU into 5,6-dihydro-5-fluorouracil (FUH2), a catabolic metabolite which will not be further regarded in this PBPK model. The enzymatic activity of DPD has been determined in both liver and tumor tissue [8,37-38]. The enzymatic activities were described by the Michaelis-Menten constant Km and the velocity of the enzymatic reaction V_{max} for the individual enzymes and respective substrates. Mean Km and V_{max} values were calculated from in vitro data and V_{max} values were further optimized to fit the patient plasma concentrations by using the optimization module of GastroPlus™. In vitro enzyme expression values (mg enzyme/g tissue) were reported for CES 1 and CES 2 in liver microsomes and TP and DPD in tumor tissue. TP and DPD liver expression values were adopted from the tumor expression values. CDA expression levels have not been reported in literature yet, therefore CDA liver and tumor expression

has been optimized to fit the observed patient data. The input parameters for the PBPK model are summarized in Table 1. After validation of the PBPK model with plasma concentration-time profiles of CCB, DFCR and DFUR from the PK study and 5FU data from literature, the model was used to depict the influence of co-variates on the concentration in plasma, liver and tumor for all four compounds. Co-variates such as renal impairment, age or administration of the drug with food have been reported to be responsible for interpatient variability [39-41]. The co-variate body weight was already considered in the administered dose by integrating the body surface area of the patient into the individual dosage calculation. The blood flow rate in tumor tissue can vary depending on the physiology of the patient and the tumor entity and should be considered as co-variate alongside the liver blood flow rate. Additionally, variations in enzyme activities have been reported as potent co-variates, due to either genetic polymorphisms in the metabolic enzymes or physiological differences. Therefore, the influence of variations by 0.1-10-fold in the model parameters enzyme expression and V_{max} have been evaluated for the disposition of the active moiety 5FU and its precursors in plasma, liver- and tumor tissue.

Table 1

Results

Patient characteristics

28 patients were entered into this study and randomly assigned to study arm A or B. Four patients did not receive the complete study treatment, thus being ineligible for the PK evaluation. One of them experienced a severe infusion related allergic reaction to CTX at the first administration and one patient exhibited a rapidly declining ECOG status. Another patient developed early progressive disease after two cycles of therapy. The fourth patient was not able to start the therapy due to generalized edema. Hence, 24 patients, 12 patients in each arm, completed the three cycles and were therefore included in the analysis reported in this investigation. The patient demographics have already been reported by Rachar et al [14].

PK profile of CCB and its metabolites

Fig. 2 Plasma concentration-time profile of CCB (a) and its metabolites DFCR (b) and DFUR (c) in the third treatment cycle, including the GastroPlus™ simulations for plasma, liver- and tumor tissue. Simulated plasma-, liver- and tumor concentration-time profiles of 5-FU (d)

Table 2

The plasma PK data of the third treatment cycle is summarized in Table 2 and lies within the reported range after application of 1000 mg/m² CCB [35,39-42]. Plasma concentration-time profiles of CCB, DFCR and DFUR are displayed in Fig. 2, alongside with the simulated concentration-time profiles of the PBPK model for all four compounds. The described mean values of C_{max} and AUC_{0-6} did not significantly differ in arm A and arm B and coincide with already reported PK data of CCB monotherapy, indicating that there is no PK interaction between the three applied drugs, as was demonstrated in previous publications for CCB with CTX and for CCB with OX [14,43-44]. Nonetheless, a high variability was visible in the evaluated PK profiles, particularly in CCB

concentrations, with deviations of C_{max} by 3.5-fold and AUC_{0-6} by 3-fold compared to the calculated mean. Plasma concentration results from the simulation were predicted in a similar range as observed in patients and were additionally calculated in liver and tumor tissue. The 5FU concentrations in the model were validated with literature data [35,39-40], since 5FU was not analyzed in the patients participating in the current PK study. The simulation was additionally calculated in dosages ranging from 500 mg/m² to 1500 mg/m² to confirm the reported dose linearity and to validate the PBPK model. C_{max} and AUC_{0-6} values increased linearly from 500 mg/m²-1500 mg/m² for CCB, DFCR and DFUR, only 5FU concentrations did not follow linearity with changing CCB dosages. In the 1500 mg/m² dosage, 5FU C_{max} and AUC_{0-6} increased by additional 54% and 44%, respectively in both, plasma and liver, and by 16% for C_{max} and 13% for AUC_{0-6} in tumor tissue. The application of 500 mg/m² resulted in additionally decreased C_{max} and AUC_{0-6} in both plasma and liver by 30% and 24% and in tumor tissue by 12% and 10%, respectively.

Treatment-emergent adverse events/toxicities

Of the 24 patients in the PK study, two patients developed a G 3 TEAE; one in form of severe diarrhea in the three treatment cycles and another patient in form of lymphopenia in cycle 3. It has been reported that a higher grade of toxicity can be correlated to a higher systemic exposure to DFUR [9], therefore the PK data of both patients with G 3 TEAEs have been evaluated accordingly. Both patients displayed increased CCB concentrations by 2.5-4-fold throughout the duration of the study, however showed DFCR and DFUR values close to the mean values, thus no correlation could be made in these cases with an elevated DFUR exposure. G 2 TEAE according to U.S. NCI-CTCAE v.4.0, based on SOC-PT, were observed for: gastrointestinal disorders in 3 patients/ 5 events comprising diarrhea, nausea, emesis, and abdominal pain; skin and subcutaneous tissue disorders in 2 patients / 3 events consisting in erythema; general disorders and administration site conditions in 5 patients /5 events comprising asthenia, fatigue, and pyrexia; infections and infestations in 2 patients / 3 events comprising herpes simplex and urinary tract infections; metabolism and nutrition disorders in 2 patients / 2 events comprising decreased appetite or hypokalemia; psychiatric disorders in 1 patient / 1 event as sleep disorder and under investigations in 1 patient / 1 event in form of decreased weight. Overall, 11 patients experienced 20 TEAEs G 2 (median 2; range 1-5 events per patient). G 2 haematotoxicity with lower values of Hb was seen in 9 patients / 16 controls, lymphopenia in 7 patients / 15 controls, neutropenia in a single patient / control and thrombopenia not at all. Overall, haematotoxicity was observed in 13 patients and 32 controls, respectively. Altogether, in 18 patients, 52 TEAEs/toxicities G 2 were recorded. No further significant deviations from normal values of laboratory parameters were registered.

PBPK model

Fig. 3 Influences of the physiological co-variates gender (a), renal impairment (b), liver blood flow (c) and tumor blood flow (d) on the AUC of CCB, DFCR, DFUR and 5FU in plasma, liver- and tumor tissue

To illustrate possible mechanisms behind the observed variability, which may be linked to toxicity and therefore treatment failures, the PBPK model was used to demonstrate the effects of several co-variates on the disposition of CCB, DFCR, DFUR and 5FU in plasma, liver and tumor compartments. The influences on the AUC of the four compounds are displayed in Fig. 3. Physiological variations in a study population can comprise age, gender and

body weight of which the current dosing scheme already includes body weight as variable through the calculation of the body surface area for the applied dosage of CCB. Thus, age and gender remain as basic physiological co-variates in a CCB study population. Age did not significantly affect the AUCs of CCB, DFCR, DFUR or 5FU in plasma, as reported previously [9], and neither in liver nor tumor tissue, as demonstrated in the model (data not shown). Gender differences were predicted in a 65-year-old male and female with 75 kg body weight. AUCs and peak concentrations of all four compounds were elevated by 10-20% for the female compared to the male physiology in all compartments, thus not resulting in statistically or clinically relevant changes. All four compounds are renally excreted in a low to moderate extent [35-36], thus renal impairment is expected to have an influence on the concentrations. The simulation showed that the expected effect on plasma concentrations was confirmed, but only minimal effects were observed in liver and tumor tissues. The highest effect was monitored in DFUR plasma concentrations and AUC with an increase by 22.4% and 39.8% respectively. Since all enzymes involved in the metabolism of CCB to 5FU are located in liver, tumor or both, the liver and tumor blood flow were anticipated to influence the concentrations of the compounds. Tumor blood flow can vary with tumor entity [22] and liver blood flow can differ due to physiological changes [41,45-46]. In the simulation, both parameters have been changed in a 2-fold range. Altering the liver blood flow in the specified range had minor effects on the plasma concentrations of all compounds and insignificant effects on the concentrations in liver and tumor tissue. Increasing the tumor blood flow however resulted in an elevated tumor AUC of DFCR and DFUR by 1.5-fold and a slightly reduced AUC of 5FU in tumor tissue by 16%, whereas a decreased tumor blood flow inversely resulted in a reduced tumor AUC of DFCR and DFUR by 40% and minimally increased tumor AUC of 5FU. The administration of CCB is usually recommended 30 min after a standard meal, however the administration with food can alter the PK profile, due to a delayed absorption. In the simulation the peak concentrations of all four compounds decreased on average by 35% in plasma, by 45% in liver and by 30% in tumor tissue. T_{max} was delayed by 1.6-2.2-fold, yet the AUC of CCB and its metabolites did not decrease in the observed time frame, hence the slower absorption did not alter the disposition of the compounds in the investigated compartments.

Fig. 4 Impact of variations by 0.1-10-fold in V_{max} (a,b,c) and enzyme expression levels (d,e,f) of the metabolizing enzymes of CCB to 5FU, on the plasma-, liver- and tumor-disposition of 5FU. The assessment includes the carboxylesterases (CES) 1 and 2 in liver and cytidine deaminase (CDA), thymidine phosphorylase (TP) and dihydropyrimidine dehydrogenase (DPD) in liver and tumor tissue

Due to the extensive metabolism involvement in the concept of the triple prodrug CCB, the contribution of each enzyme in liver and tumor is crucial for the disposition of CCB and its metabolites in the different compartments, plasma, liver and tumor. The influences of all involved enzymes are of specific interest concerning the 5FU disposition, as displayed in Fig. 4. Including the enzymatic activity into the PBPK model required both enzyme expression values in liver and tumor tissues, depending on the enzyme, as well as Km and V_{max} to describe the enzymatic reaction. Parameter sensitivity analysis exhibited a similarly strong dependence of the enzymatic reactions on the respective V_{max} and enzyme expression levels, therefore both parameters of each enzymatic step have been investigated regarding their contribution to the 5FU concentrations in plasma, liver and tumor. Varying V_{max} and expression levels of the first metabolic step, executed by CES 1 and CES 2, minimally impacted the AUC of 5FU in all three compartments, likewise the AUCs of the precursors DFCR and DFUR. Variations of V_{max} in the range obtained from in vitro experiments however affected the AUCs of CCB similarly in plasma, liver and

tumor by +84% to -57% for CES 1 and +73% to -45% for CES 2. Integrating reported variations of the enzyme expression levels resulted in AUC variations of CCB by ±13% for CES 1 and ±10% for CES 2 alterations in all compartments. The CDA located in the liver showed a stronger effect on the 5FU disposition in all three compartments regarding both, enzyme expression and V_{max} values. Applying the range of in vitro V_{max} values for the liver enzyme to the model decreased the AUC of 5FU by up to 36% in plasma and liver and increased by up to 66% in tumor tissue. The AUC of DFCR increased by 2- to 3-fold in all three compartments, whereas the AUC of DFUR resulted in only minimal alterations. Adjusting the V_{max} of CDA in tumor tissue in the range of in vitro values increased the DFCR tumor disposition by 94% but decreased the tumor AUC of DFUR and 5FU by 15% and 20%, respectively. Since the CDA expression levels were optimized by the software, the range of experimental values could not be applied in this step. Variations in the third metabolic conversion step by TP affected 5FU and DFUR disposition in all three compartments. However, changing V_{max} of the liver enzyme according to in vitro measurements altered the AUC of 5FU only minimally, due to the little variability observed for this parameter. Varying V_{max} of the TP located in tumor tissue in the range of in vitro values, decreased he 5FU tumor disposition by 26% but increased the DFUR disposition by up to 2.4-fold. The expression levels in tumor tissue have shown a broad range of variation and are thus likely to highly affect the disposition of 5FU and DFUR. Decreasing the expression of TP in tumor tissue in the measured range increased the AUC of DFUR by 3.6-fold and decreased the 5FU AUC by 52% in tumor tissue. Adopting the same expression range of the TP tumor enzyme to the TP liver enzyme would result in extensive variations in disposition for DFUR and 5FU in all three compartments. The AUC of DFUR would be subjected to a possible increase up to 4.2-fold in plasma and liver and 3.2-fold in tumor. The AUC of 5FU would decrease by 70% in plasma and liver and could increase up to 2.5-fold in tumor tissue. The last enzymatic step involved in the metabolic cascade is executed by the DPD, which inactivates 5FU through catabolic metabolism. A high enzymatic activity and expression would be expected to decrease the 5FU levels in all compartments. The V_{max} of the liver DPD was reported to show little variability in experiments, however, adapting even the small changes in V_{max} of the liver DPD to the model resulted in high variations of 5FU AUCs by 3-fold in plasma and liver and 1.65-fold in tumor tissue. Changing the V_{max} of DPD located in tumor tissue in the range observed in experiments decreased the AUC of 5FU by 43%. Decreasing the expression levels of DPD in the model tumor tissue according to in vitro measurements did not significantly change the 5FU disposition in any compartment, however, adopting the same range to the liver enzyme would result in massive increases of 5FU disposition in plasma and liver by 37-fold and in tumor by 10-fold.

Discussion

This study inquired the sequential metabolism of CCB to 5FU in the compartments plasma, liver and tumor including the assessment of co-variate influences on the disposition of the four compounds CCB, DFCR, DFUR and 5FU. It also evaluated the applied antitumor therapy and related toxicity in patients, operating under the general assumption, that higher concentrations of chemotherapeutic agents are responsible for a higher observed toxicity. Both, plasma concentrations of CCB, DFCR and DFUR as well as TEAEs have been monitored in all patients of the present PK study. The mean plasma concentrations of all three compounds were within the reported range, however showed a high standard deviation. Especially CCB concentrations varied strongly, both inter- and intraindividually. During the 9 weeks of treatment with changing sequences of CCB application in combination

with CTX and OX, two out of 24 patients developed G 3 toxicities. Both patients were associated with highly elevated C_{max} and AUC_{0-6} values of CCB, though normal values of DFCR and DFUR, thus not following the previously reported correlation of high DFUR exposure and safety aspects [9]. It has however been reported that higher DFUR concentrations correlate with the incidence of hand-foot-syndrome, which has not been observed as G 3 TEAE in any patient during the treatment period. The PBPK model was created to better understand the reasons behind the high variations observed in patient's plasma concentrations as well as to illustrate consequences from physiological changes, co-medication or dosage changes on the disposition of 5FU and its precursors in various compartments.

As previously reported, age and gender did not have any clinically relevant effects on the concentrations of all four compounds in plasma, liver or tumor, even though the simulated physiologies varied regarding arterial, venous and liver blood flow, volume of arterial and venous supply as well as systemic clearance. In addition, also separately changing the liver blood flow in a 2-fold range resulted in negligible changes in all compartments. The possibility of hepatic dysfunction affecting the disposition of CCB and its metabolites has been described in literature as non-clinically relevant with insignificant changes in plasma concentrations of hepatically impaired patients [41]. Since all four compounds are excreted renally in a low to moderate extent with higher extraction rates for DFCR and DFUR, it was shown in both, patients and the PBPK model, that plasma concentrations of both compounds increase with reduced renal clearance. Tumor concentrations on the other hand were minimally altered through the reduced systemic clearance. Patients with severe renal impairment were reported with considerably elevated DFUR plasma concentrations and were associated with G 3 and 4 TEAEs. Even patients with mild renal impairment suffered from significantly higher G 3 and 4 incidents than patients with normal renal function [40]. The strongest impact on plasma, liver and tumor concentrations however derived from influences in the metabolic cascade. In the current PBPK model the enzymatic activity was described by the enzyme expression in liver and tumor tissue and the kinetic parameters V_{max} and Km. Variations in expression and V_{max} values have shown to considerably contribute to the disposition of all compounds. Various studies have been dedicated to the risk assessment of the variability in enzymatic activity in CCB and 5FU therapy concerning toxicity and treatment failures. The enzymes CES 1 and CES 2 only affected the directly involved CCB and had a minimal effect on the other compounds, including the 5FU disposition.

The CDA, located in tumor and liver, is responsible for the formation of DFUR from its precursor DFCR, however the model showed that only the liver enzyme is responsible for variations in DFUR plasma concentrations and is thus involved in the development of possible TEAEs, based on the assumption that an increased DFUR exposure is correlated with higher toxicity. The CDA located in tumor tissue only affects the respective tumor concentrations, however to a lower extent than the liver enzyme. A high CDA activity of +180% of the average value has been reported in a patient, which led to severe toxicities after CCB administration [47]. According to the PBPK model, the high CDA activity led to strongly increased DFUR and 5FU concentrations and consequently caused serious AEs. Genetic polymorphisms have been detected in the CDA gene, with the consequence of high transcription of the enzyme in normal tissues and thus a higher incidence for overall toxicity in CCB treatment [48-49].

The TP mediates the conversion from DFUR to 5FU and is therefore the key enzyme in the development of the active moiety. Variations in V_{max} and expression of the TP in liver notably altered DFUR and 5FU disposition, where an increase in V_{max} and expression resulted in an expected decrease for DFUR and increase for 5FU in plasma and liver. However, the disposition of both, DFUR and 5FU decreased in tumor tissue. Yet, increasing the

expression and V_{max} of the tumor TP resulted in a decrease for DFUR and increase for 5FU in tumor tissue. This discrepancy has been discussed by Blesch et al [9], and their findings suggested that the tumor blood flow and thus the supply of DFUR as precursor from plasma plays a crucial role in 5FU formation, however as reported by Vaupel et al [22], the variations in tumor blood flow between different tumor entities were reported by approximately 2- to 5-fold and thus much smaller than the variations considered by Blesch et al. In the current PBPK model, alterations in the tumor blood flow rate and their impact on 5FU concentrations have been evaluated in a 2-fold range, hence the effect on the 5FU tumor disposition was smaller than in the previously calculated 10-fold range [9]. The TP has also been reported to stimulate angiogenesis and is potentially involved in the regulation of cell proliferation and apoptosis [50-51] and was therefore suggested to be monitored to ensure a favorable ratio between TP and DPD for a better susceptibility to the CCB therapy in patients [52].

The DPD is responsible for the inactivation of 5FU and is thus the second key enzyme in this metabolic cascade regarding efficacy and toxicity of the treatment. In the model, the liver DPD showed the most powerful impact on the disposition of 5FU in a 10-fold range of both, V_{max} and expression levels in all compartments. Even in the range of experimental measurements, the variations were substantial, which strongly supports and encourages the analysis of DPD levels in patients to detect possible deficiencies or genetic variants with lower activity before starting CCB or 5FU therapy [53-55]. The DPD in tumor tissue only showed a minor influence on the 5FU tumor disposition, thus varying DPD levels in different tumor entities were not expected to highly influence the therapy outcome.

Several strategies have been developed and comprise genotype and phenotype-based diagnostics to evaluate the risk of 5FU associated toxicities [15-18,56-58]. The field of pharmacogenetics thus plays an important role in CCB and 5FU therapy, to detect genetic variations which possibly alter the activity or expression of key enzymes. Combining the information of clinically relevant genetic variations regarding enzyme phenotype modifications with a PBPK model could therefore improve predictions for treatment efficacy or toxicity and facilitate risk assessment concerning physiology, dosages and co-medication.

Conclusion

The current PBPK model displays the influences of possible co-variates and could serve as basis for further integration of relevant changes in parameters describing the enzymatic reactions and thus providing insights into the effects of polymorphisms and co-medication on plasma, liver and tumor concentrations of CCB and its metabolites.

Acknowledgements

The authors would like to thank Veronika Rachar for providing the pharmacokinetic patient data as well as Nicole Weissenboeck and Maria Lichteneckert for clinical data management. The authors would further like to acknowledge the valuable contributions of Daniela Wolkersdorfer and Richard Greil to the study organization and administration in the frame of the AGMT, Arbeitsgemeinschaft Medikamentöse Tumortherapie gemeinnützige GmbH, the sponsor of the clinical study (Protocol # AGMT_Capecet_PK). The open access funding is provided by University of Vienna.

Compliance with Ethical Standards

Funding

The sponsor of the clinical study was the AGMT Arbeitsgemeinschaft Medikamentöse Tumortherapie gemeinnützige GmbH which was funded by Merck Austria (Protocol # AGMT_Capecet_PK). The company did not influence the production of the manuscript nor the data analysis nor the interpretation of the data presented. Clinical data management was provided by the Ludwig Boltzmann-Institute for Applied Cancer Research (LBI-ACR VIEnna). The pharmacokinetic analysis of the trial presented was partly supported by the Applied Cancer Research – Institution for Translational Research Vienna (ACR-ITR VIEnna).

Conflict of interest

AG reports honoraria for pharmacokinetic analyses from the ACR-ITR VIEnna.

CD's non-profit research institutes (LBI-ACR VIEnna and ACR-ITR VIEnna) were funded by unrestricted research grants from Merck Austria, Roche Austria, and Sanofi-Aventis, respectively. CD received compensation as a member of scientific advisory boards of Merck Austria, Roche Austria and Sanofi-Aventis, respectively. He also consulted for Merck and Roche Austria and received compensation. CD receives compensation as a member of an IDMC for two studies run by Merck.

MC reports no conflict of interest.

Ethical approval

All procedures performed in studies involving human participants were in accordance with the ethical standards of the institutional and/or national research committee and with the 1964 Helsinki declaration and its later amendments or comparable ethical standards. The study protocol was approved by the Ethics Committee of the City of Vienna.

Informed consent

Informed consent was obtained from all individual participants included in the study.

References

1. Twelves C, Wong A, Nowacki MP et al (2005) Capecitabine as adjuvant treatment for stage III colon cancer. N Engl J Med 352:2696-2704. doi:10.1056/NEJMoa043116

2. Cassidy J, Clarke S, Díaz-Rubio E et al (2008) Randomized phase III study of capecitabine plus oxaliplatin compared with fluorouracil/folinic acid plus oxaliplatin as first-line therapy for metastatic colorectal cancer. J Clin Oncol. 26:2006-2012. doi: 10.1200/JCO.2007.14.9898.

3. Cunningham D, Lang I, Marcuello E et al (2013) Bevacizumab plus capecitabine versus capecitabine alone in elderly patients with previously untreated metastatic colorectal cancer (AVEX): an open-label, randomised phase 3 trial. Lancet Oncol 14:1077-1085. doi: 10.1016/S1470-2045(13)70154-2.

4. Seidman AD, O'Shaughnessy J, Misset JL (2002) Single-agent capecitabine: a reference treatment for taxane-pretreated metastatic breast cancer? The Oncologist 7(Suppl 6):20-285.

5. Zambetti M, Mansutti M, Gomez P et al (2012) Pathological complete response rates following different neoadjuvant chemotherapy regimens for operable breast cancer according to ER status, in two parallel, randomized phase II trials with an adaptive study design (ECTO II). Breast Cancer Res Treat 132:843-851. doi: 10.1007/s10549-011-1660-6.

6. Baselga J, Zamagni C, Gómez P et al (2017) Phase III randomized, double-blind trial comparing sorafenib with capecitabine versus placebo with capecitabine in locally advanced or metastatic HER2-negative breast cancer. Clin Breast Cancer 17:585-594.e4. doi: 10.1016/j.clbc.2017.05.006.

7. Miwa M, Ura M, Nishida M et al (1998) Design of a novel oral fluoropyrimidine carbamate, capecitabine, which generates 5-fluorouracil selectively in tumours by enzymes concentrated in human liver and cancer tissue. Eur J Cancer. 34:1274-1281.

8. Tsukamoto Y, Kato Y, Ura M et al (2001) A physiologically based pharmacokinetic analysis of capecitabine, a triple prodrug of 5-FU, in humans: the mechanism for tumor-selective accumulation of 5-FU. Pharm Res. 18:1190-1202.

9. Blesch KS, Gieschke R, Tsukamoto Y et al (2003) Clinical pharmacokinetic/pharmacodynamic and physiologically based pharmacokinetic modeling in new drug development: the capecitabine experience. Invest New Drugs. 21:195-223.

10. Schüller J, Cassidy J, Dumont E et al (2000) Preferential activation of capecitabine in tumor following oral administration to colorectal cancer patients. Cancer Chemother Pharmacol. 45:291-297.

11. Mader RM, Schrolnberger C, Rizovski B et al (2003) Penetration of capecitabine and its metabolites into malignant and healthy tissues of patients with advanced breast cancer. Br J Cancer. 88:782-787.

12. US Food and Drug Administration - XELODA (capecitabine) tablets, Label https://www.accessdata.fda.gov/drugsatfda_docs/label/2015/020896s037lbl.pdf Accessed 28 March 2019

13. Maughan TS, Adams RA, Smith CG et al (2011) Addition of cetuximab to oxaliplatin-based first-line combination chemotherapy for treatment of advanced colorectal cancer: results of the randomised phase 3 MRC COIN trial. Lancet. 377:2103-2114. doi: 10.1016/S0140-6736(11)60613-2.

14. Rachar V, Czejka M, Kitzmueller M et al (2016) Assessment of pharmacokinetic interaction between capecitabine and cetuximab in metastatic colorectal cancer patients. Anticancer Res. 36:4715-4723.

15. Lam SW, Guchelaar HJ, Boven E (2016) The role of pharmacogenetics in capecitabine efficacy and toxicity. Cancer Treat Rev. 2016 50:9-22. doi: 10.1016/j.ctrv.2016.08.001.

16. Pellicer M, García-González X, García MI et al (2017) Identification of new SNPs associated with severe toxicity to capecitabine. Pharmacol Res. 120:133-137. doi: 10.1016/j.phrs.2017.03.021.

17. Loganayagam A, Arenas Hernandez M, Corrigan A et al (2013) Pharmacogenetic variants in the DPYD, TYMS, CDA and MTHFR genes are clinically significant predictors of fluoropyrimidine toxicity. Br J Cancer. 2013 108:2505-2515. doi: 10.1038/bjc.2013.262.

18. Meulendijks D, Cats A, Beijnen JH et al (2016) Improving safety of fluoropyrimidine chemotherapy by individualizing treatment based on dihydropyrimidine dehydrogenase activity - Ready for clinical practice? Cancer Treat Rev. 50:23-34. doi: 10.1016/j.ctrv.2016.08.002.

19. Jones H, Rowland-Yeo K (2013) Basic concepts in physiologically based pharmacokinetic modeling in drug discovery and development. CPT Pharmacometrics Syst Pharmacol. 2:e63. doi: 10.1038/psp.2013.41.

20. Aarons L. (2005) Physiologically based pharmacokinetic modelling: a sound mechanistic basis is needed. Br J Clin Pharmacol. 2005 60:581-583.

21. Gruber A, Czejka M, Buchner P et al (2018) Monitoring of erlotinib in pancreatic cancer patients during long-time administration and comparison to a physiologically based pharmacokinetic model. Cancer Chemother Pharmacol. 81:763-771. doi: 10.1007/s00280-018-3545-4.

22. Vaupel P, Kallinowski F, Okunieff P (1989) Blood flow, oxygen and nutrient supply, and metabolic microenvironment of human tumors: a review. Cancer Res. 49:6449-6465.

23. Schellens JH (2007) Capecitabine. Oncologist. 12:152-155.

24. Czejka M, Schuller J. (1992) [The binding of 5-fluorouracil to serum protein fractions, erythrocytes and ghosts under in vitro conditions] Bindung von 5-Fluorouracil an Serumproteinfraktionen, Erythrozyten und Ghosts unter in vitro Bedingungen. Arch Pharm. 325:69–71. doi: 10.1002/ardp.19923250203.

25. Shindoh H, Nakano K, Yoshida T et al (2011) Comparison of in vitro metabolic conversion of capecitabine to 5-FU in rats, mice, monkeys and humans--toxicological implications. J Toxicol Sci. 36:411-422.

26. Tabata T, Katoh M, Tokudome S et al (2004) Bioactivation of capecitabine in human liver: involvement of the cytosolic enzyme on 5'-deoxy-5-fluorocytidine formation. Drug Metab Dispos. 32:762-767.

27. Tabata T, Katoh M, Tokudome S et al (2004) Identification of the cytosolic carboxylesterase catalyzing the 5'-deoxy-5-fluorocytidine formation from capecitabine in human liver. Drug Metab Dispos. 32:1103-1110.

28. Godin SJ, Crow JA, Scollon EJ et al (2007) Identification of rat and human cytochrome p450 isoforms and a rat serum esterase that metabolize the pyrethroid insecticides deltamethrin and esfenvalerate. Drug Metab Dispos. 35:1664-1671.

29. Ross MK, Borazjani A, Wang R et al (2012) Examination of the carboxylesterase phenotype in human liver. Arch Biochem Biophys. 522:44-56. doi: 10.1016/j.abb.2012.04.010.

30. Zou LW, Jin Q, Wang DD et al (2018) Carboxylesterase Inhibitors: an update. Curr Med Chem. 25:1627-1649. doi: 10.2174/0929867325666171204155558.

31. Laizure SC, Herring V, Hu Z et al (2013) The role of human carboxylesterases in drug metabolism: have we overlooked their importance? Pharmacotherapy. 33:210-222. doi: 10.1002/phar.1194.

32. Quinney SK, Sanghani SP, Davis WI et al (2005) Hydrolysis of capecitabine to 5'-deoxy-5-fluorocytidine by human carboxylesterases and inhibition by loperamide. J Pharmacol Exp Ther. 313:1011-1016.

33. Satoh T, Taylor P, Bosron WF et al (2002) Current progress on esterases: from molecular structure to function. Drug Metab Dispos. 30:488-493.

34. Ueda M, Terai Y, Kumagai K et al (2001) Correlation between thymidine phosphorylase expression and invasion phenotype in cervical carcinoma cells. Int J Cancer. 91:778-782.

35. Judson IR, Beale PJ, Trigo JM et al (1999) A human capecitabine excretion balance and pharmacokinetic study after administration of a single oral dose of 14C-labelled drug. Invest New Drugs. 17:49-56.

36. Desmoulin F, Gilard V, Malet-Martino M et al (2002) Metabolism of capecitabine, an oral fluorouracil prodrug: (19)F NMR studies in animal models and human urine. Drug Metab Dispos. 30:1221-1229.

37. Takechi T, Okabe H, Fujioka A et al (1998) Relationship between protein levels and gene expression of dihydropyrimidine dehydrogenase in human tumor cells during growth in culture and in nude mice. Jpn J Cancer Res. 89:1144-1153.

38. McLeod HL, Sludden J, Murray GI et al (1998) Characterization of dihydropyrimidine dehydrogenase in human colorectal tumours. Br J Cancer. 77:461-465.

39. Reigner B, Verweij J, Dirix L et al (1998) Effect of food on the pharmacokinetics of capecitabine and its metabolites following oral administration in cancer patients. Clin Cancer Res. 4:941-948.

40. Poole C, Gardiner J, Twelves C et al (2002) Effect of renal impairment on the pharmacokinetics and tolerability of capecitabine (Xeloda) in cancer patients. Cancer Chemother Pharmacol. 49:225-234.

41. Louie SG, Ely B, Lenz HJ et al (2013) Higher capecitabine AUC in elderly patients with advanced colorectal cancer (SWOGS0030). Br J Cancer. 109:1744-11749. doi: 10.1038/bjc.2013.517.

42. Schreiber V (2014) [Pharmacokinetics and metabolic activation of capecitabine in the combination therapy with oxaliplatin and the monoclonal antibody cetuximab] Pharmakokinetik und metabolische Aktivierung von Capecitabin in der Kombinationstherapie mit Oxaliplatin und dem monoklonalen Antikörper Cetuximab. Dissertation, University of Vienna.

43. Czejka M, Schueller J, Farkouh A et al (2011) Plasma disposition of capecitabine and its metabolites 5'DFCR and 5'DFUR in a standard and dose-intensified monotherapy regimen. Cancer Chemother Pharmacol. 67:613-619. doi: 10.1007/s00280-010-1363-4.

44. Farkouh A, Scheithauer W, Buchner P (2014) Clinical pharmacokinetics of capecitabine and its metabolites in combination with the monoclonal antibody bevacizumab. Anticancer Res. 34:3669-3673.

45. Bradley SE, Ingelfinger FJ, Bradley GP (1952) Hepatic circulation in cirrhosis of the liver. Circulation. 5:419-429.

46. Twelves C, Glynne-Jones R, Cassidy J et al (1999) Effect of hepatic dysfunction due to liver metastases on the pharmacokinetics of capecitabine and its metabolites. Clin Cancer Res. 5:1696-1702.

47. Mercier C, Dupuis C, Blesius A et al (2009) Early severe toxicities after capecitabine intake: possible implication of a cytidine deaminase extensive metabolizer profile. Cancer Chemother Pharmacol. 63:1177-1180. doi: 10.1007/s00280-008-0889-1.

48. García-González X, Cortejoso L, García MI et al (2015) Variants in CDA and ABCB1 are predictors of capecitabine-related adverse reactions in colorectal cancer. Oncotarget. 6:6422-6430.

49. Caronia D, Martin M, Sastre J et al (2011) A polymorphism in the cytidine deaminase promoter predicts severe capecitabine-induced hand-foot syndrome. Clin Cancer Res. 17:2006-2013. doi: 10.1158/1078-0432.CCR-10-1741.

50. Bonotto M, Bozza C, Di Loreto C et al (2013) Making capecitabine targeted therapy for breast cancer: which is the role of thymidine phosphorylase? Clin Breast Cancer. 13:167-172. doi: 10.1016/j.clbc.2012.10.002.

51. Bijnsdorp IV, Capriotti F, Kruyt FA et al (2011) Thymidine phosphorylase in cancer cells stimulates human endothelial cell migration and invasion by the secretion of angiogenic factors. Br J Cancer. 104:1185-1892. doi: 10.1038/bjc.2011.74.

52. Ishikawa T, Sekiguchi F, Fukase Y et al (1998) Positive correlation between the efficacy of capecitabine and doxifluridine and the ratio of thymidine phosphorylase to dihydropyrimidine dehydrogenase activities in tumors in human cancer xenografts. Cancer Res.58:685-690.

53. Mercier C, Ciccolini J (2016) Profiling dihydropyrimidine dehydrogenase deficiency in patients with cancer undergoing 5-fluorouracil/capecitabine therapy. Clin Colorectal Cancer. 6:288-296.

54. Ezzeldin H, Diasio R (2004) Dihydropyrimidine dehydrogenase deficiency, a pharmacogenetic syndrome associated with potentially life-threatening toxicity following 5-fluorouracil administration. Clin Colorectal Cancer. 4:181-189.

55. Mattison LK, Fourie J, Desmond RA et al (2006) Increased prevalence of dihydropyrimidine dehydrogenase deficiency in African-Americans compared with Caucasians. Clin Cancer Res. 12:5491-5495.

56. Kuilenburg ABPV, Meijer J, Tanck MWT et al (2016) Phenotypic and clinical implications of variants in the dihydropyrimidine dehydrogenase gene. Biochim Biophys Acta. 1862:754-762. doi: 10.1016/j.bbadis.2016.01.009.

57. Meulendijks D, Henricks LM, Sonke GS et al (2015) Clinical relevance of DPYD variants c.1679T>G, c.1236G>A/HapB3, and c.1601G>A as predictors of severe fluoropyrimidine-associated toxicity: a systematic review and meta-analysis of individual patient data. Lancet Oncol. 16:1639-1650. doi: 10.1016/S1470-2045(15)00286-7.

58. Falvella FS, Cheli S, Martinetti A et al (2015) DPD and UGT1A1 deficiency in colorectal cancer patients receiving triplet chemotherapy with fluoropyrimidines, oxaliplatin and irinotecan. Br J Clin Pharmacol. 80:581-588. doi: 10.1111/bcp.12631.

Table 1 Input parameters for the GastroPlus™ PBPK model of CCB and its metabolites DFCR, DFUR and 5FU

Compounds	**CCB**	**DFCR**	**DFUR**	**5FU**
Molecular weight (g/mol)	359.4	245.2	246.2	130.08
LogP	0.6	-1.15	-1.08	-0.81
pKa (acidic (a), basic (b))	8.8 (a)	2.47 (b)	8.04 (a)	7.45 (a)
Solubility (mg/ml)	26 (pH 7.4)	-	-	-
Permeability (cm/s*10^-4)	3	-	-	-
Fraction unbound in plasma (%)	46	90	38	90
Blood plasma ratio	0.5	1.08	0.91	3
Renal Clearance (l/h)	2.3	5	10	0.5
Enzymes	**CES 1**	**CDA_{liv}**	**TP_{liv}**	**DPD_{liv}**
In vitro assay type	microsomal	cytosolic	cytosolic	cytosolic
In vitro V_{max} (nmol/min/mg P)	80	20	12	0.5
In vivo V_{max} (mg/s)	0.0075	0.016	0.099	0.011
In vitro Km (µmol/l)	2000	1600	600	3
In vivo Km (mg/l)	718.7	392.3	147.7	0.39
Tissue expression (mg/g)	2.4	0.4	0.04	0.008
Protein molecular weight (kDA)	62	16	55	111
	CES 2	**CDA_{tu}**	**TP_{tu}**	**DPD_{tu}**
In vitro assay type	microsomal	cytosolic	cytosolic	cytosolic
In vitro V_{max} (nmol/min/mg P)	80	20	12	0.01
In vivo V_{max} (mg/s)	0.336	0.065	0.099	0.000217
In vitro Km (µmol/l)	2000	1600	600	3
In vivo Km (mg/l)	718.7	392.3	147.7	0.39
Tissue expression (mg/g)	0.05	0.1	0.04	0.008
Protein molecular weight (kDA)	62	16	55	111

Table 2 Plasma concentrations of CCB and its metabolites DFCR and DFUR in treatment cycle 3 and GastroPlus™ simulation results. C_{max} and AUC_{0-6} values are calculated as arithmetic mean ±SD. T_{max} is displayed as median (min-max)

	Arm A		**Arm B**		**Simulation**
	Day 1	**Day 5**	**Day 1**	**Day 5**	
CCB					
C_{max} [µg/ml]	12.72 ± 12.93	8.46 ± 5.29	12.65 ± 10.88	11.84 ± 6.38	8.83
AUC_{0-6} [µg-h/ml]	22.24 ± 15.76	6.26 ± 3.59	21.29 ± 10.20	9.35 ± 4.63	15.47
T_{max} [h]	1.0 (0.5-1.5)	1.5 (0.5-2.0)	0.75 (0.5-2.5)	0.75 (0.5-2.0)	0.6
DFCR					
C_{max} [µg/ml]	6.24 ± 2.95	4.89 ± 2.28	7.01 ± 2.40	6.55 ± 2.62	6.32
AUC_{0-6} [µg-h/ml]	18.77 ± 7.65	4.58 ± 2.8	26.06 ± 13.46	7.79 ± 3.61	12.75
T_{max} [h]	1.0 (0.5-1.5)	1.5 (0.5-2.0)	1.0 (0.5-3.0)	1.0 (0.5-2.0)	0.72
DFUR					
C_{max} [µg/ml]	8.75± 4.05	8.89 ± 4.51	8.58 ± 2.06	8.52 ± 2.51	7.83
AUC_{0-6} [µg-h/ml]	16.98 ± 6.05	7.76 ± 5.48	21.69 ± 9.34	9.50 ± 2.85	16.49
T_{max} [h]	1.0 (0.5-1.5)	1.50 (0.5-2.0)	1.0 (0.5-3.0)	1.0 (0.5-2.0)	0.86

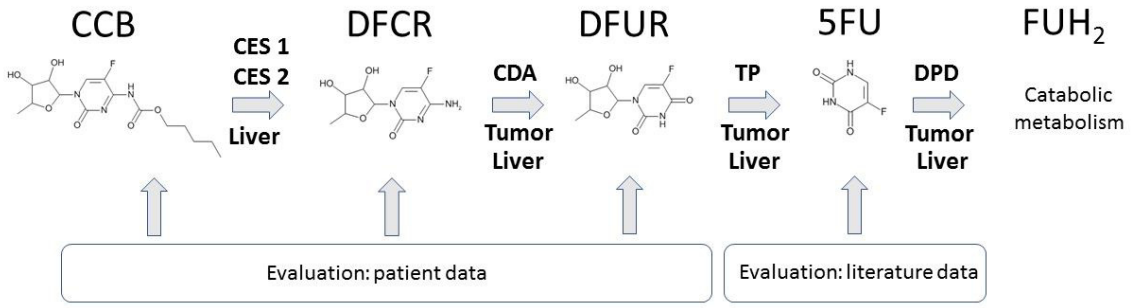
CCB
CES 1
CES 2
Liver
DFCR
CDA
Tumor
Liver
DFUR
TP
Tumor
Liver
5FU
DPD
Tumor
Liver
FUH2
Catabolic metabolism
Evaluation: patient data
Evaluation: literature data

Figure 2

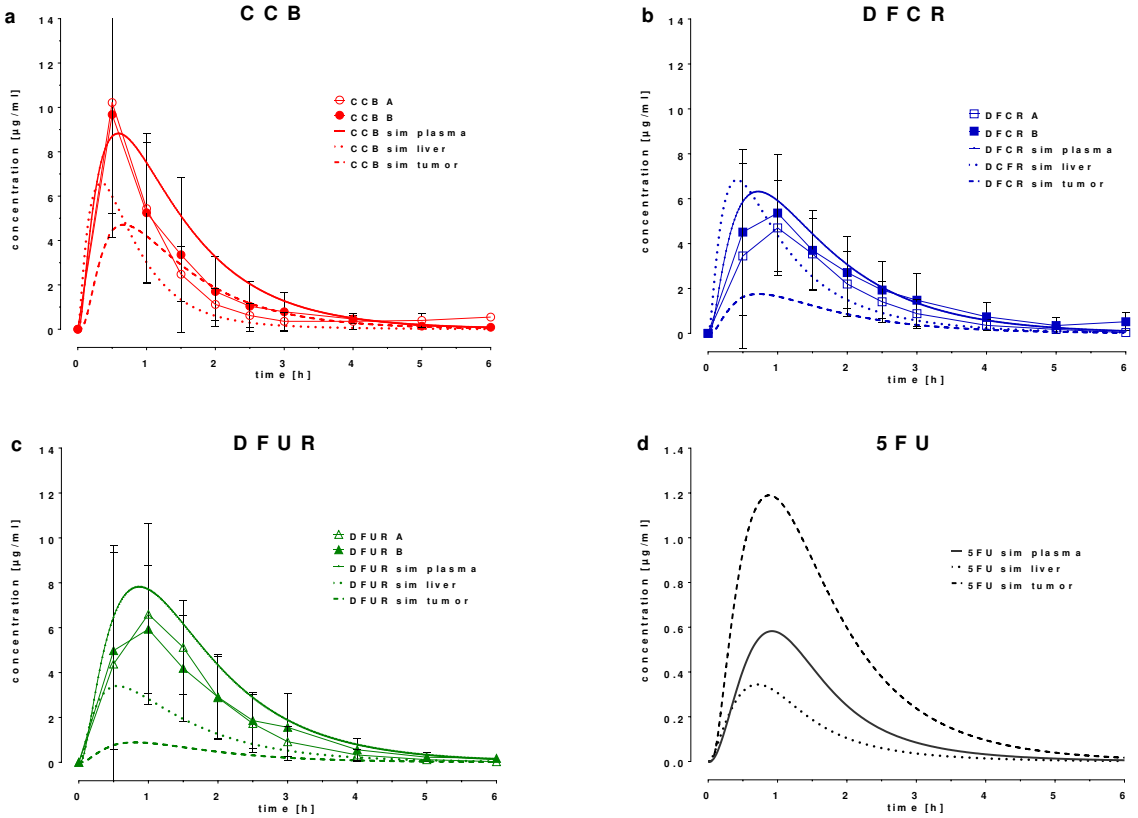

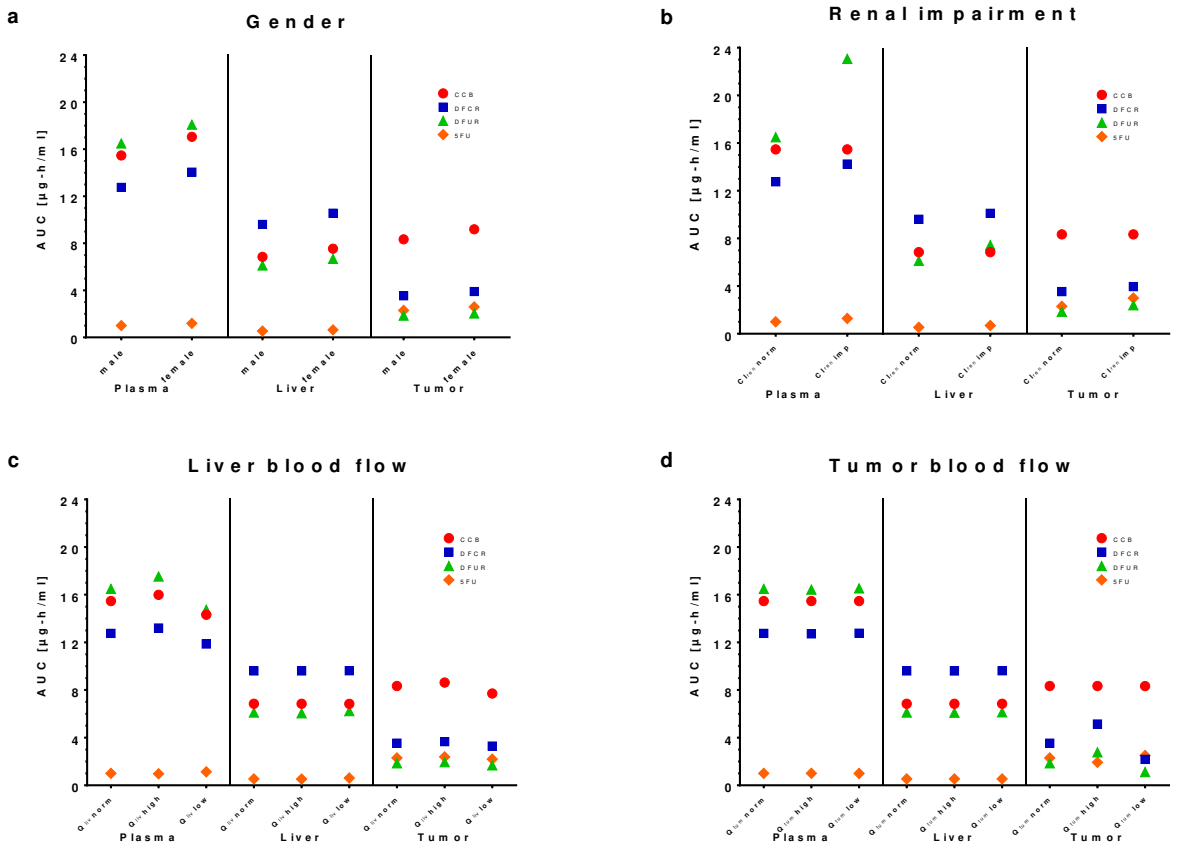

Figure 4

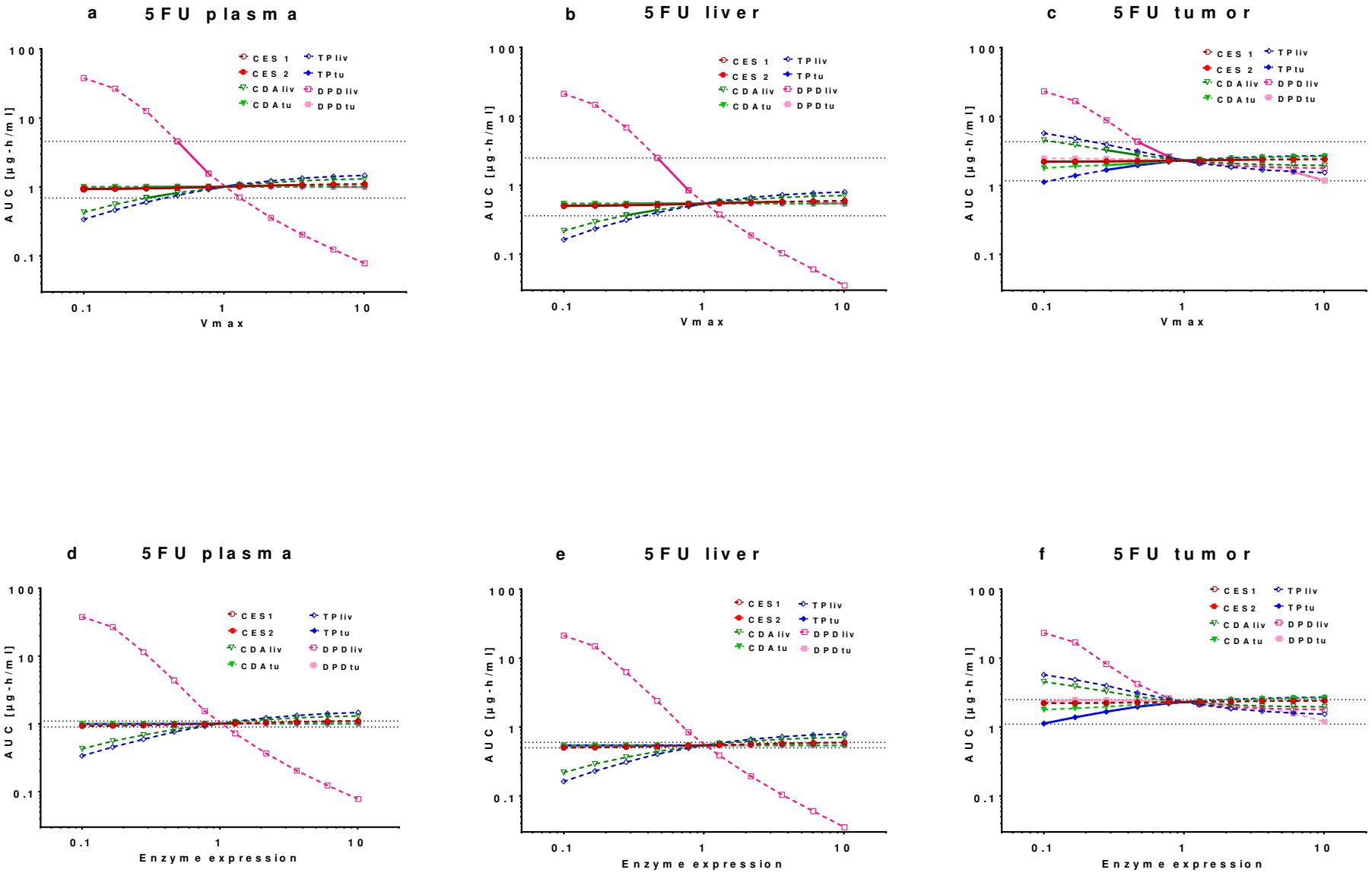

7 List of publications and poster presentations

7.1 Publications

Gruber A, Czejka M, Buchner P, Kitzmueller M, Kirchbaumer Baroian N, Dittrich C, Sahmanovic Hrgovcic A. Monitoring of erlotinib in pancreatic cancer patients during long-time administration and comparison to a physiologically based pharmacokinetic model. Cancer Chemother Pharmacol. 2018;81:763-771. doi: 10.1007/s00280-018-3545-4.

Kauffels A, Kitzmüller M, Gruber A, Nowack H, Bohnenberger H, Spitzner M, Kuthning A, Sprenger T, Czejka M, Ghadimi M, Sperling J. Hepatic arterial infusion of irinotecan and EmboCept® S results in high tumor concentration of SN-38 in a rat model of colorectal liver metastases. Clin Exp Metastasis. 2019;36:57-66. doi: 10.1007/s10585-019-09954-5.

Gruber A, Czejka M. Physiologically based pharmacokinetic modeling of the MEK 1/2 inhibitor selumetinib: impact of pharmaceutical formulation and co-variates on the plasma disposition. AAPS PharmSciTech. Submitted: May 2019.

Gruber A, Czejka M, Dittrich C. Pharmacokinetic modeling of the sequential metabolism of capecitabine to 5-fluorouracil (5FU) for evaluation of influencing factors on 5FU disposition in plasma, liver and tumor tissue and assessment of related toxicities. Cancer Chemother Pharmacol. Submitted: May 2019.

7.2 Poster presentations

Kitzmueller MK, Gruber A, Baroian N, Sahmanovic-Hrgovcic A, Schoenbichler C, Keplinger M, Czejka M. Preclinical pharmacokinetics (PK) of new tyrosine kinase inhibitors (TKIs): In vitro investigations versus in silico predictions. 2016 Conference: CESAR Annual Meeting at: Munich, Germany.

Sahmanovic Hrgovcic A, Gruber A, Dittrich C, Buchner P, Baroian N, Kitzmueller M, Czejka M. Multiple dose pharmacokinetics of erlotinib when combined with gastric acid reducing agents – a comparison with a physiologically based pharmacokinetic model. 2018 Conference: World Gastrointestinal Cancer at: Barcelona, Spain.